Inositol phosphate pathway evolution and synthesis in *Dictyostelium discoideum*

Paloma Portela Torres

MRC Laboratory for Molecular Cell Biology

A thesis submitted to fulfil the requirements for the award of Master of Philosophy in Cell Biology from University College London

April 2020

I, Paloma Portela Torres, confirm that the work presented in this thesis is my own. Where information has been derived from other sources, I confirm that this has been indicated in the thesis.

Work supported by the Medical Research Council.

Abstract

Inositol phosphates (InsPs) are polar water-soluble derivatives of the six-carbon cyclitol inositol. They are synthesized, through phosphorylation reactions, by kinases of four distinct families: IPK, IP5-2K, ITPK1 and PPIP5K, which are thought to be present across all eukaryotes. A pleiotropy of functions has been ascribed to InsPs, from nutrient storage as phytate ($InsP_6$) in plant seeds to the regulation of energy metabolism for the highly phosphorylated inositol pyrophosphates (PP-InsPs).

PP-InsPs were first identified and structurally described in the slime mould *D. discoideum*, in part due to the high concentrations of these molecules in amoeba. However, the amoeba knockout strains for the homologous enzymes synthesising PP-InsPs in humans (and yeast), IP6K (kcs1) and PPIP5K (vip1), do not present clear phenotypes.

The work presented in this thesis expanded our biochemical understanding of these kinases by identifying additional isomers of inositol pyrophosphates and *IpkA* as the main source of $InsP_8$ in the social amoeba. These findings shed light into the evolution of the inositol phosphate pathway and suggested an increased complexity of isomers and enzymes. Inositol phosphate kinase functions were identified in all domains of the tree of life as well as certain viruses, increasing our understanding of the origin and diversification of the inositol phosphate pathway.

Impact statement

The data described in this thesis provides an increased understanding of the pathways that lead to the synthesis of inositol phosphates in different organisms. Inositol phosphates are molecules harbouring a plethora of biological functions across species as well as relevance in industrial and biomedical fields.

Within academia, an increased understanding of the emergence of inositol phosphate synthesis will help us in the re-framing of evolutionary processes leading to the emergence of the contemporary eukaryotic cell.

The farming industry has tried to reduce the levels of inositol phosphates in diets of monogastric animals, including pigs and chickens. Crop engineering could be assisted by an increased understanding of inositol phosphate pathways across key harvested species.

In a clinical setting, the deciphering of relevant inositol phosphate pathways in key pathogenic microorganisms will aid in the development of targeted drug design.

Publications

Saiardi, A., Azevedo, C., Desfougères, Y., Portela-Torres, P., and Wilson, M.S.C. (2018). Microbial inositol polyphosphate metabolic pathway as drug development target. Adv. Biol. Regul. 67, 74–83.

Figures and Tables

1. Introduction

1.1. Inositol and inositol-derived molecules.

1.1.1. Structure

Inositol is a six-carbon ring classified as a cyclic polyol and therefore referred to as cyclitol. The most common isoform of inositol found in biology exists in the form of myo-inositol (Ins). The *myo* isomer adopts a chair conformation, in which an axis of symmetry runs through positions 2 and 5 of the carbon ring. The hydroxyl group on position 2 is denominated axial since its positioning is perpendicular to the plane of the ring. The remaining hydroxyls are termed equatorial since they sit roughly on the same plane as the ring itself. Hydroxyls on positions 1,3 and 5 protrude toward the side of the plane in which the 2-hydroxyl sits and those on positions 4 and 6 point slightly away from it (**Figure 1.1.**).

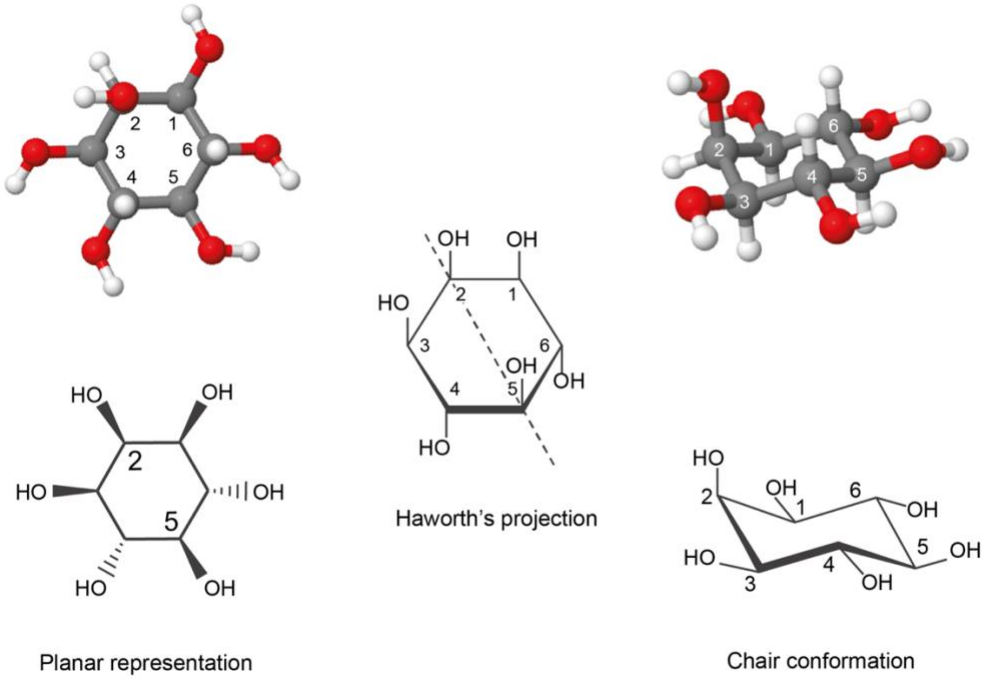

Figure 1.1. Myo-inositol structure. The six-carbon ring of myo-inositol is depicted in a three-dimensional space with corresponding chemical representations to highlight the orientation of its hydroxyl groups. Myo-inositol is represented by three schematic diagrams: Planar representation, Haworth's projection and Chair conformation. Three-dimensional structures were generated using Jmol following the Corey, Pauling and Koltun (CPK) colouring convention. Hydroxyls 1,3,4,5 and 6 adopt an equatorial position, maximising the distance between them. The hydroxyl on position 2 is axial, as can be noticed in the three-dimensional structures. The plane of symmetry turning myo-inositol into a meso compound devoid of optical activity is represented in the Haworth's projection, going through carbon positions 2 and 5.

The six hydroxyl groups of the inositol ring can serve as a scaffold for phosphorylation reactions leading to the synthesis of lipid phosphoinositides (PtdIns) and the soluble inositol phosphates (InsPs). PtdIns have an inositol backbone linked by a phosphodiester bond to a diacylglycerol (DAG) chain on position 1 of the ring. Phosphorylation at positions 3,4 and 5 creates the array of 7 molecular species found in eukaryotic cells (Di Paolo and De Camilli, 2006).

Soluble InsPs are molecules of inositol with phosphate groups (PO_4^{3-}) attached by a phosphoester bond to the carbons on the inositol ring or by a phosphoanhydride bond to pre-existing phosphates on the scaffold to generate inositol pyrophosphates (PP-InsPs). Phosphorylation at all carbons on the inositol ring forms $InsP_6$ or phytic acid (**Figure 1.2.**).

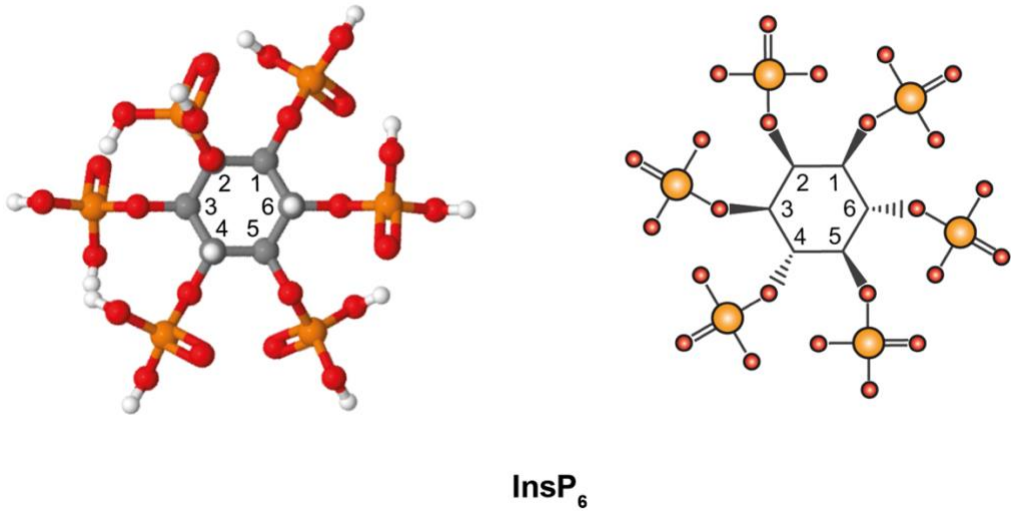

Figure 1.2. $InsP_6$ structure. The six-carbon ring with phosphate groups at all positions in a three-dimensional manner and represented as a CPK coloured planar diagram (oxygen in red and phosphate in orange).

The line of symmetry in myo-inositol runs through positions 2 and 5 (**Figure 1.1.**). Hence, inositol 2 (2-InsP) and 5 (5-InsP) phosphate are symmetric or meso compounds, whereas the internal mirror plane determined by the symmetry axis results in two enantiomeric pairs: inositol 1 (1-InsP) and 3 (3-InsP) phosphate as well as inositol 4 (4-InsP) and 6 (6-InsP) phosphate. Distinguishing the structure of the enantiomeric pairs of InsPs is not possible using most available techniques, given their magnetic equivalence.

PP-InsPs constitute a group of InsPs with diphosphate or triphosphate groups bearing high energy phosphoanhydride bonds. The structure of PP-InsPs in yeast/mammalian cells (Gu et al., 2016; Lin et al., 2009) was found to differ from that present in *D. discoideum* (Albert et al., 1997; Laussmann et al., 1996, 1997). $InsP_7$ in the amoeba was described as 6-$InsP_7$, whereas 5-$InsP_7$ was the isomer defined in mammalian and yeast cells. In the case of $InsP_8$, *D. discoideum* was found to have 5,6-$InsP_7$ and the mammalian/yeast isomer was described as 1,5-$InsP_8$ (**Figure 1.3.**). This discrepancy among PP-InsP isomers was unprecedented and has ever since remained uninvestigated. Indeed, enzymes responsible for the synthesis of InsPs are evolutionarily conserved (**1.2.1.**).

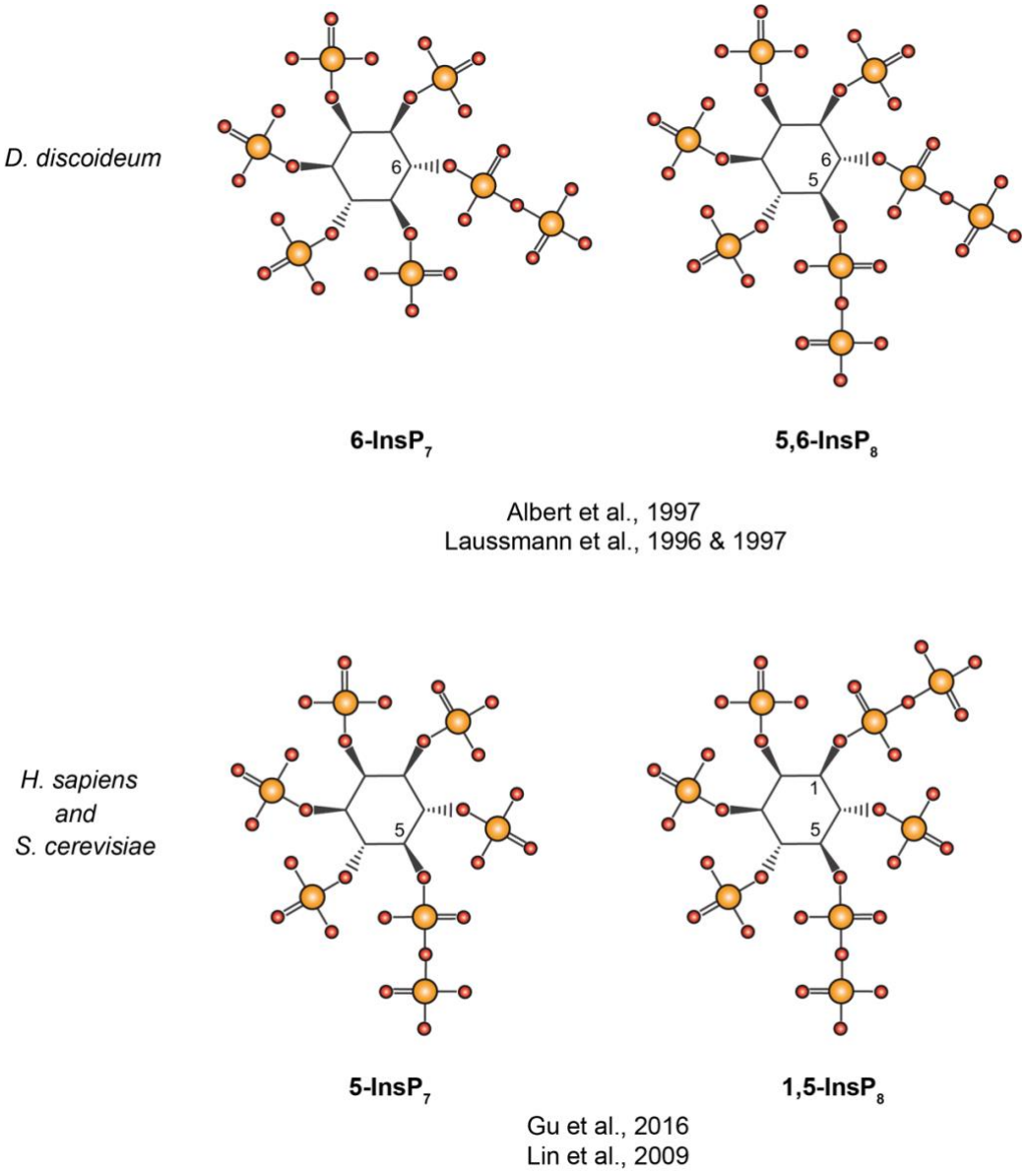

Figure 1.3. Described $InsP_7$ and $InsP_8$ isomer differences between *D. discoideum*, *H. sapiens* and *S. cerevisiae*. NMR studies from *D. discoideum* in-vivo generated inositol pyrophosphates established positioning of the phosphate moieties at carbon 6 for $InsP_7$ and carbons 5 and 6 for $InsP_8$. In vitro experiments using the human and yeast kinases determined their isomeric specificity for the synthesis of 5-$InsP_7$ and 1,5-$InsP_8$.

The structure of PP-InsPs in *D. discoideum* was resolved using NMR (Laussmann et al., 1996). The PP-InsP structures discerned from *in vivo* data were $InsP_7$ with a pyrophosphate in the enantiomeric position 4/6 of the inositol ring and $InsP_8$ with pyrophosphate moieties at positions 4/6 and 5.

Later, the same group was able to derive, from in vitro data, that the naturally occurring $InsP_7$ isomer in the amoeba was 6-$InsP_7$. In an enzymatic assay with a partially purified $InsP_8$ synthesising activity in *D. discoideum*, only the synthetic $InsP_7$ enantiomer pyrophosphorylated at position 6 (and not those at positions 1,3 and 4) led to the production of $InsP_8$. This effect was recapitulated by the use of $InsP_7$ extracted from D. discoideum as a substrate (Laussmann et al., 1997).

An independent study (Albert et al., 1997) drew similar conclusions when comparing the differential (enantiomer-specific) inhibition of a phosphatase in *in vitro* assays. The purified phosphatase could be inhibited with $InsP_7$ from *D. discoideum* extracts with similar kinetics to those arising from the use of a synthetic 6-$InsP_7$ (and not 4-$InsP_7$), supporting the evidence for 6-$InsP_7$ as the isomer present in the amoeba.

Hence, a combination of *in vivo* and *in vitro* data pointed towards 5,6-$InsP_8$ as the isomer present in *D. discoideum* (Albert et al., 1997; Laussmann et al., 1996, 1997). This was found to be in contrast with more recently obtained *in vitro* data pointing at 1,5-$InsP_8$ as the isomer present in yeast and mammalian cells (Gu et al., 2016; Lin et al., 2009) (**Figure 1.3.**).

1.1.2. Function

PtdIns are the best characterised inositol-derived molecules, despite their low cellular concentration (Balla, 2013). The development of the "membrane identity" concept was in large, due to the regulation of processes including membrane and vesicle trafficking and nuclear signalling by the presence of PtdIns anchored to different cell membranes (Balla, 2013).

PtdIns can exert their function via the binding of different protein motifs (including the Pleckstrin Homology (PH), Phagocytic oxydase (PX) and Fab1p, YOTB, Vac1p and EEA1 (FYVE) domains) to these lipids. A renowned PtdIns is $PI(4,5)P_2$, which is phosphorylated by PI3Ks to synthesise $PI(3,4,5)P_3$ can be synthesised growth factor signalling, receptor tyrosine kinase (RTK) or G protein-coupled receptor (GPCR) activation. $PI(3,4,5)P_3$ is involved in the Akt/PKB-mTOR signalling pathway that can mediate chemotaxis, cell proliferation and survival (Vanhaesebroeck et al., 2012). $PI(4,5)P_2$ can also be cleaved by PLC in response to receptor activation to form DAG (which activates Protein Kinase C or PKC) and InsPs, molecules that will remain the focus of this study.

The most thoroughly described InsP is the second messenger $Ins(1,4,5)P_3$. It can be generated by different Phospholipase C (PLC) isotypes in response to a range of stimuli, leading to an increase in calcium ion release from intracellular stores (Streb et al., 1983) by binding to the $InsP_3$ receptor (Berridge, 1993).

PP-InsPs have been implicated in the regulation of a number of cell biological processes reviewed in (Shears, 2015; Thota and Bhandari, 2015; Wilson et al., 2013; Zhang et al., 2011). Specific functions attributed to PP-InsPs range from the regulation of growth and stress responses, DNA repair, vesicular trafficking, cell cycle and cell death, Akt signalling,

ribosome biogenesis, the antiviral immune response and chromatin remodelling.

Yeast with decreased $InsP_7$ and $InsP_8$ display slow growth (Dubois et al., 2002), a resistance to cell death induced by hydrogen peroxide and dependent on the checkpoint kinase Rad53 (Onnebo and Saiardi, 2009) and show defects in DNA recombination and reduced survival upon induction of DNA double-strand breaks (Onnebo and Saiardi, 2009). Yeast without PP-InsPs have small vesicles and fragmented vacuoles and impaired endocytic membrane trafficking (Dubois et al., 2002; Saiardi et al., 2000, 2002). Additionally, in yeast, S phase progression following release from cell cycle arrest requires $InsP_7$ (Banfic et al., 2013).

Mammalian cells with decreased levels of $InsP_7$ show defects in homologous recombination repair (Jadav et al., 2013). Mammalian cells have increased $InsP_8$ levels following hyperosmotic or thermal stress (Choi et al., 2005; Pesesse et al., 2004) and those overexpressing the enzyme synthesizing $InsP_7$ display increased insulin exocytosis (Illies et al., 2007). In mammalian cells, $InsP_7$ levels fluctuate in different cell cycle stages, accumulating transiently at G1, falling during S phase and likely increasing again at G2/M phase (Barker et al., 2004). Also in mammalian cells, $InsP_7$ acts as a physiological inhibitor of Akt signalling, reducing insulin-stimulated glucose uptake (Chakraborty et al., 2010). Mammalian cells lacking the enzyme synthesizing $InsP_7$ show specific alterations in histone methylation (Burton et al., 2013)

The association of PP-InsPs to all these diverse phenotypes highlights their importance. However, this research field has been somehow constrained by the technologies employed to study PP-InsPs.

1.1.3. Analytical methods to study PP-InsPs

Different techniques have been employed for studying the isomeric conformation and relative abundance of InsP and PP-InsP species in biology. These include Nuclear Magnetic Resonance (NMR), Strong anion exchange High-Performance Liquid Chromatography (Sax-HPLC), Polyacrylamide Gel Electrophoresis (PAGE) with Toluidine blue or DAPI staining and, more recently, Raman Spectroscopy.

For a structural characterization of PP-InsPs, NMR spectra can be interpreted to infer the structure of PP-InsPs molecules. A requirement for NMR studies is the availability of large amounts of purified material to be analysed. Due to the high concentrations of PP-InsPs in *D. discoideum* – described below – Dictyostelids have constituted the only systems in which the determination of the *in vivo* structures of PP-InsPs from cellular extracts (not PP-InsPs purified from *in vitro* enzymatic reactions) has been possible (Pisani et al., 2014).

An NMR technique relying on ^{13}C-inositol labelling was recently developed (Harmel et al., 2019). This ^{13}C-inositol NMR approach displays the advantage of increasing signal-to-noise ratios and obtaining clearer spectra. Further development of this technique has been achieved in the Saiardi laboratory (Yann Desfougères, personal communication) by silencing the enzyme (*ino1*/ISYNA1) that synthesises inositol phosphate from glucose 6-phosphate in the cell, further increasing labelling efficiencies.

However, different PP-InsP enantiomers cannot be distinguished by NMR due to their equivalent magnetic signals (Irvine, 2016; Lonetti et al., 2011). To distinguish between PP-InsPs enantiomeric pairs, indirect approaches have been developed that arise from the comparison of different HPLC traces. These approaches usually rely on in vitro enzymatic assays using synthetic enantiomeric standards of PP-InsPs against those from cellular

extracts. Instances in the literature include enzymatic assays analysing the isomeric substrate specificity of kinases (Laussmann et al., 1997) or the isomer-sensitive inhibition of phosphatases (rat hepatic diphosphatase) (Albert et al., 1997). In fact, two enzymes in *D. discoideum* were identified in vitro as having catalytic specificity for 6-$InsP_7$ and 5-$InsP_7$ (**Figure 5.10**) indicating that perhaps a higher isomeric diversity is present in the amoeba. Nonetheless, due to the remarkable catalytic flexibility of InsP kinases in vitro (Losito et al., 2009), the challenge remains to identify *in vivo* structures of PP-InsP species.

One possible way to bypass this limitation could rely on the use of Raman Spectroscopy. Obtention of signature spectra for chemically synthesised InsPs would allow recognition of different isomeric structures from cellular extracts. Additionally, *in vivo* (Smith et al., 2016) detection of the localisation, relative abundance and isomeric nature of InsPs could be possible using this technique.

For the quantification of PP-InsPs, Sax-HPLC is usually be carried out. Traditional Sax-HPLC analysis involves radiolabelling with myo-[^{3}H]-inositol to labelling equilibrium in which all the different InsP pools are equally labelled. The labelling equilibrium is presumably reached after cells go through several rounds of cell division (thus hours in the case of yeast or days in the case of mammalian cell lines) (Bennett et al., 2006) – a limiting factor for optimal experimental design.

Isotopic labelling can dismiss differences in labelling efficiency across specimens, precluding accurate estimations of PP-InsPs concentrations. Representative data derived from this technique is strongly dependent on the turnover of inositol and inositol-derived molecules. As cellular availability of unlabelled inositol (directly synthesised from glucose) can be altered, ratios of labelled to unlabelled inositol can show variability across experiments. Indeed, expression levels of the inositol synthase Ino1 have been reported to be positively (Shen et al., 2003; Steger et al.,

2003) and negatively (King et al., 2010) regulated by different enzymes and levels of InsPs.

To bypass the need for radiolabelling, a non-radiometric HPLC technique was developed that involved metal dye detection (MDD HPLC). In MDD HPLC, transition metals bind with high affinity to polyanions (such as inositol phosphates) as well as a cation-specific dye for their indirect optical detection and quantification (Mayr, 1988).

The acidic conditions in HPLC – highly acidic in MDD mildly acidic in more traditional Sax-HPLC methods – have been shown to result in the hydrolysis of the pyrophosphate bonds in PP-InsPs, leading to their degradation to InsPs and their consequent underrepresentation in HPLC data (Pisani et al., 2014).

PAGE coupled to Toluidine blue or DAPI staining was conceived as a method for the accurate quantification of cellular levels of $InsP_6$ and PP-InsPs. The high concentration of polyacrylamide (normally 35%) coupled to the use of a high voltage during electrophoresis allows separation of molecules with the resolution of a single phosphate group (~80 Da). The PAGE method provides an accurate snapshot of net PP-InsPs concentrations bypassing radiolabelling efficiency biases and minimising sample exposure to acidic conditions that can lead to their misevaluation (Losito et al., 2009; Pisani et al., 2014). Its much lower cost and higher throughput can compensate for a relatively higher sensitivity of HPLC.

1.2. Inositol phosphate kinases

1.2.1. Enzymes

There are two main catalytic functions that inositol phosphate kinases carry out: phosphorylation and pyrophosphorylation. Enzymes catalysing the formation of phosphoester bonds to the different positions on the inositol ring include Inositol Polyphosphate Multikinase (IPMK), Inositol Tetrakisphosphate 1-Kinase 1 (ITPK1), Ins(1,4,5)P_3 3-Kinase (IP3-3K) and Inositol Pentakisphosphate 2-Kinase (IP5-2K or IPPK); whereas enzymes generating high-energy phosphoanhydride bonds include Inositol hexakisphosphate Kinase (IP6K) and Diphosphoinositol Pentakisphosphate Kinase (PPIP5K). Consensus phosphorylation and pyrophosphorylation positions (Saiardi et al., 2018) for these enzymes are displayed in **Figure 1.4**.

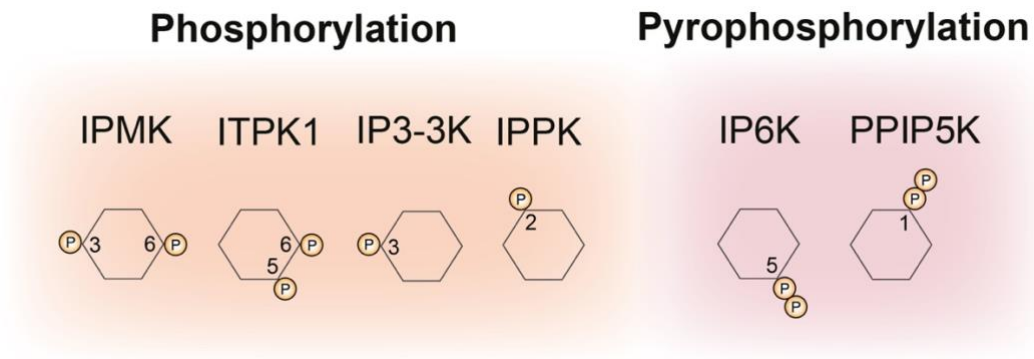

Figure 1.4. Inositol phosphate kinase enzymes and their enzymatic activity. Enzymes are divided mainly on their catalysis of a phosphoester (Phosphorylation) or a high-energy phosphoanhydride bond (Pyrophosphorylation). The position of the carbon ring they have been described to phosphorylate (IPMK, ITPK1, IP3-3K and IPPK or IP5-2K) or pyrophosphorylate (IP6K and PPIP5K) is depicted.

In terms of the controversy between the PP-InsP isomers found in the social amoeba and yeast/humans, the enzymes thought to be responsible for this difference are IP6K (E.C.2.7.4.21) and PPIP5K (E.C. 2.7.4.24). In *S. cerevisiae* and *H. sapiens*, IP6Ks have specific activity towards position 5 on the inositol ring (Draškovič et al., 2008), whereas PPIP5Ks place a pyrophosphate on position 1 (Wang et al., 2012).

The IP6Ks can phosphorylate both $InsP_5$, $InsP_6$ and $InsP_7$ *in vitro* (Draškovič et al., 2008; Saiardi et al., 1999, 2001a). Substrate selectivity for these kinases varies by organism-specific isomer. Mammalian IP6K1 has a 5-fold higher affinity for $InsP_6$ over $InsP_5$, whereas IP6K2 has a 20-fold higher affinity (Saiardi et al., 1999).

Effects of knocking out the IP6K homologue in *S. cerevisiae* (*kcs1*Δ) result in a decrease in fitness (Saiardi et al., 2000). A similar growth defect and reduced infectivity are seen in the *kcs1*Δ of the pathogenic yeast *C. neoformans* (Lev et al., 2015). The *IP6K1-/-* knockout mouse shows reduced insulin secretion and obesity resistance (Chakraborty et al., 2010). The IP6K2-/- knockout mouse shows upregulated DNA repair and ionising radiation resistance (Morrison et al., 2009). Finally, the *IP6K3-/-* knock out mouse shows reduced motor function coordination, independent of kinase activity and PP-InsP levels (Fu et al., 2015).

Among the single *IP6K-/-* knockout mice generated, no complete depletion of IP6K activity and therefore, of PP-InsPs is achieved. Generation of a multiple knockout mouse by traditional methods is difficulted by the presence of IP6K1 and IP6K2 in close proximity on the same chromosomal locus. A recently published double knockout of IP6K1 and IP6K2 in human HCT116 cells revealed decreased phosphate flux, dependent on regulation of phosphate exporter xenotropic and polytropic retrovirus receptor 1 (XPR1) activity by PP-InsPs (Wilson et al., 2019). Given that nephron-specific *XPR1-/-* mice show defects in bone physiology, phosphate homeostasis and renal dysfunction (Ansermet et

al., 2017), a revisiting of the mouse phenotypes should be carried out in a multiple knockout mouse.

An additional class of enzymes, PPIP5Ks was found to synthesise inositol pyrophosphates. First characterised in *S. cerevisiae* as Vip1 (Mulugu et al., 2007), these enzymes are characteristically large (~130 kDa) due to their dual-domain nature. PPIP5Ks usually have a kinase and an acid phosphatase domain. The kinase domain catalyses the addition of a phosphate group by a phosphoanhydride bond on position 1 of the inositol ring (Wang et al., 2012). The phosphatase domain, as characterised in the PPIP5K homologue of *S. pombe* (Asp1) is specific towards pyrophosphate moieties at position 1 (Wang et al., 2015). This capacity to synthesise and degrade its product grants these enzymes a considerable regulatory potential.

The *vip1Δ S. cerevisiae* has no detectable $InsP_8$ and a drastic increase of its precursor $InsP_7$. No effects on fitness are detected on *vip1Δ S. cerevisiae* whereas *asp1Δ S. pombe* is a temperature-sensitive mutant (Feoktistova et al., 1999). The knockout of both isoforms of PPIP5K HCT116 cells leads to a decrease in 1,5-$InsP_8$ and an increase of 5-$InsP_7$ (Gu et al., 2017). This led to a decrease in cell proliferation and altered mitochondrial metabolism, not attributable to the decrease in $InsP_8$ and likely arising from the resulting non-physiological $InsP_7$ levels (Wilson et al., 2019). No knockout mouse model of fully devoid of PPIP5K activity is available.

Despite the availability of certain PP-InsP knockout cell lines and organisms, the complete depletion of PP-InsP levels in a multicellular organism has not yet been achieved. Due to the partially characterised inositol pyrophosphate synthesis pathway in the social amoeba (Livermore, 2016), a revisiting of this organism was required to further elucidate inositol pyrophosphate function.

1.2.2. Pathways

The most thoroughly characterised inositol phosphate (Berridge, 2009) and precursor of higher phosphorylated species is $InsP_3$. It was described to originate from a lipid-dependent route was identified involving phosphoinositides and PLC (Streb et al., 1983). A novel cytosolic route of $InsP_3$ synthesis has been recently characterised (Desfougères et al., 2019), whereby an inositol phosphate synthase (ISYNA1/ino1) and ITPK1 can generate $InsP_3$ using a glucose metabolite as a substrate, independently of lipid phosphoinositides (**Figure 1.5**).

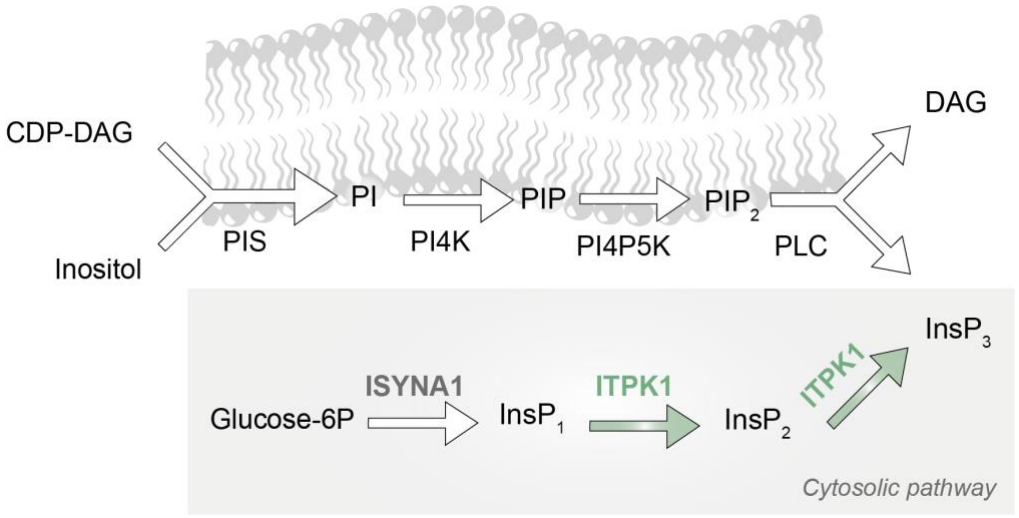

Figure 1.5. Inositol phosphate synthesis pathways. A canonical lipid-dependent pathway and a recently discovered cytosolic pathway are depicted. Synthesis of $InsP_3$ from glucose-6P mediated by ISYNA1 and ITPK1 is highlighted (Desfougères et al., 2019). CDP-DAG: Cytidine Diphosphate Diacylglycerol; PI: Phosphatidyl Inositol, PIP: Phosphatidyl Inositol Phosphate, PIP_2: Phosphatidyl Inositol Bisphosphate; DAG: Diacylglycerol; PIS: Phosphatidyl Inositol Synthase; PI4K: Phosphatidyl Inositol 4-Kinase; PI4P5K: Phosphatidyl Inositol-4-phosphate 5-Kinase; PLC: Phospholipase C; ISYNA1: Inositol-3-Phosphate Synthase 1.

Further phosphorylation of the inositol phosphates is achieved by a combination of enzymes acting in tandem. A consensus (Saiardi et al., 2018) pathway of phosphorylation pyrophosphorylation based on human data is depicted in **Figure 1.6**.

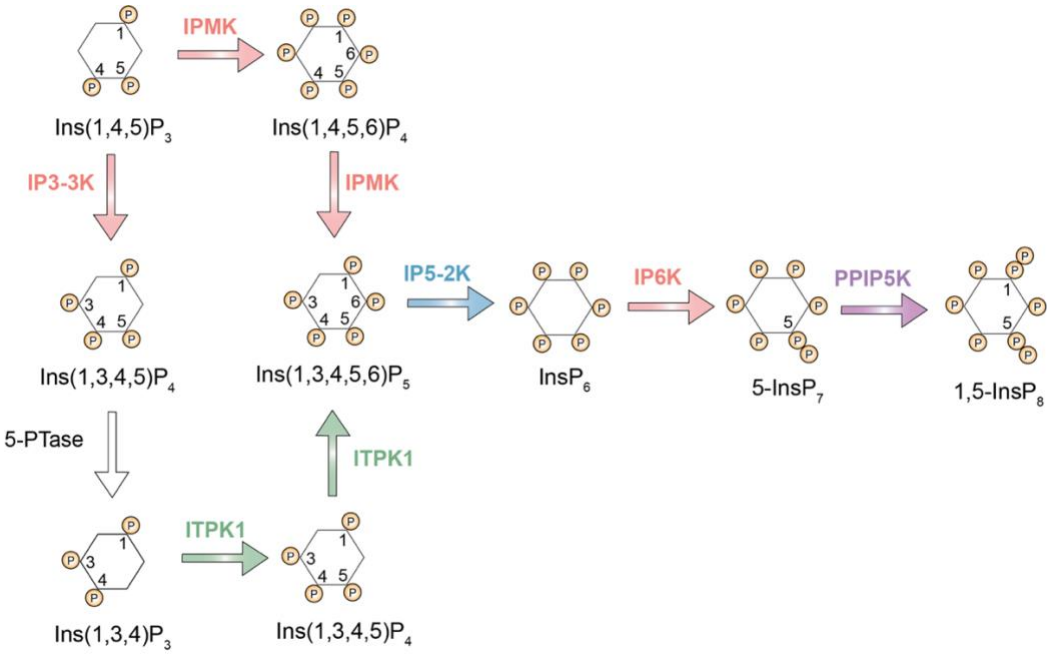

Figure 1.6. Synthesis pathway of inositol phosphates and pyrophosphates from $InsP_3$. Two alternative pathways have been described for the synthesis of phytate ($InsP_6$): a two-step IPMK pathway and a more complex ITPK1 pathway requiring an IP3-3K enzyme and an additional phosphatase (5-PTase). The alternative catalysis by IP6K and PPIP5K of $InsP_7$ and $InsP_6$ respectively has been omitted for simplicity. Kinase activity is depicted by arrows and the positions of the inositol ring that the activity concerns is shown. Enzymes are colour-coded based on their evolutionary relationships, as discussed below (**1.2.3**).

Alternative versions of this pathway are present across different organisms. Notably, yeast has been described to lack an ITPK1 enzyme, and calcium signalling regulated by IP3-3K has been claimed to be restricted to metazoa (Saiardi et al., 2018).

1.2.3. Evolution

Inositol phosphate kinases can be grouped into four families: the inositol 5/6 kinase or ITPK1 family; the IP5-2K or IPPK family; the PPIP5K family and the Inositol Phosphate Kinase "IPK" superfamily, comprising IPMKs, IP3-3Ks, and IP6Ks (**Figure 1.7**).

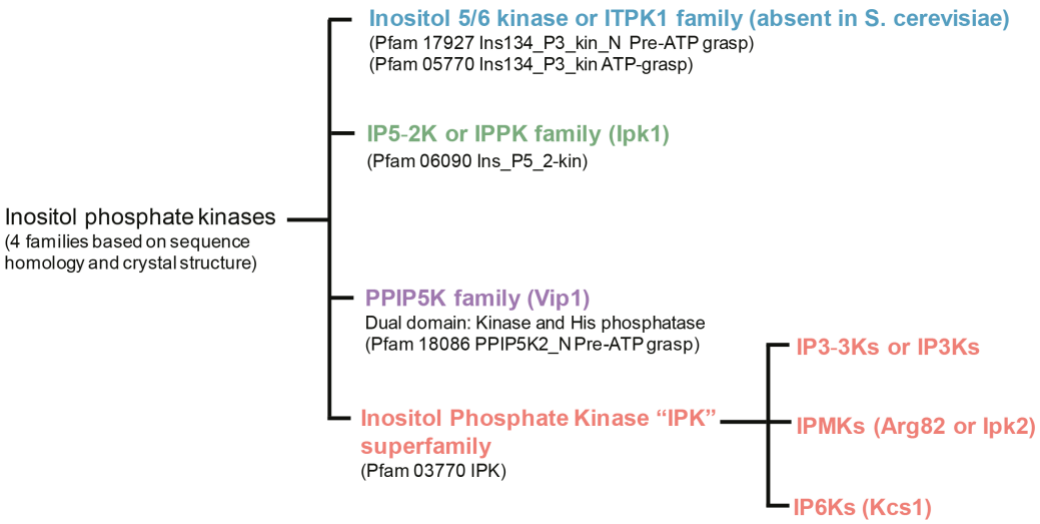

Figure 1.7. Inositol phosphate kinase families. Four families are identified based on sequence homology and structural information: ITPK1, IPPK, PPIP5K and IPK (with different activities: IP3-3Ks, IPMKs, and IP6Ks). His phosphatase: histidine phosphatase. Pfam codes are given for the available family entries and families are colour coded so that purple and pink depict the possibility of pyrophosphorylation within members of the given family.

For the synthesis of lower phosphorylated inositol phosphate species, evolution seems to have developed two multifunctional kinases, ITPK1 and IPMK (IPK member) that are essential in the many phosphorylation steps leading to the synthesis of the same isomer of $InsP_5$. The possibility of redundancy observed in developing these two alternative pathways is excluded when considering the isomeric specificity of these kinases. In

the case of the human pathway, depicted in **Figure 1.6**, an IP3-3K (IPK member) is essential in switching off calcium release (Schell, 2010) and it acts in coordination with ITPK1 to recycle any generated Ins(1,3,4,5)P4.

The $InsP_5$ isomer generated by IPMK or ITPK1 is then phosphorylated at the only non-equatorial position of the inositol ring. The axial 2-OH position is phosphorylated IP5-2K or IPPK, a group of enzymes that seemingly descends from the IPK family (Gonzalez et al., 2010).

The unexpected results from a phylogenetic analysis of IPK enzymes suggest that they are their most ancient member would be IP6Ks, which would have given rise to the catalytically flexible IPMKs and later to IP3-3Ks (Bennett et al., 2006; Wang et al., 2014). The preferred substrate for IP6Ks enzymes is indeed $InsP_6$, and for the synthesis of this molecule, an array of enzymes is required, as previously discussed. These observations suggested the crosstalk of different enzymes for the early establishment of inositol phosphate synthesis pathways. Altogether, this reasoning highlighted the need for adoption of an evolutionary approach towards a comprehensive understanding of the inositol field.

1.3. Inositol phosphate synthesis in *D. discoideum*

1.3.1. *D. discoideum* as a model

Dictyostelium discoideum is a eukaryotic motile soil microorganism (10–20 μm diameter) that gained popularity as a model organism following its discovery in 1933 by Kenneth Raper (Escalante and Cardenal-Muñoz, 2019). Experimental tractability of *D. discoideum* in a laboratory setting and the possibility of growing this organism under diverse conditions (substrate or liquid, static or shaking etc.) make of it an ideal model for the study of basic cell biological questions.

D. discoideum cells show the property of existing as motile and independent amoeboid cells and as a multicellular organism. Amoeba cells follow a developmental programme upon nutrient deprivation (**Figure 1.8**) that results in their differentiation as “aggregation competent” cells and the formation of a multicellular mass which follows a morphogenesis process culminating in the formation of a spore-containing fruiting body. Spores in a fruiting body can germinate under favourable conditions to continue the life cycle, whereas stalk cells undergo altruistic programmed cell death (Annesley and Fisher, 2009).

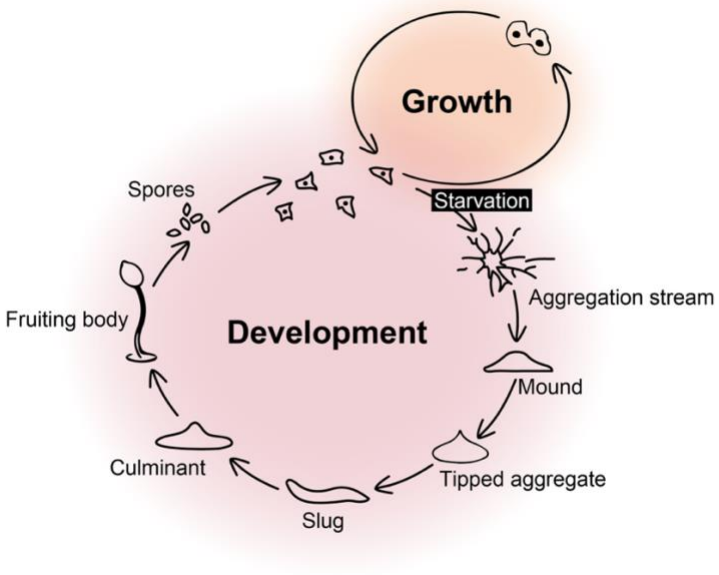

Figure 1.8. The life cycle of *D. discoideum*. Two main stages are identified Growth (vegetative state) and Development (differentiation). Amoeba cells follow a differentiation process upon starvation, lasting around 24 hours and culminating with the formation of fruiting bodies that will then turn into spores able to germinate under favourable nutritional conditions. Development-deficient phenotypes are usually easily identified based on fruiting body morphology.. Figure adapted from (Maeda and Chida, 2013; Myre, 2012).

This life cycle provides remarkable phenotypic “read-outs” in *D. discoideum* experiments. Amoeba development served as a model for

describing the process of chemotaxis (Bonner and Savage, 1947; McCutcheon, 1946). Indeed, PI(3,4,5)P_3 localisation at the leading edge of the amoeba was proposed to be responsible for motility during chemotaxis (Iijima et al., 2002), in a mechanism that remains controversial (see below). Inositol pyrophosphate levels have been described to increase during the process of development in a mechanism yet uncharacterised.

Most importantly, the similarity of the *D. discoideum* genome to those of animal cells serves a great purpose in highlighting its potential as a cell biology model. Indeed, many homologous genes between *D. discoideum* and metazoa have been lost in fungi (Escalante and Cardenal-Muñoz, 2019). Particularly, the *D. discoideum* kinome contains 24 classes of protein kinases that were seemingly lost in the branching of common ancestors leading to the commonly used yeast model organism *S. cerevisiae* (Goldberg et al., 2006).

1.3.2. Relevance in the inositol phosphate research field

D. discoideum was instrumental from the mid-1980s to the early 1990s for the development of the inositol field (Europe-Finner and Newell, 1985; Europe-Finner et al., 1991; Stephens et al., 1988, 1991). The initial discovery of PP-InsPs in 1992 traces back to the social amoeba (Mayr et al., 1992). InsP_7 and particularly, InsP_8 levels were found to increase during development in the social amoeba.

The accumulation of inositol pyrophosphates during amoeba development suggests a role for these molecules during this process. In this context, a 2003 study by Luo et al. showed an increase in aggregation speed of an *ip6k* null strain and described a role for InsP_7 in the inhibition of the membrane localisation of the cytosolic regulator of adenylyl cyclase

(CRAC) (Luo et al., 2003). CRAC is a major regulator of the chemotaxis process during the early phases of amoeba development (Insall et al., 1994). However, such an effect was described to be mediated by the ability of $InsP_7$ to interfere with the interaction of the PH domain of CRAC to the lipid PIP_3. Given that deletion of PIP_3 in the amoeba does not prevent chemotaxis (Hoeller and Kay, 2007; Nichols et al., 2015), and due to the heterogeneity and experimental difficulties of measuring development timings in the amoeba (experimental observation), the mechanism proposed by Luo et al. remains unconfirmed.

Structural NMR studies were made possible in *D. discoideum* due to the high concentrations of pyrophosphates in its cell extracts (Laussmann et al., 1996, 1997). The recently characterised (Desfougères et al., 2019) lipid-independent pathway for InsPs synthesis was initially identified in *D. discoideum* (Stephens and Irvine, 1990).

Despite the initial influence of *D. discoideum*, by the end of the 1990s, it had faded as a model organism for the study of inositol phosphates, being superseded by the budding yeast *S. cerevisiae*. The discovery of the phosphate signalling (PHO) pathway in *S. cerevisiae* and its available sequenced genome (Lenburg and O'Shea, 1996) established it as the preferred experimental model, despite the low abundance of inositol phosphate species in this organism. The availability of the *D. discoideum* genome in 2005 allowed a revisiting of this organism for biochemical and cell biological research (Eichinger et al., 2005).

In *D. discoideum*, despite high inositol phosphate levels, the standard technique of radiolabelling and HPLC analysis is burdensome and expensive, often requiring specialized equipment (Azevedo and Saiardi, 2017; Losito et al., 2009). The introduction of a PAGE method for the analysis of unlabelled inositol phosphate species stained with Toluidine blue or DAPI (**Figure 2**) has rapidly brought to light the complexity of phosphorylated inositol molecules in many different biological systems

(Losito et al., 2009), allowing a straightforward analysis of inositol species in *D. discoideum*. Furthermore, InsPs in *D. discoideum* can be simultaneously visualised along with inorganic polyphosphate (polyP) on a PAGE gel.

PolyP is composed of variable-length (10s-100s) linear chains of phosphate bound to one another by high energy phosphoanhydride bonds. It gained increasing relevance among the inositol field following the discovery of the role of 5-InsP$_7$ in directly promoting the synthesis of PolyP in yeast (Lonetti et al., 2011; Wild et al., 2016). PolyP has been suggested to be implicated in a broad spectrum of cellular roles, including utilising the energy stored in its phosphoanhydride bonds for biochemical reactions (Ahn and Kornberg, 1990; Hsieh et al., 1993; Ohashi et al., 2012), acting as a phosphate buffer by storing free phosphate (Kornberg et al., 1999), pathogen virulence (Moreno and Docampo, 2013), protein folding and post-translational protein modification (Azevedo et al., 2015).

The presence of polyP has been studied in bacteria and eukaryotes (Rao et al., 2009). Its mechanism of synthesis has been described yeast, and it is mediated by the Vtc4 protein. Vtc4 has homologous enzymes in eukaryotes such as kinetoplastids, but remains absent from most eukaryotic genomes (Desfougères and Saiardi, 2020). Although the presence of polyP has been reported in mammalian cells (Morrissey et al., 2012), no enzyme responsible for its synthesis has been identified (Desfougères et al., 2020). One of the key advantages of the study of polyP in *D. discoideum* relies on the identification of the enzyme synthesising this molecule in the social amoeba. PPK is a *D. discoideum* enzyme acquired from bacteria by horizontal gene transfer and *ppk1*$^-$ amoeba show decreased fitness (Livermore et al., 2016a). Interestingly, polyP accumulates dramatically during amoeba development, in an analogous manner to PP-InsPs.

1.3.3. Open avenues for the study of inositol phosphates

The *D. discoideum* genome encodes seven inositol phosphate kinase enzymes: *ip6k*, *ppip5k*, *ipmk*, *ipkA*, *ipkB*, *ipk1*, *itpk1* (**Table 1**) (Livermore, 2016). Out of these, only the *ip6k* (gene name *i6kA*) has been characterized (Luo et al., 2003). The possible functions for some of these enzymes came to light following the generation of unpublished *ip6k - /ppip5k –* knockouts in which residual levels of $InsP_7$ and $InsP_8$ could be detected (Livermore, 2016). As opposed to the four kinases found in yeast (Tsui and York, 2010), the seven *D. discoideum* kinases pointed towards a higher complexity of inositol phosphate synthesis in the amoeba, more similar to mammalian cells than that of yeast.

Table 1.1. Inositol phosphate kinases in *D. discoideum*

Gene id	Annotated gene name	Chrom.	Annotated gene product	KDa	Gene name	Yeast homologue	Mammalian homologue
DDB_G0278739	*I6ka*	3	Inos. phosphate kinase	81	*Ip6k*	Kcs1	IP6K 1-3
DDB_G0284617	N/A	4	n/a	56	*Ppip5k*	Vip1	PPIP5K 1-2
DDB_G0281737	N/A	3	Inos. polyphosphate multikinase	33	*Ipmk*	Arg82	IPMK
DDB_G0271760	*ipkA1*	2	Inos. polyphosphate multikinase	36	*Ipka*	N/A	N/A
DDB_G0283863	N/A	4	Inos. hexakisphosphate kinase	70	*Ipkb*	N/A	N/A
DDB_G0288351	N/A	5	Inos. pentakisphosphate 2-kinase	59	*Ipk1*	Ipk1	IPPK
DDB_G0269746	*Itpk1*	1	Inos. tetrakisphosphate 1-kinase	38	*Itpk1*	N/A	ITPK1

The need for characterisation of the remaining inositol phosphate kinases became evident under the light of incomplete depletion of PP-InsPs from the double knockout amoeba *ip6k -/ppip5k -*. Indeed, IP6K and PPIP5K had been identified as the only genes carrying out pyrophosphorylation of cellular substrates. However, uncharacterised additional sources of inositol pyrophosphates were brought to light following the analysis of this double mutant (**Figure 1.9**).

Furthermore, the isomeric discrepancy between *D. discoideum* and mammalian/yeast PP-InsPs highlighted the possibility that, if such enzymatic difference was verifiable, enzymes non-homologous to those found in humans/yeast could be responsible for the synthesis of the main differing isomers found in the amoeba, as shown in **Figure 1.9**.

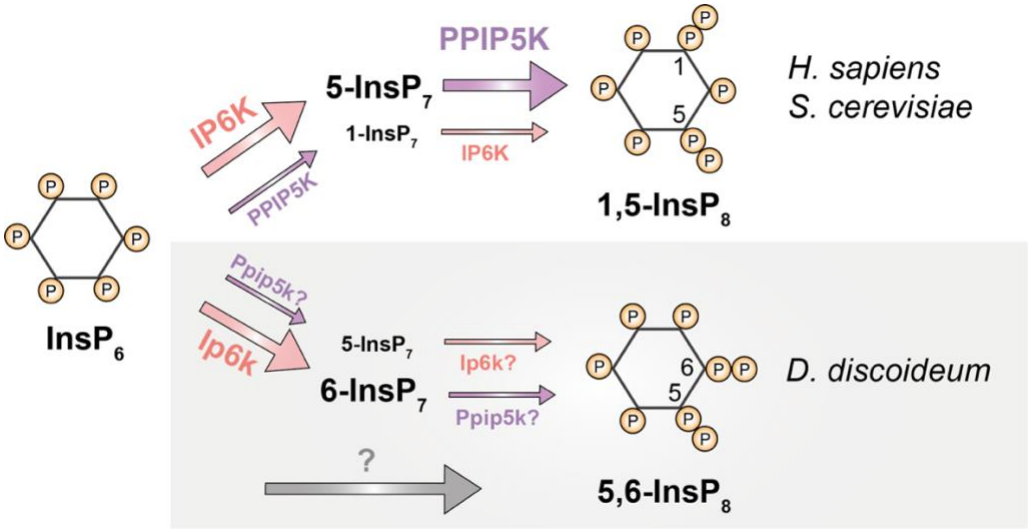

Figure 1.9. Current understanding of inositol pyrophosphate synthesis in *D. discoideum*. Despite evolutionary conservation of IP6K and PPIP5K enzymes, different isomers of $InsP_7$ and $InsP_8$ have been described in humans/yeast and the social amoeba. IP6K has been described to synthesise the majority of $InsP_7$ and a small fraction of $InsP_8$, while for PPIP5K the opposite applies. A large pool of 6-$InsP_7$ has been described to be synthesised by Ip6k in *D. discoideum*, while a smaller 5-$InsP_7$ pool could arise from alternative catalysis by Ppip5k. The isomer 5,6-$InsP_8$ has been described in the amoeba and thought to be synthesised primarily by Ppip5k and, perhaps to a lesser extent by Ip6k as is the case in humans/yeast. Given that the double knockout *ip6k - /ppip5k -* is not fully devoid of inositol pyrophosphates, alternative sources of these molecules are suggested to be present in the amoeba.

2. Materials and methods

2.1. Bacteria

2.1.1. Bacterial strains

Escherichia coli was employed for molecular cloning. Available chemically competent cells (Hanahan 1983) were employed for routine cloning. The NEB® 5-alpha Competent *E. coli* (High Efficiency) was used for higher efficiency cloning.

Klebsiella aerogenes was employed for *D. discoideum* growth in bacterial lawns and selection of candidate mutant clones.

2.1.2. Bacterial growth and storage

Bacteria were grown in Luria-Bertani (LB) media, in liquid culture (shaking at 220 rpm) or on LB-Agar (2%) plates. Antibiotic selection was performed by adding Kanamycin (50 µg/mL) or Ampicillin (100 µg/mL) to the plates. Glycerol stocks were prepared by mixing an overnight bacterial culture with 50% glycerol in a 1:1 volume ratio. Stocks were kept at -80°C.

2.1.3. Bacterial transformation

Chemically competent cells were transformed by incubation on ice for 30 minutes (usually with 100 ng of plasmid DNA or 7ug of ligation mixture. Heat shock was performed at 42°C for 1 minute, following chilling on ice for 2 minutes. Cells were resuspended in antibiotic-free LB media and

incubated for 1h at 37°C and 220 rpm. Selection of positive clones was performed by plating the cultures and cultivating them overnight on given antibiotics.

NEB® 5-alpha Competent *E. coli* cells were transformed according to the manufacturer's instructions.

2.2. Manipulation of nucleic acids

Routine nucleic acid manipulations were performed according to manufacturer's instructions for small (Qiagen Ltd. Mini kit, NEB Inc. Monarch® Plasmid Miniprep Kit) or large (Promega Ltd. PureYield™ plasmid Midiprep kit) scale plasmid DNA purification and DNA fragment purification (Qiagen Qiaquick™ Gel Extraction and PCR Purification Kit). Restriction enzymes were purchased from NEB Inc. or Promega Ltd. and T4 DNA ligase was purchased from Promega Ltd. Traditional restriction enzyme cloning was employed for most constructs (silencing and optimised enzyme expression). The non-optimised kinase constructs were obtained using Gateway® Recombination Cloning Technology (Thermo Fisher Scientific Inc.).

2.2.1. Agarose gel electrophoresis

DNA size was resolved in 1% agarose gels containing 1x TAE buffer (40 mM Tris Acetate, 1 mM EDTA) and 0.1 µg/ml ethidium bromide. Samples were loaded with a 6x DNA loading buffer (either: 10 mM Tris-HCl pH 8.0, 1 mM EDTA pH 8.0, 50% (vol/vol) glycerol and 0.005% orange G dye) and a 1 Kb DNA ladder (NEB) was employed.

2.2.2. DNA ligations

Digested inserts and plasmid vectors were typically mixed at a 3:1 molar ratio and ligated with usually 5 units of DNA ligase (Promega Ltd.). Reactions were incubated at room temperature overnight or 4°C overnight.

2.2.3. Polymerase Chain Reaction (PCR)

Primer oligonucleotides (Integrated DNA Technologies Inc.) were resuspended and stored in nuclease-free water at 100 picomoles/ul. Takara Ex Taq DNA polymerase or Invitrogen™ Platinum™ SuperFi™ DNA Polymerase according to manufacturer's instructions.

2.2.4. Colony PCR

Bacterial colony PCR was performed to identify candidate recombinant plasmids cloned successfully. Insert and vector-specific plasmids were used for these purposes. Individual clones were picked from agar Petri dishes and resuspended in 20µl of sterile H_2O, from which 1µl was used for a 10µl PCR reaction.

D. discoideum colony PCR was used for screening successfully gene-edited clones. Crude genomic preparation of *D. discoideum* clones was obtained by picking a colony and resuspending it in 20µl of crude genomic extraction buffer (1x TaKaRa Reaction buffer, 1 pM/µl 10% NP-40 and 0.1U/µl Proteinase K) for 5 minutes. These were incubated for 45 minutes at 55°C and 10 minutes at 95°C. The obtained genomic DNA was used as a template (diluted by 1:10) in PCR reactions.

2.2.7. Plasmid DNA constructs and oligonucleotides

A list of oligonucleotides employed is available in **Table 2.1**. The plasmid DNA employed are described as follows:

C-terminal GFP tagging was carried out using pDM450 (Veltman et al., 2009): [act15] || gene:GFP || hygR || gateway MCS || Extrachr (Ddp1-based) ||

N-terminal GFP tagging was performed using pTX-GFP (Levi et al., 2000): [act15] || 8xHis - GFP fusion - myc || neoR || Extrachr (Ddp1-based) ||

Transcriptional silencing was carried out using pDM304-DIRS1-lLTR_rLTR (Friedrich et al., 2015): lLTR rLTR || neoR || Extrachr (Ddp1-based) ||

Knockout generation was mediated using pTM1285 (Sekine et al., 2018): Cas9-NLS-GFP || sgRNA || neoR || (pBluescript II Backbone plasmid) ||

Table 2.1. Oligonucleotides

C-terminal GFP tagging

Human IP6K1 primers:

hIP6K1F CACCATGTGTGTTTGTCAAACCATGGAAGT

hIP6K1R CACCATGTGTGTTTGTCAAACCATGGAAGT

Human PPIP5K1 kinase primers:

hPPIP5K1F CACCATGTGGTCATTGACGGCCAGTGAG

hPPIP5K1_KinaseR TATGGTGTTCCCCAGAATCTTGGCACAGTCA

Human PPIP5K1 Pptase primers:

hPPIP5K1_PptaseF CACCATGCGGGAGCTTGCCCCACAGTT

hPPIP5K1R ATTTATCTCCTCAGGGACCTCCTGGGC

N-terminal GFP tagging

Human IP6K1 primers:

Dd_op_hIP6K1F GCGGGATCCATGTGTGTATGTCAAACTATGGAAGTAGG

Dd_op_hIP6K1R GCGCTCGAGTTGATTCTCATCACGCATTTGCTCC

Human PPIP5K1 kinase primers:

Dd_op_hPPIP5K1_KinF GCGGGATCCATGTGGTCATTAACAGCATCTGAGG

Dd_op_hPPIP5K1_KinR GCGCTCGAGCATGGTACCACTTGTAGTAGGAACG

Human PPIP5K1 Pptase primers:

Dd_op_hPPIP5K1_PptsF GCGGGATCCATGGAGTTGAGATGTGTAATTGCTATTATTC

Dd_op_hPPIP5K1_PptsR GCGCTCGAGTCCTGGAGAGAAGTGTAACTCAAC

Transcriptional silencing

IpkA trigger primer:

DdIpkA_5'_BglII GCGAGATCCAAGTTGTAGCAGGTTGAACACC

DdIpkA_3'_SpeI GCGACTAGCAGTGACTGCAGTGAATGTACG

IpkB trigger primer:

DdIpkB_5'_BglII GCGAGATCTACCAACAGTAGTAATAATAAC

DdIpkB_3'_SpeI GCGACTAGTCTCAATTGGTGCGTCAACTCC

Knockout generation

IpkA annealed oligonucleotides:

crIpkAsens AGCATGGTAAGGAATGGATAGTGT

crIpkAantis AAACACACTATCCATTCCTTACCA

IpkB annealed oligonucleotides:

crIpkBsens AGCATTATTTAAACTATGAACTGA

crIpkBantis AAACTCAGTTCATAGTTTAAATAA

IpkA screening primers:

crIpkAsens AGCATGGTAAGGAATGGATAGTGT

crIpkAscreen TCATTGATTCAATGATTTCAGGTC

IpkB screening primers:

crIpkBsens AGCATTATTTAAACTATGAACTGA

crIpkBscreen ATGGAACTTGATATGATAC

2.3. *D. discoideum*

2.3.1. Media and buffers

D. discoideum was routinely grown in liquid HL5 media (Formedium™) supplemented with 100 µg/ml penicillin and 100 µg/ml streptomycin (Gibco) and 1.4% glucose. Selection of transformed cells was performed in media supplemented with Hygromycin B (25-35 µg/ml) or G418 (5-30 µg/ml). For the purposes of selection, 2% agar SM (Formedium™) plates were employed. Thick plates (around 35 ml per dish) were poured and semi-dried to allow for optimal bacterial growth. Labelling of C-13 NMR cultures was carried out in inositol-free SIH media (Formedium™) with ^{13}C-inositol (400µM).

Development and pseudo-development buffers were employed at pH 6.4. The following buffers were employed: KK2 (20 mM potassium phosphate or 1.6 mM KH_2PO_4 with 40 mM K_2HPO_4), MES (20 mM 2-(N-morpholino)ethanesulfonic acid or $C_6H_{13}NO_4S$), HEPES (20 mM 2-[4-(2-hydroxyethyl)piperazin-1-yl]ethanesulfonic acid or $C_8H_{18}N_2O_4S$) and TRIS (20 mM 2-Amino-2-hydroxymethyl-propane-1,3-diol or $C_4H_{11}NO_3$).

2.3.2. *D. discoideum* strains

Axenic strains AX2 and AX4 and candidate *ipkA* and *ipkB* mutants (A1, A2, B1 and B2 or GWDI_30_E_2, GWDI_58_H_12, GWDI_31_A_7 and GWDI_545_A_6) were obtained from the Dicty Stock Center (Northwestern University in Chicago, IL, USA).

2.3.3. *D. discoideum* growth and storage

Strains were cultivated at 22°C in HL5 media, either in Petri dishes or in flasks at 120 rpm. Cells were diluted every 1-2 days to avoid confluency of dishes and cell densities exceeding 5 x 10^6 cells/ml. For clonal selection, transformed AX2 cells were diluted (~1 x 10^3 cells/ml) and low cell numbers plated on SM plates *K. aerogenes* with (~100 µl of saturated overnight culture).

Long-term storage of strains on cryovials was performed following stock preparation. For long-term stock preparation, 5 x 10^7 cells were stored per cryovial. Cells in exponential growth cultures were harvested by centrifugation at 500g for 4 min. Pellets were chilled on ice for 5 min and resuspended in 1 ml of cold HL5 with 10% DMSO. Following incubation on ice for 5 minutes, cells were incubated for 1-2 h at -20°C and transferred to a -80°C freezer. Stocks were thawed by resuspension in 10 ml of HL5 on a Petri dish. Following incubation for 1 h, DMSO-containing media was replaced by fresh HL5 and, if necessary, replaced by media supplemented with antibiotic 24 h after thawing.

2.3.4. Electroporation

Cells in exponential growth were centrifuged at 500 g for 2 min and washed twice in cold H50 buffer (20 mM HEPES, 50 mM potassium chloride, 10 mM sodium chloride, 1 mM magnesium sulfate, 5 mM sodium bicarbonate, 1 mM sodium phosphate monobasic) and resuspended in H50 at a concentration of 10^8 cells/ml. Cells (5x10^6 per transformation) were transferred to a 10 ml conical centrifuge tube on ice containing 4 µg of plasmid DNA. A volume of 100 µl of the suspension was transferred to an electroporation cuvette (1 mm gap size, VWR™). Cells were pulsed

twice at 0.85 kV and 25 µF, with 5 sec between each pulse. Cells were recovered on ice for 5 min, resuspended and plated on Petri dishes with HL5. Selection media was added 24 h after transformation and replaced every 2-3 days, with drug selection in liquid media lasting 10 days.

2.3.5. Construction of mutants

Genome editing was mediated by CRISPR/Cas9, following the protocol described in (Muramoto et al., 2019; Sekine et al., 2018). For the generation of the single-guide RNA (sgRNA) expression plasmid, a target sequence was defined using Rgenome's Cas-Designer. The ordered sense oligonucleotide was composed of the 20 nucleotides preceding (and hence excluding) the protospacer adjacent motif (PAM) 5′-NGG-3′ in the genomic target region. The antisense oligonucleotide was complementary to the sense and sequences 5′-AGCA-3′ (sense) and 5′-AAAC-3′ (antisense) were added to achieve complementarity with overhangs digested by BpiI.

Oligonucleotides were mixed in equal molar amounts and denaturated for 5 min at 95°C and cooled for 70 minutes with decreasing temperatures (slope of -1°C per minute) to achieve annealing at 25°C in a thermal cycling machine. Annealed oligonucleotides are simultaneously digested and ligated by Golden Gate Cloning with initial cycles of 5 min at 37°C and 15 min at 16°C. After five initial cycles, digestion for 1 h at 37°C by BpiI ensured linearisation of any un-integrated plasmid and prevented the uptake of any undigested plasmid during bacterial transformation. Bacterial colony PCR was performed with the sense oligonucleotide and a primer within the sgRNA vector (tracr-Rv AAGCTTAAAAAAAGCACCGACTCGGTGCC).

All-in-one CRISPR/Cas9 vector constructs for *ipkA* and *ipkB* were purified and transformed into *D. discoideum* AX2 by electrophoration. Following a short period of selection (1-3 days) with G418, cells were plated onto SM plates with *K. aerogenes*. After ~4 days *D. discoideum* plaques cleared from bacteria were used for colony PCR (**2.2.4.**) using the screening primers (**2.2.7.**). Candidate clones were detected by the lack of amplification, indicating that the genomic region 5' to the PAM sequence did not match that of the native *D. discoideum* genome and that a genome-editing event likely occurred.

2.3.6. Starvation

D. discoideum cells were starved by immersion in a buffer (pseudo-development) or by development in filter-buffer or buffer-agar substrate. A cell number of $20x10_6$ was developed in 35 mm diameter dishes. Cells in the exponential growth stage were washed in the buffer of choice and plated onto the given substrate, following incubation at 22°C. Images and cell extracts were obtained at different time points including: 0 h (vegetative), 1 h (starvation), 8 h (aggregation), 16 h (slug stage) and >24 h (fruiting body).

For pseudo-development, cells were plated directly in a Petri dish with the buffer of choice and harvested using a cell scraper. For development in filters, three Whatman® Grade 3 filter papers were layered and covered by a Whatman® Grade 50 quantitative filter paper (hardened low-ash) soaked in the given development buffer and followed by removal of excess liquid. Cells were resuspended in 500µl of buffer and allowed to flow into the filter by delivery with a P1000 pipette in an outward spiral movement. Cells were harvested by centrifugation for 5 min at 500 G in 10 ml conical centrifuge tubes. For development in agar-buffers, cells

were resuspended in 200µl of buffer and plated with a sterile glass spreader. A plastic scraper was employed for harvesting cells.

2.3.7 Fruiting body images

Cells were allowed to develop as described and fruiting body images were obtained after 24h or 48 h of development. Images were taken on a camera on an adjustable zoom light microscope and all images were obtained at the same magnification.

2.4. Protein analysis

2.4.1. SDS-PAGE

Protein separation based on molecular weight was performed using the NuPAGE™ (Invitrogen™) system. Precast polyacrylamide gradient gels (4-12% Bis-tris gels by Invitrogen™) were run in NuPAGE™ MES SDS running buffer. The molecular weight marker (PageRuler™) was used. Gels were run at 170 mV according to manufacturer's instructions.

2.4.2. Immunoblot analysis

Proteins were transferred to a nitrocellulose membrane in transfer buffer (25 mM Tris, 192 mM glycine) using the Invitrogen™ transfer cell at 4°C for 1h at 30 V. Membranes were briefly stained with Ponceau-S Stain and scanned. Membranes were blocked with 5% (w/v) skimmed powdered

milk in TBST (TBST; 137 mM NaCl, 2.7 mM KCl, 19 mM Tris base, 0.1% Tween 20) for 30 min at room temperature.

Membranes were incubated at room temperature for one hour with primary α-GFP (1:5000 in 3% skimmed milk TBST) antibody and secondary α-mouse antibody (1:50000 in 3% skimmed milk TBST). Membranes were washed for 10 minutes three times with TBST in between incubations and before HRP processing. Luminata™ Crescendo Western HRP Substrate (Millipore™) was employed to generate a chemical luminescent signal, which was detected by an ImageQuant™ system (GE Healthcare).

2.5. Inositol phosphate analysis

2.5.1. Raman spectroscopy

Raman spectra of dried on 10 mM solutions of inositol phosphates were obtained using a Renishaw Raman RA816 Biological analyser at 785 nm (158 mW of power) utilising a 1500 l/mm grating. Spectra obtained in collaboration with Riana Gaifulina and Geraint Thomas at University College London.

2.5.2. NMR

D. discoideum si*ino1* AX2 cells were grown in SIH media supplemented with ^{13}C-inositol (400µM). ^{13}C-inositol was synthesised by Robert Puschmann (Dorothea Fiedler's laboratory, Leibniz-Forschungsinstitut für Molekulare Pharmakologie (FMP), Berlin, Germany) (Harmel et al., 2019). Purified extracts of $InsP_6$ $InsP_7$ and $InsP_8$ were obtained from these cultures as described in (Loss et al., 2011). In brief, whole-cell extracts from 350ml labelled cultures were extracted with perchloric acid and run on single-lane 35% PAGE gels. Bands corresponding to each inositol pyrophosphate species were cut and eluted over 24 hours by rotation in alternating solutions of water and 50% methanol. Subsequent TiO_2 purification of InsPs was performed as previously described (Wilson et al., 2015).

The NMR analysis of our inositol pyrophosphate samples was carried out by Robert Puschmann in Dorothea Fiedler's laboratory at the Leibniz-Forschungsinstitut für Molekulare Pharmakologie (FMP) in Berlin, Germany. Two dimensional ^{1}H-^{13}C analysis was performed using a Bruker AVANCE III spectrometer at 600MHz and 300K.

2.5.3. Perchloric acid extraction

The procedure used is adapted from the yeast protocol (Azevedo and Saiardi, 2006), as described in (Pisani et al., 2014). D. discoideum cells at the vegetative stage or following development (**2.3.6.**) were harvested and washed twice with the starvation buffer of choice by centrifugation at 500 G for 2 min. Cell pellets were transferred to 1.5 ml tubes and resuspended in 1 M perchloric acid (40 µl for $20x10^6$ cells)., followed by incubation on ice and frequent vortexing for 5 minutes. Extracts were centrifuged at 18000 G for 10 min and supernatants transferred to new tubes, followed by neutralisation with 1 M potassium carbonate with 3 mM EDTA (19 µl for $20x10^6$ cells). Samples were neutralised by placing them with open lids on ice for 2-3 h or at 4°C overnight.

2.5.4. PAGE and Toluidine blue staining of InsPs

Inositol phosphates were resolved as previously described (Losito et al., 2009). Each gel experiment was on average performed twice (n=2), resulting in a qualitative representation of inositol phosphates present in cell extracts. Densitometry analyses were impeded by the low number of repetitions of a given experiment due to time constraints.

Gels were hand cast using 35% polyacrylamide (40% acrylamide and bis-acrylamide solution, 19:1) in TBE and 200 µl 10% APS; 15 µl TEMED. This solution was poured between two glass plates (24x16x0.1 cm) for polymerization.

Gels were pre-run for 30 minutes at 750 V and 3 mA. Neutralised perchloric acid extracts were mixed with 6xDye (0.01% Orange G; 30% glycerol; 10 mM TrisHCl pH 7.4; 1 mM EDTA) and loaded onto gels, along with any $PolyP_{13}$ or $InsP_6$ standard. Gels were run at 660 V and 5 mA at

4 °C overnight until the Orange G front had run through 2/3 of the gel. Gels were stained with a Toluidine blue solution (20% methanol; 2% glycerol; 0.05% Toulidine Blue, T3260 Sigma-Aldrich) at room temperature for 30 minutes with gentle agitation. Gels were destained twice for 20 minutes in 20% methanol and scanned with an Epson Perfection 4990 Photo Scanner.

2.6. Evolution

2.6.1. Identification inositol phosphate kinase gene family members

Collection of candidate homologue protein sequences across different organisms was carried out through a combination of methods, representative sequences are reflective of databases as accessed in August 2019. Protein sequences were manually cross-referenced to have a representative protein isoform per gene. A total of 228 sequences were collected.

Hidden Markov Model (HMM) searches against the UniProtKB database were performed using the HMM models for all four enzymes available from Pfam (IPK: PF03770.16, PPIP5K-N: PF18086.1, ITPK1-N or Ins134_P3_kin_N: PF17927.1, ITPK1 or Ins134_P3_kin: PF05770.11 and Ins_P5_2-kin: PF06090.12). Default 0.01 sequence threshold and 0.03 hit threshold were used for HMM searches using the HMMER biosequence analysis tool from EMBL©-EBI.

Protein Basic Local Alignment Search Tool (BLAST) searches using all inositol phosphate kinase members found in *S. cerevisiae* and *H. sapiens* were performed with a permissive cutoff e-value of 0.01 (Pearson, 2013) was employed given the high sequence diversity of kinase members of these families, accommodating 3 catalytic activities as is the case for the

IPK family. HMM and BLAST searches were performed by restricting the search to the taxonomy of organisms as depicted in (**Table 6.1**).

Identification of annotated family homologues for IPK, IP5-2K and ITPK1 was performed by accessing the available InterPro family entries (IPK: IPR005522, ITPK1: IPR008656 and IP5-2K: IPR009286). Family members were restricted by taxonomy to identify kinases across different species.

2.6.2. Identification of inositol phosphate kinase absences

To avoid the detection of a kinase absence due to incomplete genome sequencing, proteomes were analysed from species whose genomes have been completely sequenced. Reference proteomes were used to provide comprehensive coverage of species across the tree of life. The absence of different kinases was identified by collecting InterPro family entries among eukaryotic reference proteomes for IPK, ITPK1 and IP5-2K.

A database of available eukaryotic reference proteomes was accessed through UniProt. Those eukaryotic proteomes identified by a proteome identifier (UPID, e.g.: UP000000000) that did not have an entry for either of the three inositol phosphate kinases analysed in InterPro were annotated. Individual absences in the taxa corresponding to the proteome identifiers were collected.

A tree of reference eukaryotic proteomes was generated and branches in which all species of a given taxon had the same kinase absence were annotated as *bona fide* absences across the whole taxon. Other taxa without complete loss of a kinase family in all constituent species were collapsed and left uncoloured. The results were displayed in a tree of eukaryotic species with reference proteomes generated through the NCBI

Taxonomy tool Common Tree (ncbi.nlm.nih.gov/Taxonomy/CommonTree/wwwcmt.cgi). The final figure was obtained by manually annotating the tree using the FigTree software.

2.6.3. Generation of evolutionary trees

An evolutionary tree with branch lengths proportional to divergence time was generated using TimeTree (Institute for Genomics and Evolutionary Medicine Center of Biodiversity, Temple University). The generated Newick file was used to generate the tree in the figure using FigTree. Species falling outside the tool coverage were manually added adjacent to those of the same taxa as described by the Open Tree of Life reference taxonomy (tree.opentreeoflife.org). Viruses were not branched from the tree of life due to their uncertain evolutionary origin (Krupovic et al., 2019). Kinase numbers as described in (**2.6.1.**) were manually annotated and colour coded for each species.

3. Inositol pyrophosphate structure in *D. discoideum*

3.1. Introduction

The inositol field has historically relied on NMR for resolving the isomeric structure of inositol pyrophosphates present across different organisms. These were first identified in *D. discoideum* from an HPLC trace that detected the presence of molecules of higher polarity than the fully phosphorylated $InsP_6$ ring (Europe-Finner et al., 1991). Due to the advantages posed by PP-InsP concentrations in the amoeba, isomeric structures of these molecules were defined by NMR (Albert et al., 1997; Laussmann et al., 1996, 1997). Subsequently, inositol pyrophosphate structures were described in yeast and humans from the derived analysis of *in vitro* reaction products (Gu et al., 2016; Lin et al., 2009).

The isomers described in human cells differed from those found in *D. discoideum*. $InsP_7$ was described as 6-$InsP_7$ in the amoeba and 5-$InsP_7$ in humans. In the case of $InsP_8$, the isomer described for *D. discoideum* was 5,6-$InsP_8$ while the human and yeast one was 1,5-$InsP_8$ (**Figure 1.3**). This was of particular interest for this study, since the enzymes synthesising them from $InsP_6$ are evolutionarily conserved, as will be discussed later.

Such difference in the isomeric species could arise from the fact that data regarding human structures are derived from *in vitro* reactions. Small changes in reaction conditions, such as changes in pH (Draškovič et al., 2008), have been demonstrated to alter the isomeric nature of the products formed, possibly generating the disparity among the reported structures of amoeba and human/yeast inositol pyrophosphate isoforms.

An alternative approach such as Raman spectroscopy could be an ideal candidate for the corroboration of differences in such structures if applied

successfully across *D. discoideum*, human and yeast. Furthermore, the application of enantioselective Raman spectroscopy (Rullich and Kiefer, 2018) could provide additional information that NMR does not resolve, regarding the exact positioning of the phosphoanhydride-bonded phosphates on inositol pyrophosphates.

Considering recent developments in NMR technology, and the relative antiquity of the NMR technique and instruments employed for *D. discoideum* studies, a revisiting of these gained priority. The development of a novel NMR method (Harmel et al., 2019) using ^{13}C-inositol for the reduction of possible sources of noise was key for this investigation.

Finally, the advantages provided by the amoeba model for the study of cellular inositol phosphate levels could be exploited. Biochemical snapshots obtained by the PAGE method could inform on the *in vivo* function of the human kinases when expressed in an exogenous system, providing further information on the isomeric compatibility of inositol pyrophosphates across species.

3.2. Results

3.2.1. Detecting PP-InsP isomers with Raman

To determine the feasibility of studying inositol pyrophosphate isomers in *D. discoideum* with a novel technique for the field, Raman spectromicroscopy, an initial approach was undertaken. This approach aimed at the identification of PP-InsPs in a cellular sample of the social amoeba, potentially allowing the identification of the concentration and subcellular localisation of different isomers. The initial goal was set to determine whether the Raman signal from cellular *D. discoideum* would

provide enough information to distinguish between isomers of inositol pyrophosphates.

Dried solutions of different inositol pyrophosphate isomers were analysed (**Figure 3.1**). A Raman signal was obtained for $InsP_6$, 5-$InsP_7$ and 1-$InsP_7$. Such signal was distinct, allowing the identification of samples of unlabelled solutions and highlighting the potential for Raman imaging in *D. discoideum* cellular samples.

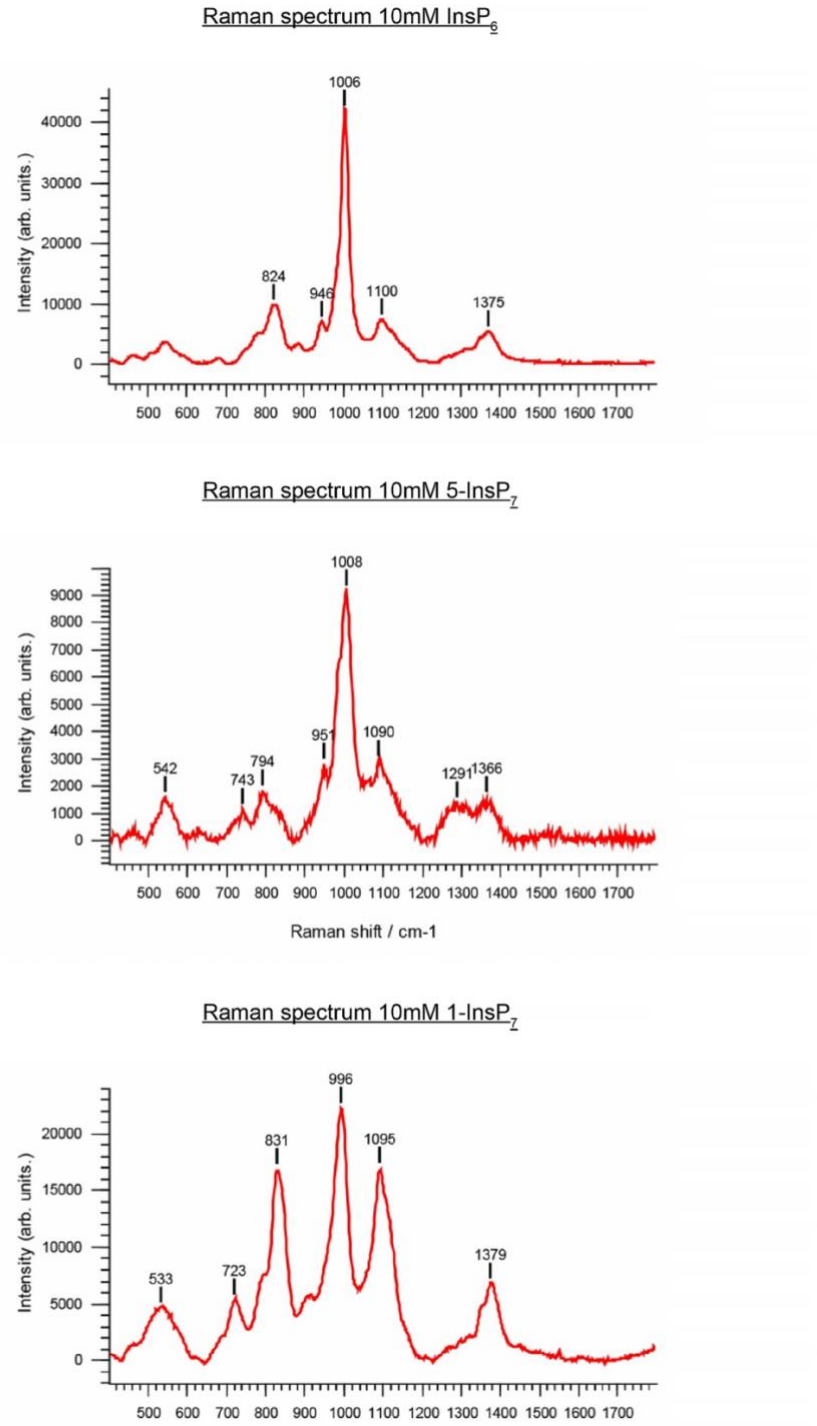

Figure 3.1. Raman spectra of standard inositol phosphate species. Raman spectra of synthetic dried 10 mM solutions of $InsP_6$, 5-$InsP_7$ and 1-$InsP_7$ obtained with a Renishaw Raman microspectroscopic system. All spectra were averaged across five-point measurements, truncated in the fingerprint region and baseline corrected. Obtained in collaboration with Riana Gaifulina and Geraint Thomas from UCL.

3.2.2. Describing isomers by ^{13}C-inositol NMR

For obtaining finer detail regarding the precise structure of inositol pyrophosphates in *D. discoideum*, ^{13}C-inositol NMR was employed (**Figure 3.2**). Labelling of the amoeba was promoted by the use of si*ino1* AX2 cells, which rely on a source of extracellular inositol for survival. Cells were labelled in the laboratory and extracts were sent to Dorothea Fiedler's laboratory at the Leibniz-Forschungsinstitut für Molekulare Pharmakologie (FMP) in Berlin, Germany for their NMR analysis by Robert Puschmann.

The analysis of $InsP_7$ purified from *D. discoideum* cell extracts corroborated the presence of a pyrophosphate moiety in the enantiomeric carbon position 4/6 (Laussmann et al., 1996). It also opened a way for the identification of previously undescribed forms of $InsP_7$ in the social amoeba, such as those phosphorylated at position 1/3.

Following analysis of the $InsP_8$ spectrum, a substantially increased diversity of isomers was revealed. The previously described positions 4/6 and 5 seemed to bear a pyrophosphate, but others such as 1/3 and 2 also seemed to be subject to pyrophosphorylation in amoeba $InsP_8$ species.

Such increase in isomeric complexity required its coupling to a molecular biology approach to identify the key enzymatic players required for the production of inositol pyrophosphates in *D. discoideum*.

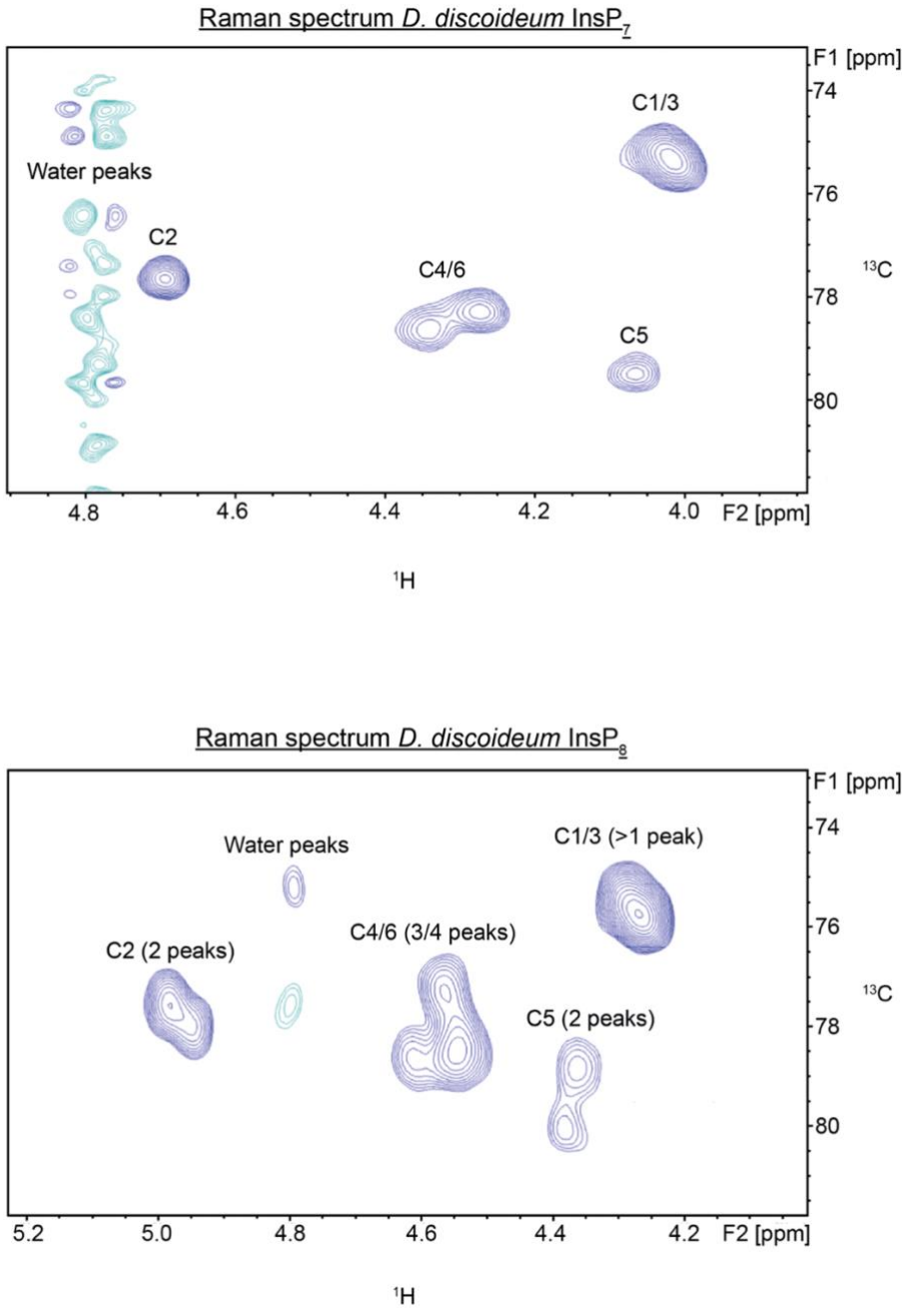

Figure 3.2. NMR spectra of *D. discoideum* InsP$_7$ and InsP$_8$. Two-dimensional NMR spectrum for InsP$_7$ and InsP$_8$ from *D. discoideum* cellular extracts, obtained with a Bruker AVANCE III spectrometer at 600MHz and 300K. The X-axis represents the $_1$H spectrum and the Y-axis corresponds to the $_{13}$C spectrum. The $_{13}$C-$_1$H coupling is presented; this resonance is influenced by the presence of a pyrophosphate moiety by splitting the signalling peak. NMR analysis was carried out by Robert Puschmann in Dorothea Fiedler's laboratory at the Leibniz-Forschungsinstitut für Molekulare Pharmakologie (FMP) in Berlin, Germany.

3.2.3. Reconstitution experiments

To elucidate the isomeric nature of inositol pyrophosphates in *D. discoideum*, reconstitution experiments were performed. These were designed on the premise that endogenous isomeric availability would act as a limiting factor for the production of novel inositol pyrophosphates.

Previously available knockouts (*ip6k -, ppip5k - and ip6k -/ppip5k -*) were employed for this purpose, coupled with the expression of C-terminal GFP-tagged versions of the homologous human kinases (hIP6K and hPPIP5K). The inositol phosphate profiles of the amoeba lines employed are represented in **Figure 3.3**.

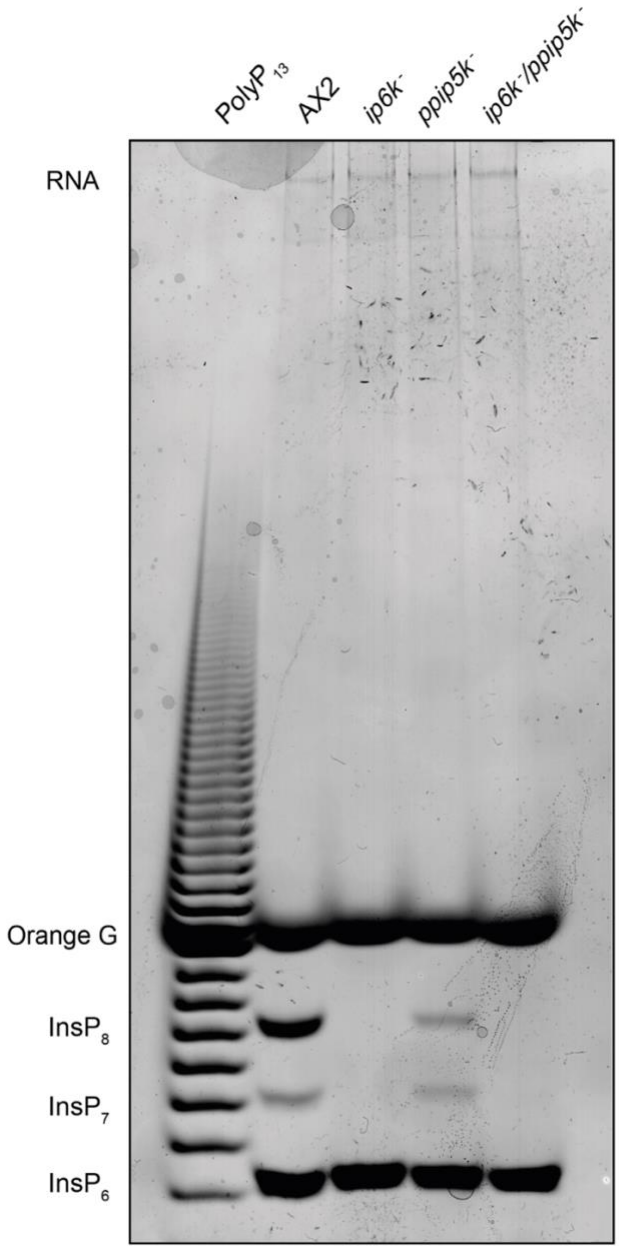

Figure 3.3. PAGE gel of *D. discoideum* wild type and available knockout strains. Wild type strain AX2 and available inositol pyrophosphate mutants (*ip6k* -, *ppip5k* - and *ip6k* -/*ppip5k* -) of the same genetic background are represented. Inorganic polyphosphate of average length 13Pi (PolyP13) is used as a ladder, a solution of OrangeG dye is used for sample loading. Staining with Toluidine blue reveals negatively charged molecules such as RNA and inositol phosphates. A considerable reduction in InsP7 and InsP8 is observed for *ip6k* -, *ppip5k* - and *ip6k* -/*ppip5k* -. However, inositol pyrophosphate depletion is not achieved in any of the knockouts analysed as seen in subsequent gel images obtained using a higher staining sensitivity.

The large size of PPIP5K suggested its expression in the form of cropped domains. The length of both phosphatase and kinase domains of this bifunctional enzyme was analysed as shown in **Figure 3.4**. To increase the likelihood of a maximised protein stability, the kinase domain was cropped generously, avoiding the inclusion of any of the phosphatase domain in the recombinant protein product.

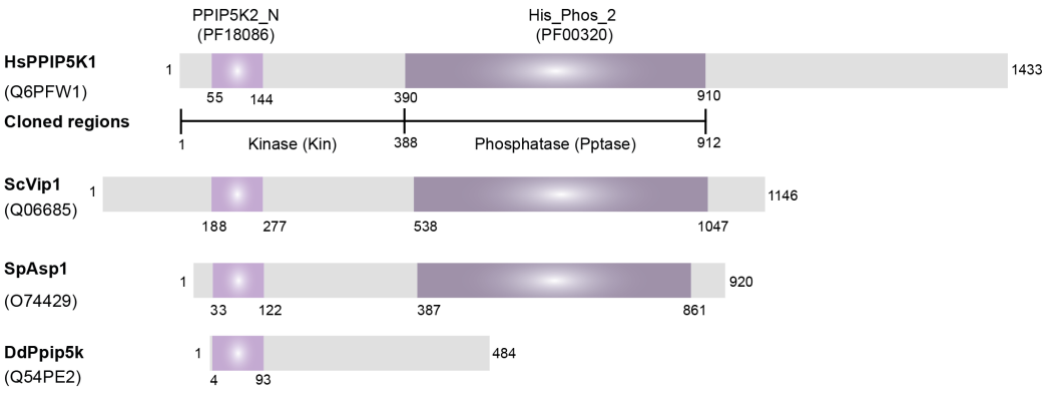

Figure 3.4. Domain distribution of PPIP5K enzymes. The Pfam kinase and phosphatase domains are represented in light and dark purple respectively. Three representatives (Sc: *S. cerevisiae*, Sp: *S. pombe* and Dd: *D. discoideum*) were employed to determine the desired length for expression of the human PPIP5K1 (HsPPIP5K1) kinase (Kin) and phosphatase (Pptase) segments to maximise protein fragment stability.

The expression of the full-length, C-terminally tagged human IP6K did not show a clear increase in the probed inositol phosphates in the cellular extract of *D. discoideum* (**Figure 3.5**).

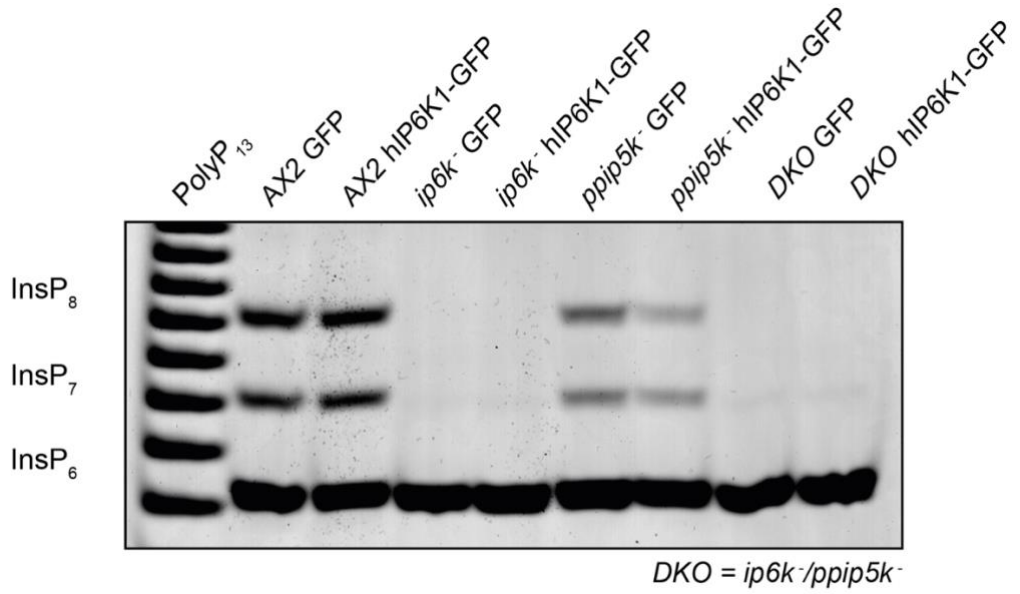

Figure 3.5. Expression of the human IP6K1 in *D. discoideum*. Expression of the C-terminally GFP-tagged full-length human IP6K1 (hIP6K1) in *D. discoideum* did not indicate sustainable differences in inositol phosphate levels. A Western blot or fluorescence signal for the expression of this enzyme was not detectable.

In the expression of the human PPIP5K, the exceptionally large size of this enzyme and its bifunctional catalysis led to its separation into its constituent domains (kinase and phosphatase). No significant changes in inositol phosphate levels were detected upon the expression of the C-terminally tagged human domains in *D. discoideum* (**Figure 3.6**).

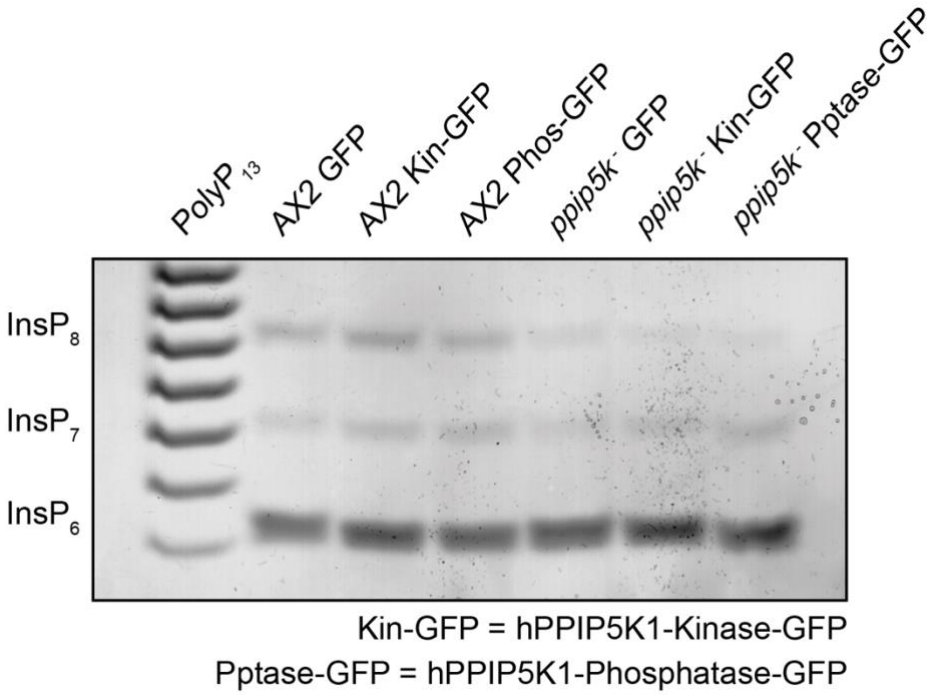

Figure 3.6. Expression of cropped kinase and phosphatase regions of the human PPIP5K in *D. discoideum*. Expression of the C-terminally GFP-tagged Kinase and Phosphatase and regions did not result in a sustained alteration of inositol phosphate levels in the amoeba. Western blot and fluorescence signals were not detectable.

There was a lack of Western blot signal for the GFP-tagged human enzymes in cellular extracts (data not shown). The AT-rich nature of the amoeba genome (Eichinger et al., 2005) has proved to be a hurdle in the expression of exogenous proteins (Arya et al., 2008). Additionally, the use of C-terminal tags could reduce the stability of the fusion protein product, resulting in a decrease in expression levels. Given the inability to detect the expression of the constructs by Western blots, a different strategy was employed.

Codon-optimisation of the original protein sequences was designed through an interface from IDT™ SciTools® and manually adjusted to achieve the compatibility of restriction sites for molecular cloning, as

depicted in **Figure 3.7**. The resulting sequences were synthesised by IDT™ and cloned onto a vector used for tagging proteins with N-terminal GFP.

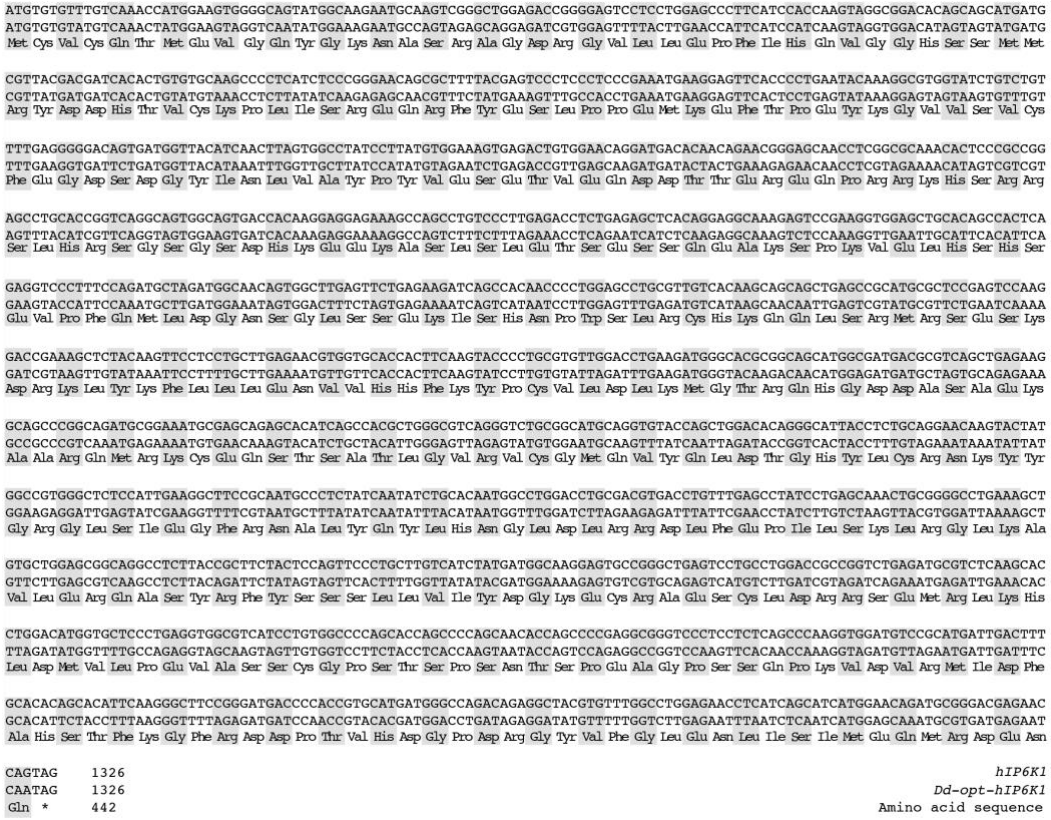

Figure 3.7. Codon optimisation of the human IP6K1 for expression in *D. discoideum*. Optimisation of the kinase sequence was obtained to match codon usage bias in *D. discoideum*. The AT-rich nature of amoeba genome (Eichinger et al., 2005) results in an abundance of substitutions favouring these two nucleotides. Codon optimisation was obtained with an IDT™ SciTools® tool and manually adjusted to prevent the presence of unwanted restriction sites. Figures of optimisation of PPIP5K1 kinase (**Figure 7.1**) and phosphatase (**Figure 7.2**) fragments are found in the Appendix section (**7**).

Expression of the protein constructs was achieved, as detected by Western blotting of cellular extracts (**Figure 3.8**). Expression of the optimised coding sequence for the human IP6K lead to an increase in $InsP_7$ in both wild type and *ip6k* - amoebae, suggesting the ability of

human IP6K to use cellular $InsP_6$ in *D. discoideum* as a substrate for the production of $InsP_7$.

The codon-optimised kinase domain of the human PPIP5K lead to a partial increase in $InsP_7$, suggesting a certain and previously reported (Lin et al., 2009) promiscuity of this enzyme for different inositol pyrophosphates. Expression of the corresponding phosphatase domain seemed to lead to a decrease in $InsP_8$ when expressed in the amoeba, indicating that a fraction of *D. discoideum* $InsP_8$ can serve as a substrate for this enzyme.

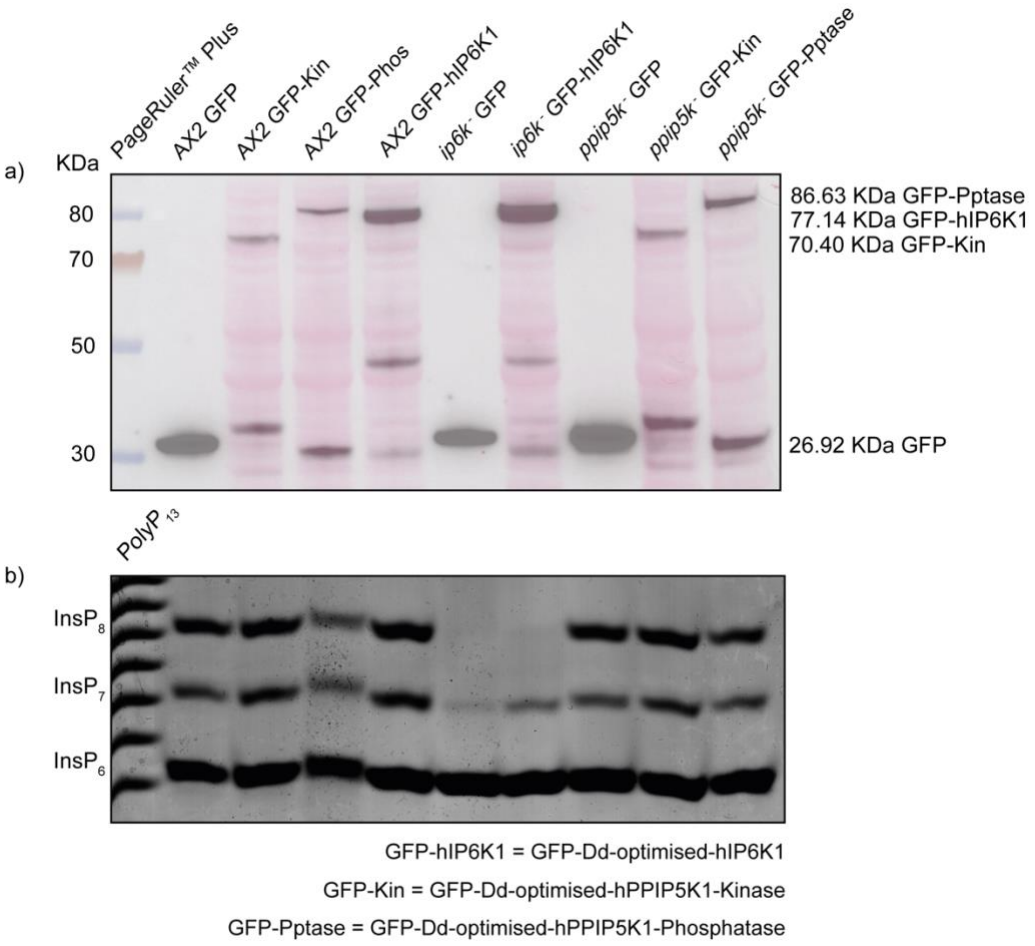

Figure 3.8. Expression of the codon optimised human IP6K1 and PPIP5K1 kinase and phosphatase fragments and their effect on inositol phosphate levels in *D. discoideum*. The scanned western blot overlayed with the Ponceau-stained membrane in panel a) reveal a lower band of free GFP as well as the detected expression of the GFP-tagged proteins in the different *D. discoideum* strains. The inositol profiling image in panel b) detects the activity of the human IP6K1 in *D. discoideum* resulting in an increase in $InsP_7$ levels in both wild-type AX2 and *ip6k* -.The effect of expression of the kinase and phosphatase regions of the human PPIP5K1 on inositol pyrophosphate levels was inconclusive, suggesting the activity of both towards a fraction of $InsP_7$ and $InsP_8$ respectively. Optimised gene fragments of these enzymes were synthesised and subcloned into a ptx-GFP *D. discoideum* vector for C-terminal GFP tagging.

3.3. Discussion

Raman spectroscopy proved to be a promising and, to our knowledge, previously unexplored method for the detection of distinctive inositol pyrophosphate isomers. Its application in *D. discoideum* by comparison of cellular signals to those of standards coupled with deconvolution of different signals could be facilitated by the high concentrations of such species in the social amoeba. Technical limitations of this method arise from the early days of its development. However, the data obtained in these studies established itself as a promising attempt at an approach that could gain track in the near future.

To obtain structurally detailed images of inositol pyrophosphate species that could verify or update relatively dated data obtained with older NMR instrumentation (Laussmann et al., 1996), a ^{13}C-inositol NMR approach was undertaken. This revealed an unparalleled diversity of inositol pyrophosphates in the social amoeba that does not come in conflict with that published but extends the number of potential pyrophosphate positions largely. Increased sensitivity in our method could be held responsible for such inconsistency, and the revealed alternative isomers could account for a smaller fraction of cellular inositol pyrophosphates in the social amoeba.

The low concentrations of inositol pyrophosphates in mammalian cells largely prevent obtaining structural information by NMR. The *D. discoideum* model was employed to obtain further *in vivo* detail regarding the isomeric similarities found between human and amoeba inositol pyrophosphates.

That the human version of *ip6k*, hIP6K could produce $InsP_7$ in *D. discoideum* comes as no surprise, since the fully phosphorylated ring of $InsP_6$ does not present alternative isomeric arrangements that could lead to steric hindrance precluding it from acting as a substrate for the hIP6K

enzyme. It seems clear that the inositol ring phosphorylated at all six carbons can act as a scaffold even for those enzymes exogenous to the cellular organism.

The increase of $InsP_7$ detected in *ip6k* - *D. discoideum* most likely arises from the proposed generation of 5-$InsP_7$ by the human IP6K, as demonstrated in vitro (Gu et al., 2016). This product does not lead to a recovery of *ip6k* - to wild type $InsP_7$ and $InsP_8$ levels, indicating that the presence of this isomer in the amoeba is sub-efficient for the reconstitution of the amoeba inositol pyrophosphate pathway.

A fraction of this $InsP_7$ is pyrophosphorylated to generate $InsP_8$. Since this experiment was performed in an *ip6k* - background, the proposed alternative catalytic activity of IP6Ks as $InsP_8$-synthesising enzymes for the formation of the predominantly described *D. discoideum* isomer 5,6-$InsP_8$ would be discarded.

In the case of hPPIP5K, the discerned high isomeric complexity of the inositol pyrophosphate pool in the amoeba (**Figure 3.2**) could account for the results obtained. Expression of its kinase domain led to a clear increase of an $InsP_7$ and, to a lesser extent, $InsP_8$. A small increase in $InsP_8$ can be accounted for by the use of cellular 6-$InsP_7$ in *D. discoideum* as a sub-optimal substrate by hPPIP5K, which is claimed to have 5-$InsP_7$ as an optimal substrate in humans (Gokhale et al., 2013). The substantial increase in $InsP_7$ could arise by the proposed (Lin et al., 2009) alternative catalytic activity of PPIP5K in mammalian cells, phosphorylating $InsP_6$ to generate a pool of 1-$InsP_7$.

The phosphatase domain of this enzyme is described to be specific for the carbon at position 1 of the mammalian 1,5-$InsP_8$. As seen by NMR, *D. discoideum* has a pool of $InsP_8$ phosphorylated at position 1 (**Figure 3.2**) that this enzyme could be using as a substrate, leading to a reduction in $InsP_8$ levels.

These results supported the proposed idea of increased diversity in the isomeric conformations of inositol pyrophosphate species in the amoeba, therefore raising a question concerning their enzymatic source.

4. Inositol pyrophosphate synthesis *in D. discoideum* – *ip6k* and *ppip5k*

4.1. Introduction

The availability of partially characterised knockout strains in the laboratory instigated their further investigation. Single and double knockouts of *ip6k* and *ppip5k* had been generated by homologous recombination. Such strains failed to show any phenotype when developed in KK2-agar. Two hypotheses could be formulated at this stage.

Firstly, additional sources of inositol pyrophosphates could compensate for the knocking out of *ip6k* and *ppip5k*, leading to the synthesis of sufficient amounts of these molecules for cellular function. According to this hypothesis, their overcoming of limitations in inositol pyrophosphate synthesis following the knockout of the two main enzymes having homologues in humans and yeast would be independent of the environment.

Alternatively, a potential phenotype found in the double knockout strain could be masked by the ideal nutrient-rich environment usually found in laboratory conditions. For example, an excess in cellular phosphate availability could mask any possible link between inositol pyrophosphates and phosphate homeostasis. A constraint to these conditions could reveal a previously dismissed phenotype.

To test the latter hypothesis, it is worth noticing that standard development conditions remarkably induce starvation of most nutrients and ions excluding potassium and phosphate. Indeed, the commonly used development medium is constituted by just 20 mM K-Phosphate buffer at pH 6.4. Due to the nature of our investigation, extracellular phosphate saturation could skew the results obtained, leading to a lack of apparent phenotype. Emulation of non-laboratory developmental

conditions would hence rely on a limitation of ion availability, specifically in the case phosphate, since its availability could alter the phosphate flux in the slime mould.

An alternative buffer solution deprived of phosphate could be employed for our experiments. Such a solution would mimic the pH found in the development buffer KK2 (pH 6.4) and ideally have a certain buffering capability.

4.2. Results

4.2.1. Inositol phosphate levels during regular development

To initially characterise the sources of different inositol pyrophosphates during a physiological process such as *D. discoideum* development, the previously available knockouts were analysed under standard conditions, to corroborate previous observations. Since polyP is synthesised during development, one could expect a limitation in the phosphate available for the synthesis of inositol pyrophosphates by uncharacterised sources during development.

All four strains are shown in **Figure 4.1**, with each lane representing strains having spent 24h in the standard growth medium HL5 or having followed starvation with KK2-agar as a substrate. The developed strains show a remarkable induction of inorganic PolyP production, as previously described (Livermore et al., 2016a).

All strains accumulate inositol pyrophosphates following development. There is no complete depletion of inositol pyrophosphate levels even in the double knockout, despite it lacking the two main enzymes known to be necessary for the synthesis thereof in humans and yeast.

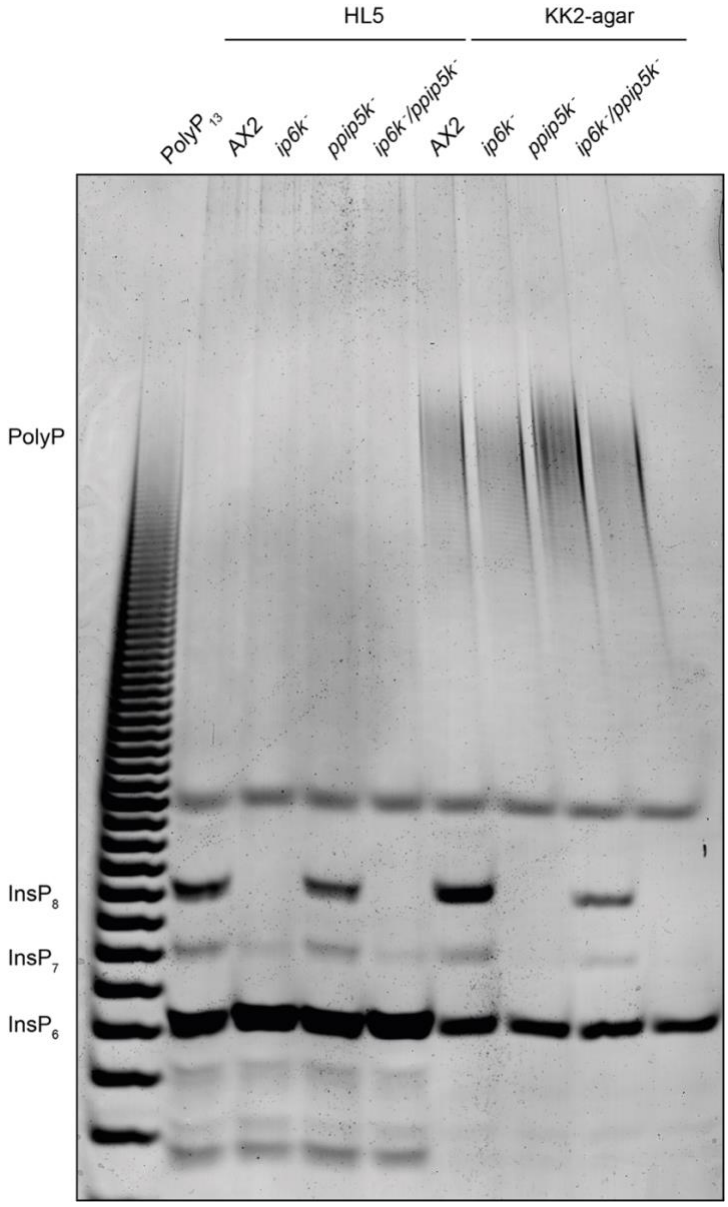

Figure 4.1. Vegetative state and development of available *D. discoideum* inositol phosphate mutants under standard conditions. Wild type AX2 and mutant (*ip6k* -, *ppip5k* - and *ip6k* -/*ppip5k* -) strains were analysed in the exponential growth the stage (HL5) at 1-3x10$_6$ cells/ml or developed in a KK2-Agar plate. Equal cell numbers were employed (20x10$_6$ cells/lane) and differences in total cell mass are attributable to a loss of material arising in the extraction procedure. An accumulation of inorganic polyphosphate (polyP) and inositol pyrophosphates is detected in all strains following development, as well as an increase in inositol pyrophosphates. A loss in cell extract material due to experimental procedures is detected in all KK2 agar strains, decreasing the observed levels of all inositol phosphate species analysed. Bands below InsP$_6$ correspond to different InsP$_5$ species as well as ATP and GTP.

A developmental time course highlights the synthesis and progressive accumulation of $InsP_7$ in the double knockout strain, as shown in **Figure 4.2**.

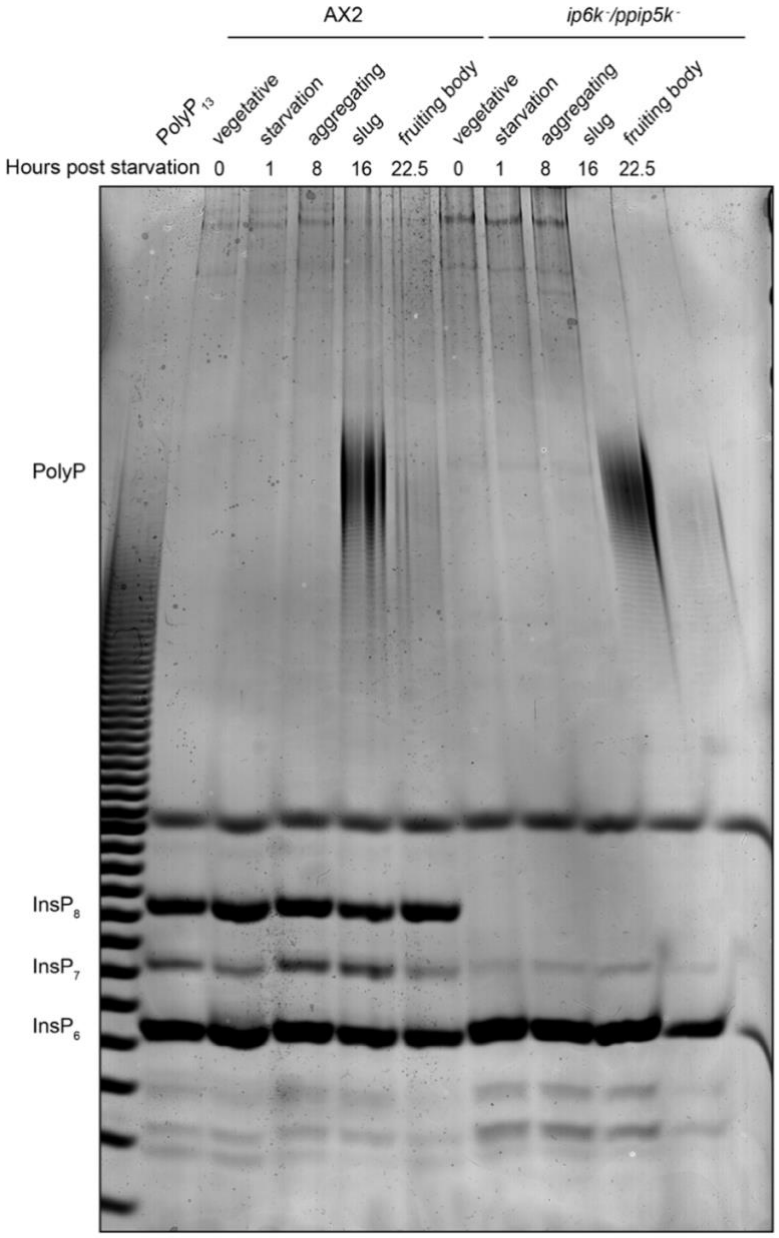

Figure 4.2. Developmental timecourse for the *D. discoideum* wild type and double knockout strains under standard conditions. Wild type AX2 and double knockout (*ip6k -/ppip5k -*) strains were analysed at different time points when developed under standard conditions a KK2-agar substrate. Levels of inositol pyrophosphates increase in both wild-type and *ip6k -/ppip5k –* strain as development progresses. Extraction of polyp is sub-optimal in the later stages of development due to experimental constraints.

4.2.2. Inositol phosphate levels during pseudo-development

The efficiency of extraction of polyP and inositol pyrophosphates is reduced at the later stages of *D. discoideum* development, in which the spore is being formed and becomes less accessible. This limitation was therefore bypassed by deploying an assay that arrests *D. discoideum* at the mound stage (R. Kay laboratory, personal communication). The phosphate-rich nature of KK2, the preferred starvation buffer for this model organism, prevented us from achieving a phosphate-starvation state. The developed assay would arrest the amoebae mid-development under different starvation conditions.

The initial candidate for phosphate starvation was MES, given its buffering range and that amoeba development under these conditions had previously proven successful in the laboratory. Development in water was added as a control since it should not accommodate pH changes. The wild type strains successfully achieved pseudo-development in the formulated assay. Development in both KK2 and H_2O showed PolyP production, as well as an increase in inositol pyrophosphate levels compared to those in the vegetative state. Interestingly, there was a complete depletion of polyP production when cells were developed in the MES buffer (**Figure 4.3**).

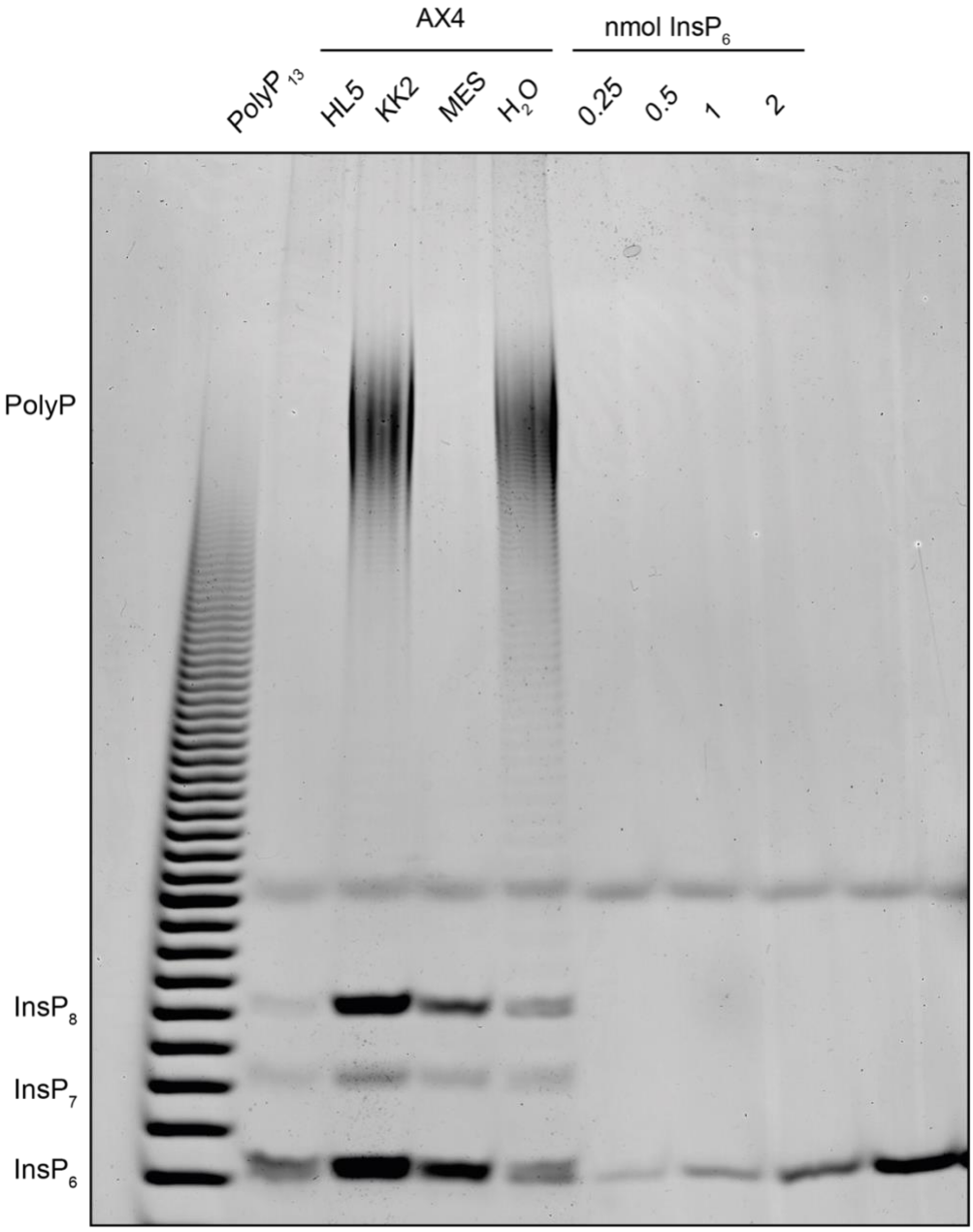

Figure 4.3. Pseudo-development of wild type *D. discoideum* in different buffers. Wild type AX4 strains were analysed following a pseudo-development consisting in the submersion of cells in different starvation buffers or water and resulting in arrest at the mound stage for 24 hours. A growth stage (HL5) sample is added as a control and different amounts of $InsP_6$ are used as a standard. PolyP production was detected in all development lanes except for in the case of MES.

To further investigate the source of this strong and interesting phenotype, different additional buffers were employed at the same pH. The similarity between the structures of MES and HEPES would provide structural-related information. The different pKas of HEPES and TRIS compared to MES would give us insights into the effects of the addition of titration salts during pH adjustment of the buffers. In order to obtain information on any potential links to inositol pyrophosphate production, the *ip6k -/ppip5k -* double knockout *D. discoideum* strain was also employed in these assays.

No depletion of PP-InsPs was achieved in the double knockout strain, even under the conditions of phosphate starvation during development (MES, HEPES, TRIS). Interestingly, the water control successfully followed development, highlighting the lack of necessity of buffering capacity of a given development solution (**Figure 4.4**). These results indicated the independence of PP-InsP synthesis by uncharacterised enzymes from extracellular phosphate.

All strains excluding those developed under MES were capable of polyP synthesis during pseudo-development. This indicated that the process of pH adjustment and the addition of salts to the development buffer would be trivial for the production of polyP. Interestingly, HEPES showed a decrease in polyP production when compared to TRIS, hinting at a potential structure-based inhibitory effect of MES.

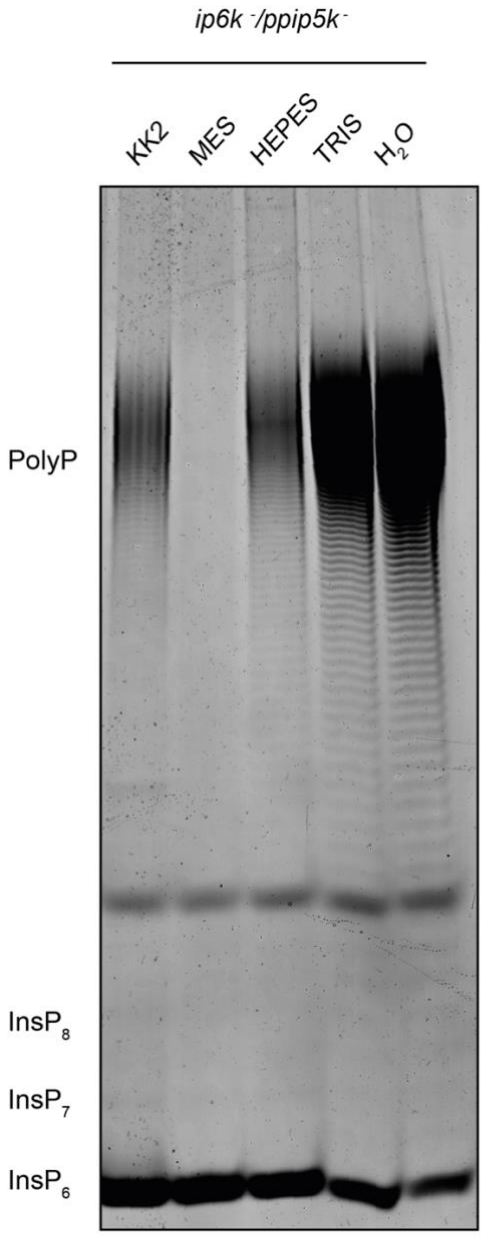

Figure 4.4. Pseudo-development of double knockout *D. discoideum* in different buffers. The double knockout (*ip6k -/ppip5k -*) was analysed following 24 hours of pseudo-development in different buffers and a water control. PolyP production was detected in all development lanes except for in the case of MES.

In order to test the hypothesis of an inhibitory effect of MES on polyP production during *D. discoideum* starvation, we proceeded to dilute different proportions of buffers with either MES or H_2O (**Figure 4.5**). PolyP

production was inversely proportional to MES concentration in the development buffer, somewhat independent of phosphate concentration. These results substantiated a detrimental effect of MES on polyP synthesis in the amoeba during development.

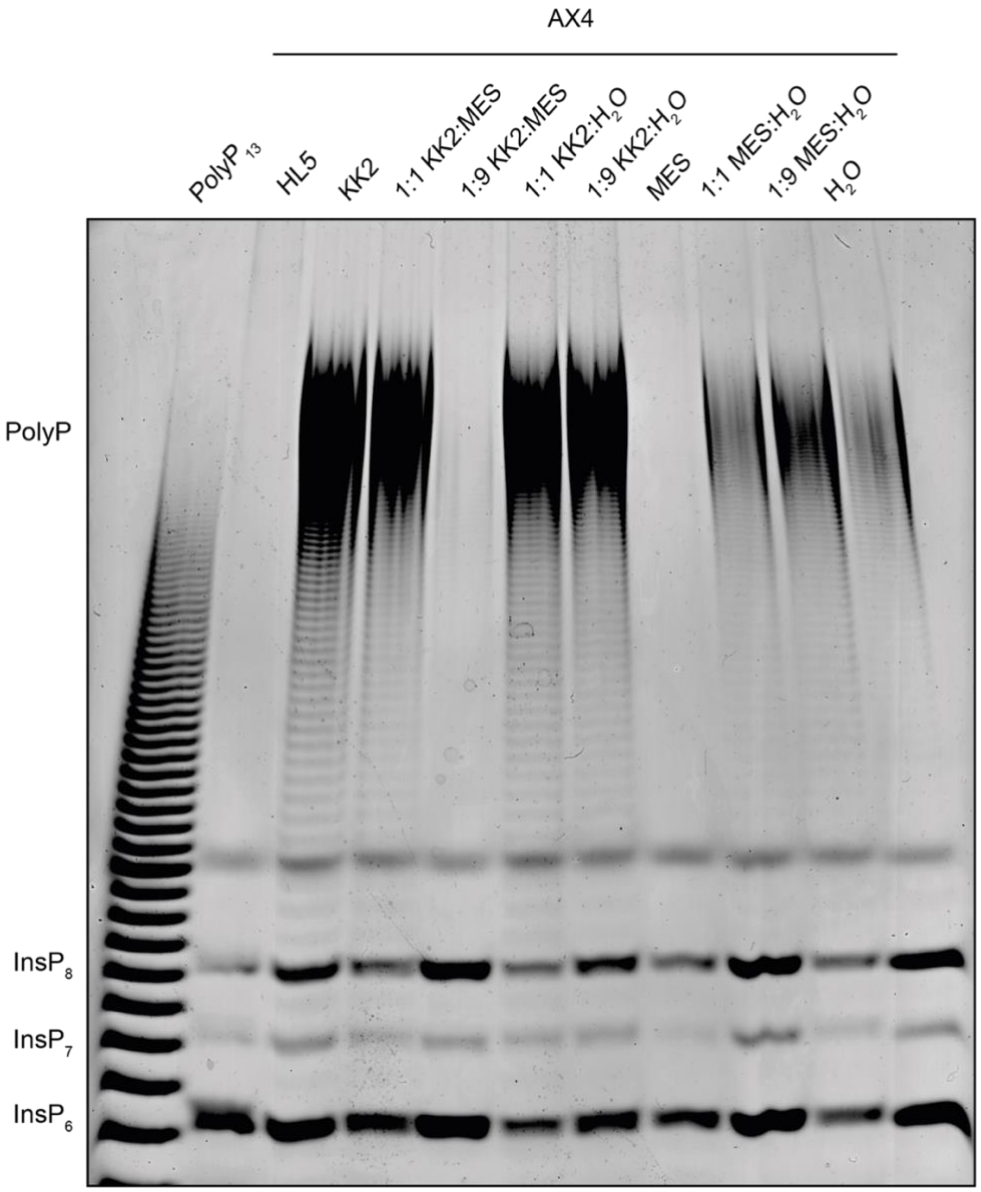

Figure 4.5. Pseudo-development of wild type *D. discoideum* in different buffer mixtures. The AX4 wild type strain was pseudo-developed for 24 hours in buffers of different MES concentrations. The concentration of synthesised PolyP increased inversely proportional to MES concentration in the buffer mixture. The H_2O only lane showed a reduced synthesis of PolyP versus expected levels, likely due to experimental variability.

4.2.3. Phenotypic characterisation of available mutants

All strains succeeded to follow development under standard conditions (KK2-agar) and form fruiting bodies, the final stage in *D. discoideum* development (**Figure 4.6**).

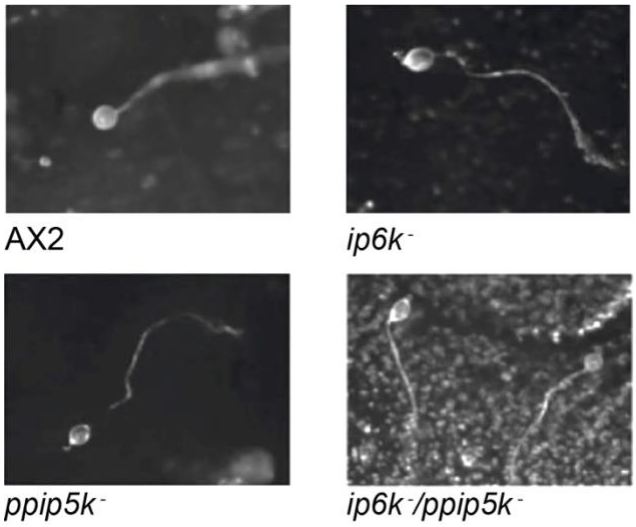

Figure 4.6. Fruiting bodies of wild type and available inositol phosphate mutant *D. discoideum* strains. The AX2 and mutant (*ip6k* -, *ppip5k* - and *ip6k* -/*ppip5k* -) strains were developed under standard KK2-agar conditions. Light microscopy images were obtained for each strain, showing no developmental phenotype.

To detect any developmental phenotype of the lack of *ip6k* and *ppip5k* that may have gone unnoticed by the quantification of inositol phosphate species, the process of development was examined under complete phosphate starvation. Since the absence of phosphate from agar used in development plates is not guaranteed, an alternative approach was undertaken. Cellulose filters can be submerged in a buffer and the resulting substrate can be employed for development assays. Despite variable differences in timing, not attributable to differing buffer conditions,

all strains completed development, culminating in the formation of fruiting bodies under phosphate starvation (**Figure 4.7**).

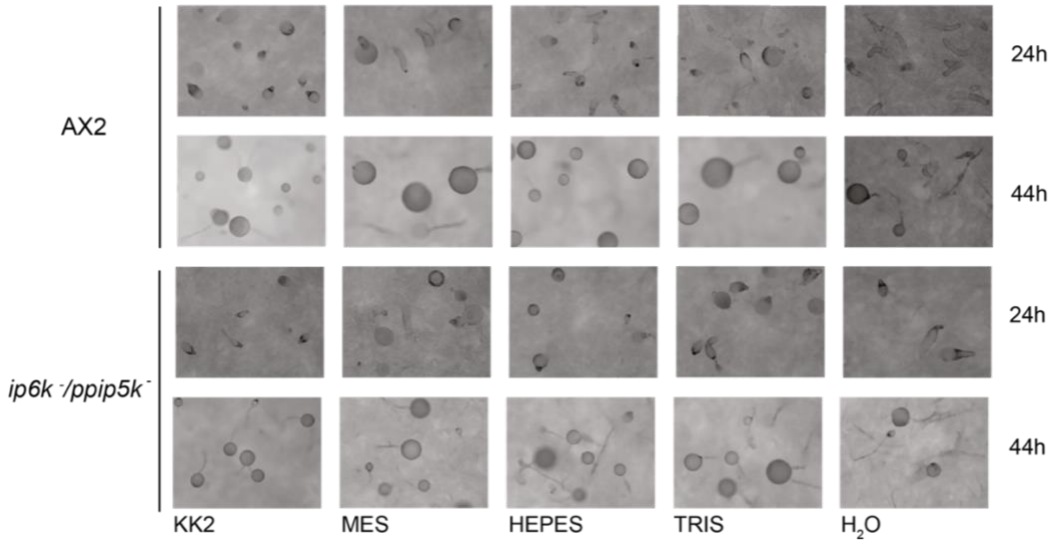

Figure 4.7. Fruiting bodies of wild type and double knockout *D. discoideum* strains. The AX2 and double knockout *ip6k-/ppip5k-* were developed in buffered (KK2, MES, HEPES, TRIS) and unbuffered (H_2O) cellulose filters and pictures were obtained. Developmental timings were inconsistently variable, and no phenotype was detected, even in the unbuffered H_2O conditions.

These results highlighted a lack of developmental phenotype from the deletion of homologous enzymes to those synthesising inositol pyrophosphates in human and yeast. It also brought to light the necessity of obtaining an amoeba strain completely devoid of inositol pyrophosphates for an expansion of their functional characterisation.

4.3. Discussion

The previously characterised (Pisani et al., 2014) increase in inositol pyrophosphate levels during development still held for the available knockout strains, reinforcing the developmental upregulation of inositol pyrophosphate production by alternative sources during *D. discoideum* development.

An analysis of the inositol phosphate concentrations under different developmental conditions demonstrated that extracellular phosphate availability does not act as a limiting factor for the upregulation of inositol pyrophosphate.

The inhibitory effect of MES on polyP production resulted in a serendipitous yet fruitful discovery. Structural insights reveal the difference between MES and HEPES (**Figure 4.8**). Such difference could be accountable for the inversely proportional synthesis of polyP when MES is employed as a starvation buffer for the social amoeba.

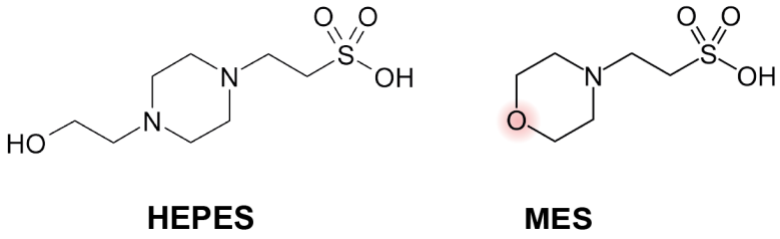

Figure 4.8. Chemical structure of HEPES and MES buffers. The similarity between MES (2-morpholin-4-ylethanesulfonic acid) and HEPES (2-[4-(2-hydroxyethyl)piperazin-1-yl]ethanesulfonic acid) structures resides in the carbon ring and the ethanesulfonic acid moiety. The oxygen in the morpholine ring of MES is likely responsible for the inhibitory effect of this buffer on PolyP synthesis, as the similarly structured HEPES does not have this effect.

A time limitation of this study resided in the lack of analysis of germination efficiencies of spores found in the last stage of development. Such an experiment could argue whether the developmental effect of a considerable pool of inositol pyrophosphates takes place at the germination level. However, to obtain findings that are not exclusive to the developmental process of germination in *D. discoideum*, the line of enquiry proceeded in an alternative direction.

The lack of an *ip6k -/ppip5k -* developmental phenotype in the process of fruiting body formation could be attributable to incomplete depletion of inositol pyrophosphates in the analysed strains. Hence, to identify the effect of cellular availability of inositol pyrophosphates, a full depletion of these was deemed necessary and therefore prioritised.

5. Inositol pyrophosphate synthesis in *D. discoideum* – *ipkA* and *ipkB*

5.1 Introduction

For the identification of additional sources of inositol pyrophosphates in *ip6k -/ppip5k -* amoeba different approaches could be considered. An unbiased approach could reside in the biochemical purification of the enzymes required through means of an affinity column. Since previously uncharacterised inositol phosphate kinase genes were present in the *D. discoideum* genome, a focused approach was selected.

Two genes, renamed as *ipkA* and *ipkB*, were identified as candidates for the function of inositol pyrophosphate synthesis in the social amoeba. Both are members of the IPK superfamily and lack clear mammalian or yeast homologues, preventing the prediction of their precise catalytic function.

The Genome-Wide *Dictyostelium* Insertion (GWDI) library, with mutant *D. discoideum* strains, would be a first resource for obtaining of *ipkA* and *ipkB* knockout strains. The GWDI project provides a collection of over twenty thousand mutants for insertions in given genes of interest. These have often not been employed for experimental approaches and need further validation of their particular mutation.

A drawback of this library is the genetic background of the strains, AX4. This differs from wild type and inositol phosphate mutant strains available, which have an AX2 background. For optimal laboratory practice and the accurate comparison of inositol phosphate levels and phenotypes across different mutants, all experiments should be performed on a single genetic background. Despite this limitation, the availability of mutants could be a valuable asset in determining *ipkA* and *ipkB* function.

An additional short-term approach for the elucidation of *ipkA* and *ipkB* involvement in the synthesis of inositol pyrophosphates is gene silencing. This method of transcriptionally repressing protein expression could lead to a substantial decrease in inositol pyrophosphate synthesis, given that inositol pyrophosphate synthesis is not limited by external phosphate availability and that internal factors seem to be at play. This method could be particularly efficient if one of these two enzymes could be silenced on a mutant background of the other, resulting in a combinatorial decrease in total IPK family protein expression.

For obtaining stable *ipkA* and *ipkB* knockout lines, homologous recombination is often employed. In this work, we resourced to a recently developed CRISPR/Cas9 technique in the social amoeba, given its experimental accessibility and claimed high efficiency in the generation of mutant strains.

5.2 Results

5.2.1. GWDI strain analysis

To characterise the cellular function of *ipkA* and *ipkB*, knockouts from the Genome-Wide *Dictyostelium* Insertion (GWDI) project were ordered. These mutants are in a different *D. discoideum* background (AX4) and usually their loss of function mutation remains unverified. Nonetheless, their availability could prove to be instrumental for looking into the function of these two genes.

Under growth conditions, there was no substantial difference in the levels of inositol pyrophosphates between wild type and GWDI mutants. No difference was seen either under KK2 pseudo-development (**Figure 5.1**).

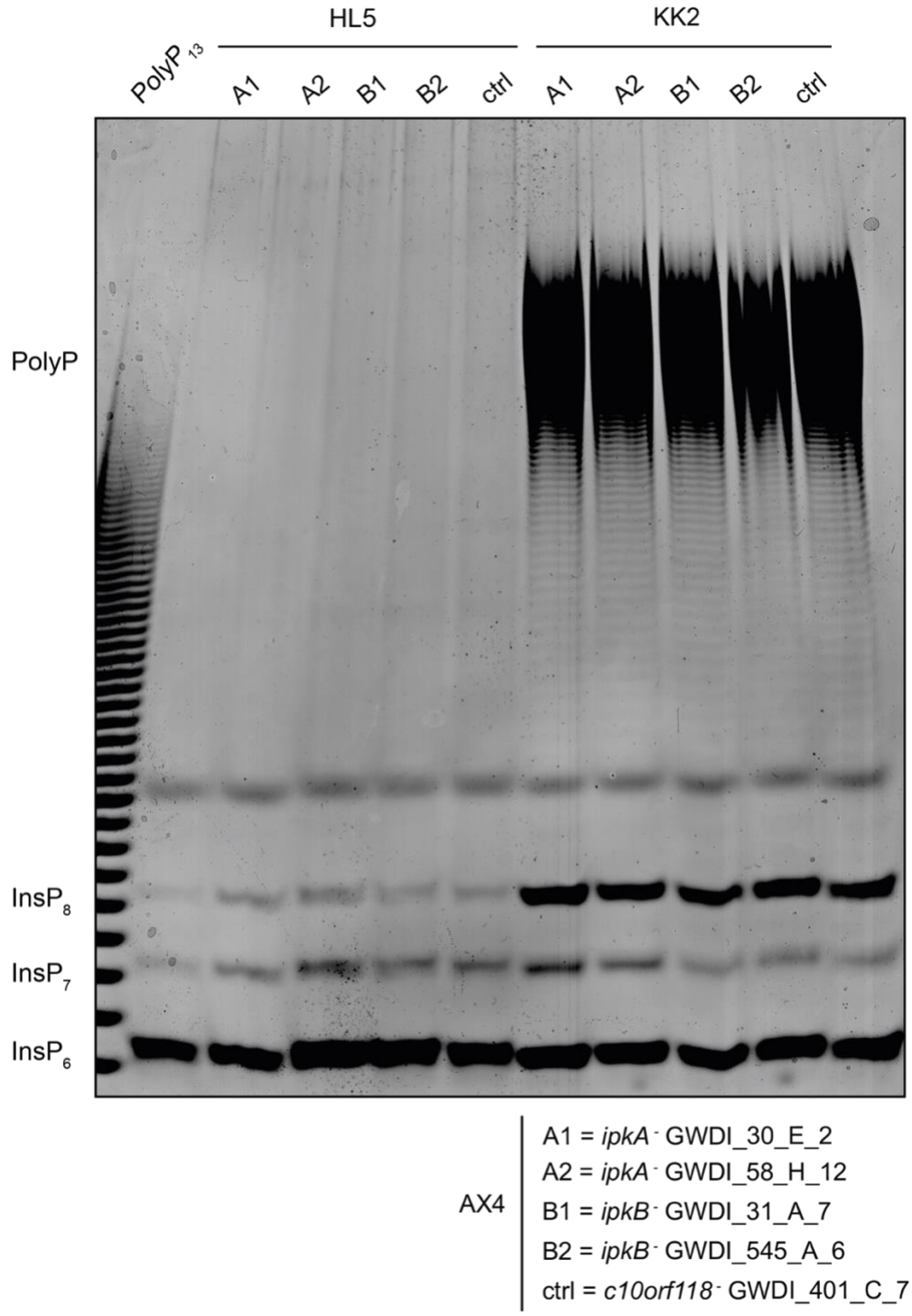

Figure 5.1. Inositol phosphate profiles of selected GWDI mutants in the vegetative and KK2 pseudo-development stages. Candidate GWDI *ipkA* and *ipkB* loss of function mutants analysed by PAGE in the growth stage and after having followed starvation in KK2 buffer. No clear differences are observed at either vegetative or KK2 pseudo-development stage.

It was under phosphate starvation during MES pseudo-development that the A1 strain (GWDI_30_E_2) showed a reduction in $InsP_8$ levels (**Figure 5.2**).

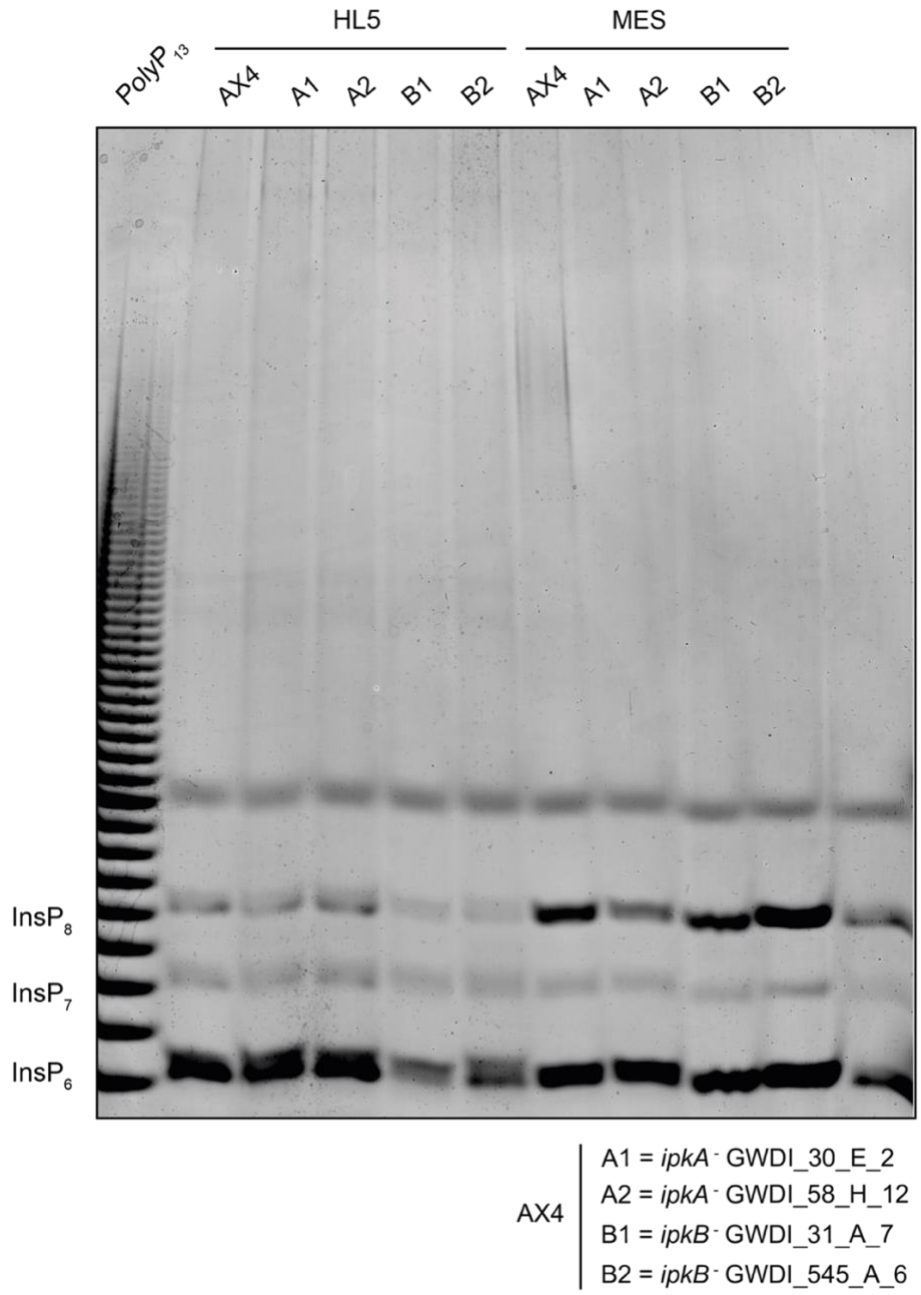

Figure 5.2. Inositol phosphate profiles of selected GWDI mutants in the vegetative and MES pseudo-development stages. Candidate GWDI *ipkA* and *ipkB* loss of function mutants analysed by PAGE in the growth stage and after having followed starvation in MES buffer. No clear differences are observed at the vegetative state, while a decrease in $InsP_8$ is detected in the A1 (GWDI_30_E_2) mutant.

5.2.2. Silencing approach and silencing of GWDI strains

Given the possibility that ipkA and ipkB may act through a synchronous mechanism to co-produce a larger pool of inositol pyrophosphates, a combinatorial silencing approach was undertaken. This plasmid-based method, described in **Figure 5.3** would rapidly yield silenced strains for the investigation of their inositol phosphate levels.

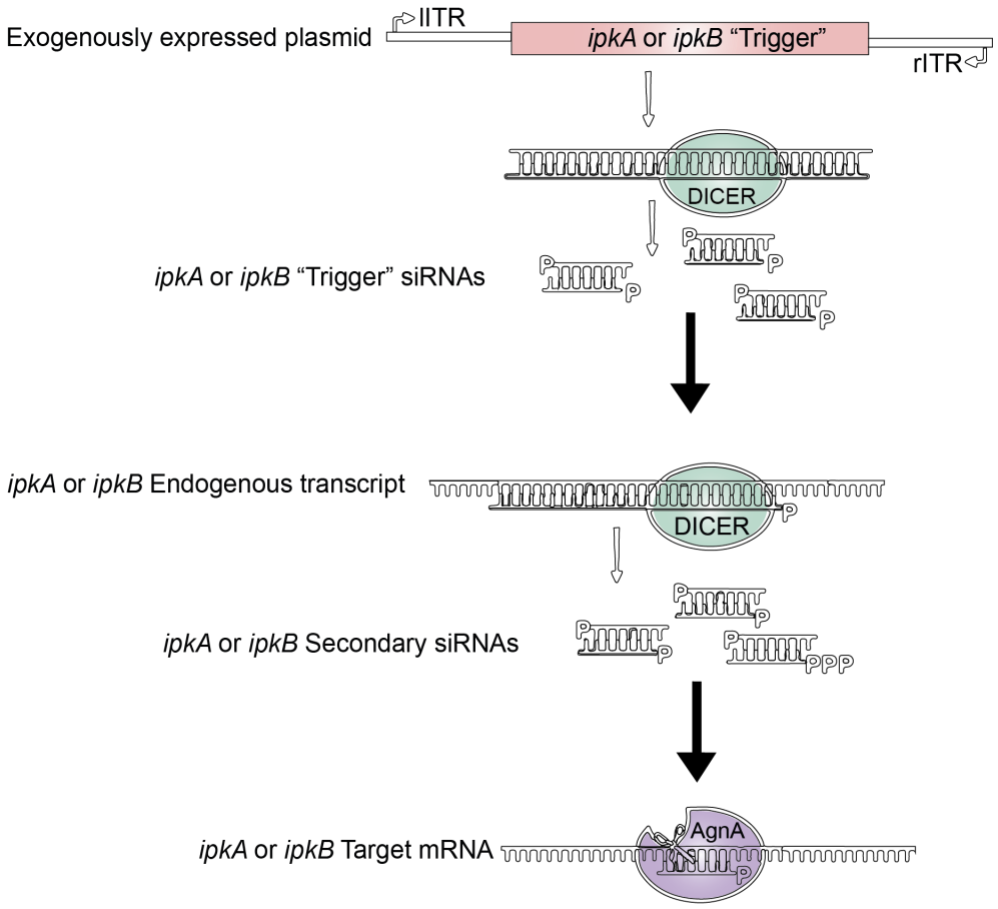

Figure 5.3. Schematic of the plasmid-based silencing strategy. The Dicer/AgnA system for RNAi is depicted. Trigger sequences were designed for the silencing of *ipkA* or *ipkB* respectively. Trigger sequences are expressed from left and right promoters (lITR,and rITR) resulting in a double stranded RNA that is targeted by dicer to form Trigger siRNAs. SiRNAs target endogenous enzyme transcripts which are cleaved by AgnA resulting in downregulation of ipkA or ipkB gene expression. Figure adapted from Friedrich et al. 2015.

Expression of the *ipkB* silencing plasmid in the *D. discoideum* GWDI strains A1 and A2 did not seem to result in a reduction of inositol pyrophosphate levels (**Figure 5.4**).

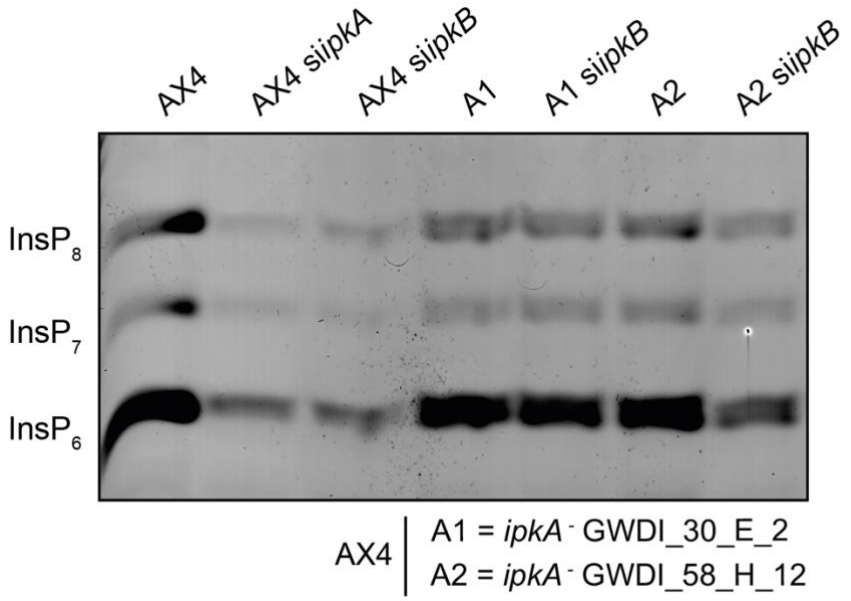

Figure 5.4. Gene silencing in wild type and candidate GWDI *ipkA*- strains. Plasmid-based silencing of *ipkB* in wild type AX4 and GWDI mutants A1 and A2. qPCR experiments confirming the effectiveness of gene knockdown were not obtained. No clear decrease in inositol pyrophosphate levels was observed in the wild-type or mutant strains analysed.

Expression of the *ipkA*-silencing plasmid in the GWDI B1 and B2 strains did result in a reduction of $InsP_8$ levels in the amoeba (**Figure 5.5**), pointing at evidence for its involvement in inositol pyrophosphate synthesis.

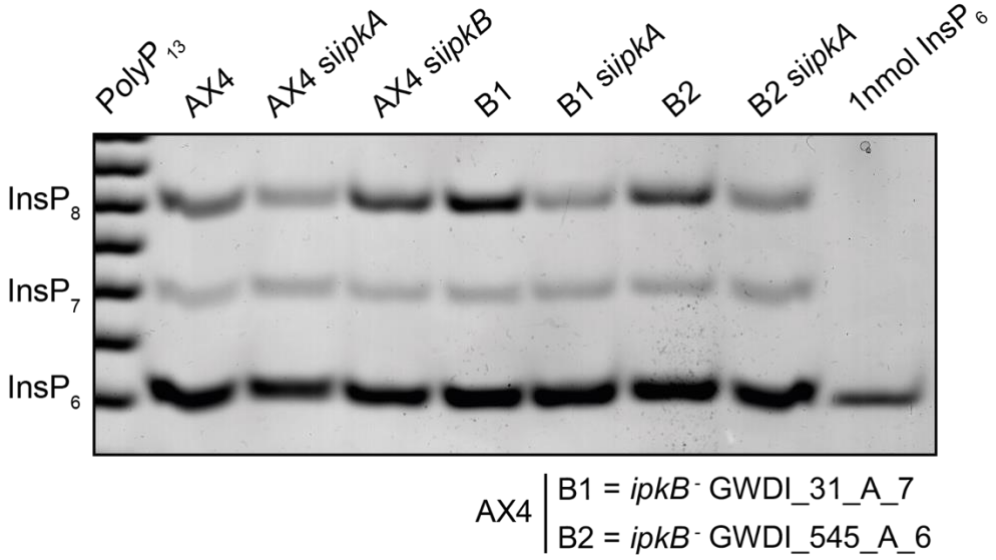

Figure 5.5. Gene silencing in wild type and candidate GWDI *ipkB*- strains. Silencing of *ipkA* in the wild type AX4 and both B1 and B2 GWDI mutants resulted in a decrease in $InsP_8$ levels. There seemed to be no cumulative effect on inositol pyrophosphate levels in the silencing of *ipkA* in the candidate *ipkB*- mutants B1 and B2.

Due to the inconsistent results from RT-qPCR transcript quantification (data not shown), and due to the still incomplete depletion of inositol phosphate levels in the silenced GWDI strains, a non-transient approach was undertaken.

5.2.3. Knockout generation

The GC-rich nature of the *D. discoideum* genome (Eichinger et al., 2005), as well as its high-efficiency homologous recombination (Katz and Ratner, 1988), had long halted the progress in the application of CRISPR/Cas9 methods in the social amoeba. We deployed a recently published “all-in-one” vector system(Sekine et al., 2018) (**Figure 5.6**) for the generation of novel mutant strains.

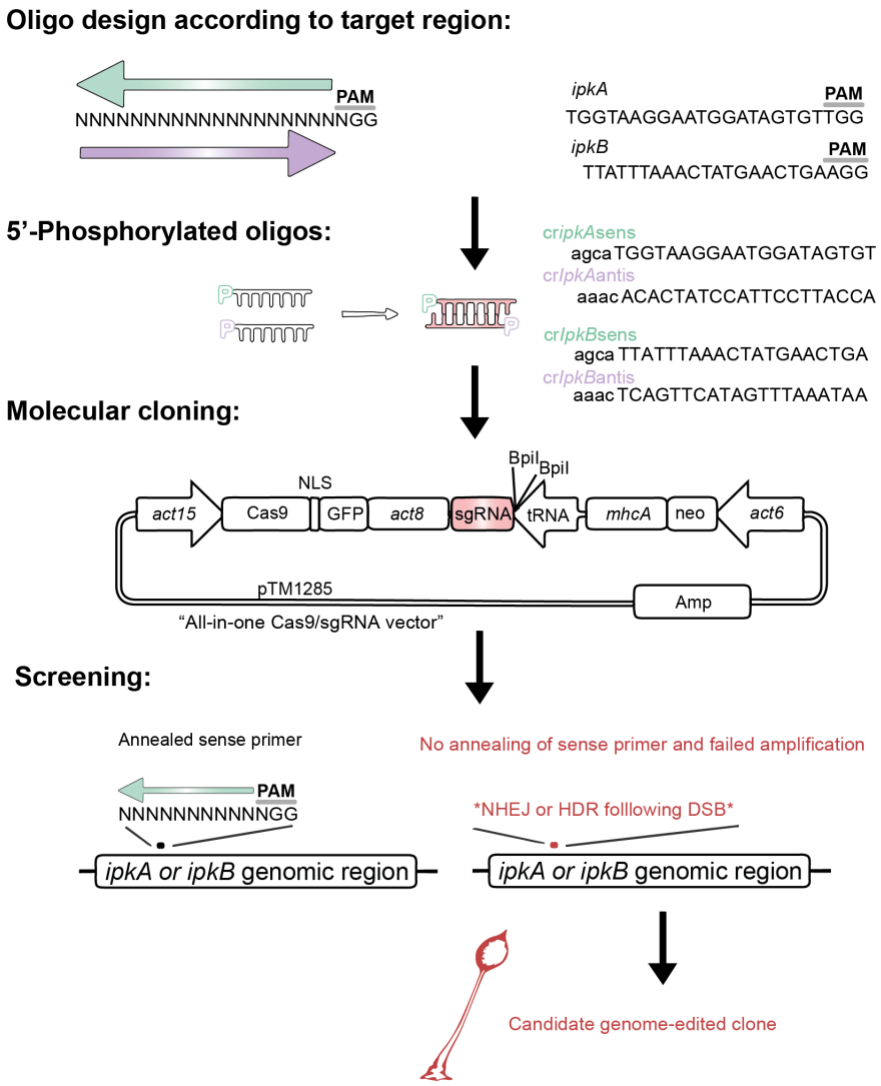

Figure 5.6. Cas9/sgRNA knockout generation pipeline in *D. discoideum*. Sense and antisense oligos are designed according to a PAM-comprising target region selected using Rgenome's Cas-Designer. The 5' phosphorylated oligos are ordered and cloned into the all-in-one Cas9/sgRNA vector following annealing. Positive transformed clones are detected by the lack of DNA amplification in a polymerase chain reaction using a sense and screening primer. Genome editing following DNA double-strand break (DSB) upstream of the PAM sequence may occur in the form of non-homologous end joining (NHEJ), leading to insertions and deletions (indels) or homology-directed repair (HDR) in the presence of a donor construct. In the case of genome editing, annealing of the sense primer will be prevented and failed amplification will indicate the likelihood of a mutant *D. discoideum* clone. A summary of this method is found in (Muramoto et al., 2019; Sekine et al., 2018).

Following transformation of the Cas9/sgRNA vector and following selection process, twelve clones each were screened from *ipkA* and *ipkB* plates. In the case of *ipkB*, there was no clear reduction in inositol pyrophosphate levels in the candidate clones screened by PCR (**Figure 5.7**).

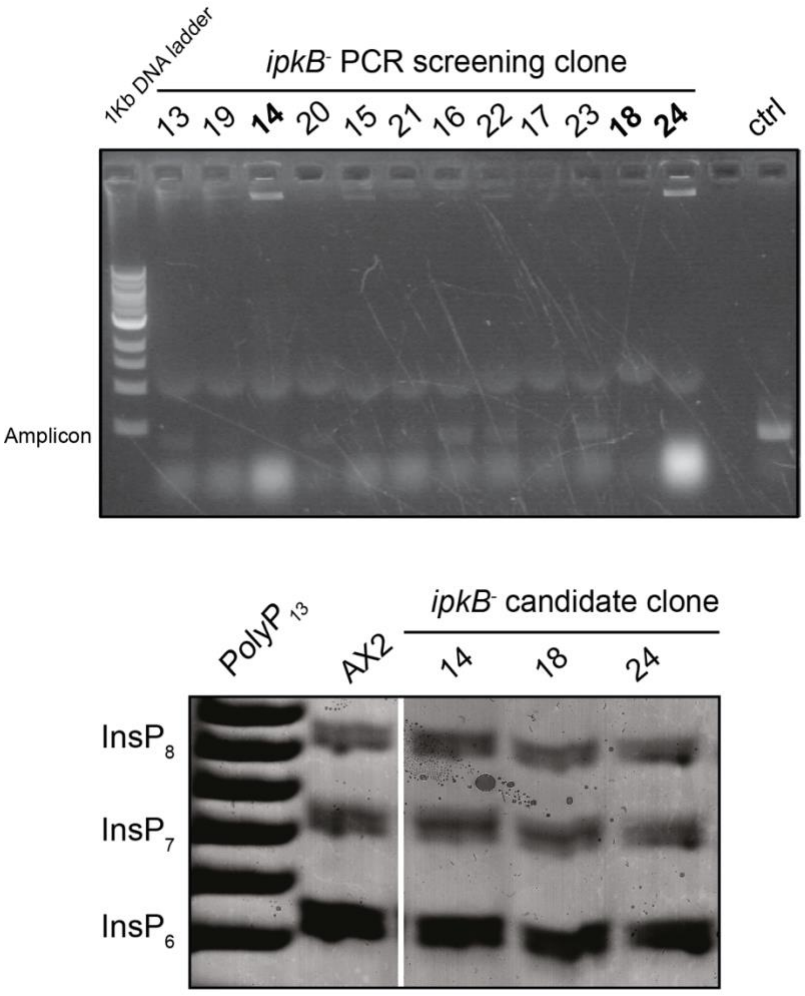

Figure 5.7. Cas9/sgRNA *ipkB* knockout candidates *D. discoideum*. Screening by PCR (top image) revealed weak amplification of the amplicon band (see ctrl: control lane) in clones 14, 18 and 24. However, inositol profiling (bottom image) of these amoeba strains revealed no substantial difference in inositol phosphate levels in the *ipkB* knockout candidate clones.

PCR screening in the case of *ipkA* yielded a higher number of candidate clones (**Figure 5.8**). Upon analysis of these by PAGE, a remarkable depletion of $InsP_8$ was detected in 4 out of 5 clones. Such reduction in $InsP_8$ levels provided evidence for the role of IpkA as a previously uncharacterised source of inositol pyrophosphates in the social amoeba.

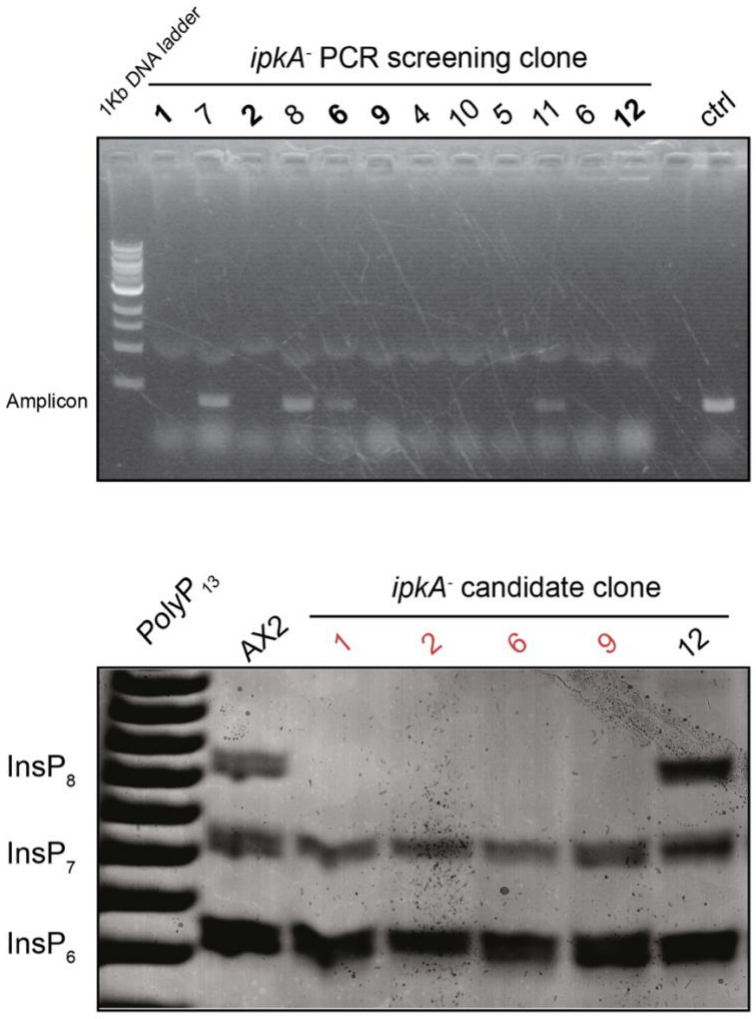

Figure 5.8. Cas9/sgRNA *ipkA* knockout candidates *D. discoideum*. Screening by PCR (top image) revealed weak amplification of amplicon (see ctrl: control lane) in clones 1, 2, 6, 9 and 12. Inositol profiling (bottom image) of these amoeba strains revealed a drastic increase in $InsP_8$ in all candidate clones excluding clone 12. The uniformity and strength of the obtained phenotype argues for an effective gene editing in these clones.

5.3. Discussion

To identify the additional source of inositol pyrophosphates in the social amoeba, the readily available mutant strains were initially analysed. Due to time limitations, the verification of *ipkA* - and *ipkB* - GWDI mutants as *bona fide* knockouts was not achieved. Instead, silencing provided increasing evidence towards the involvement of *ipkA* - and *ipkB* - in inositol pyrophosphate synthesis, without supporting evidence for their action *in tandem*. The time-efficient analysis of these strains provided evidence of the potential involvement of these genes in the synthesis of inositol pyrophosphates and directed posterior lines of investigation.

Evidence regarding the role of *ipkB* following generation of CRISPR mutants remained unclear and, and it was discontinued due to time limitations. However, the generation of mutant lines by CRISPR/Cas9 provided clear evidence for the involvement of *ipkA* in the synthesis of $InsP_8$ in *D. discoideum*. This striking phenotype is not achieved in the *ppip5k* - mutant, that shows a small reduction in $InsP_8$ levels, which still accumulate during development. Additionally, the partially purified enzymatic activity described by (Laussmann et al., 1997) was that of an enzyme synthesising $InsP_8$ in the amoeba and with a size of approximately 40 kDa, consistent with IpkA (36 kDa) and in contrast with Ppip5k, which has a molecular weight of 56 kDa (**Table 1.1.**).

The fact that a development-dependent increase in $InsP_8$ is seen in *ppip5k* - points at the involvement of *ipkA* in this process, given that a large majority of this inositol pyrophosphate seems to be synthesised by this enzyme in the social amoeba, and that the expression of this enzyme is developmentally upregulated (Livermore, 2016). An $InsP_8$-synthesising catalytic function is not expected from enzymes of the IPK family, which either phosphorylate the inositol scaffold (IPMKs, IP3-3Ks) or add a pyrophosphate moiety in the synthesis of $InsP_7$ (IP6Ks).

One could speculate that *ipkA* is responsible for the synthesis of isomeric forms of $InsP_8$ that are only specific to *D. discoideum*, given its lack of clear homologues outside Amoebozoa. When looking at closely related species in Amoebozoa, *H. pallidum* and has been previously described to synthesise a large pool of 5,6-$InsP_8$ and a smaller one of 1,5-$InsP_8$ (Laussmann et al., 2000).

The study by Laussmann *et al.* described 5,6-$InsP_8$ as the only $InsP_8$ isomer present in *D. discoideum*. Since inositol pyrophosphate concentrations (expressed as nmol per cell number) are higher in *H. pallidum*, the analysis by Laussmann *et al.* could have precluded the identification of isomers present in lower concentrations in *D. discoideum*, and only detecting those in its close relative within Amoebozoa. As detected in this study by the highly sensitive C-13 NMR, a larger array of different inositol pyrophosphate isomers is present in *D. discoideum*.

It can therefore be hypothesised that IpkA is responsible for the synthesis of the largest pool of inositol pyrophosphates in *D.* discoideum, taking the form of 5,6-$InsP_8$ and that other isomers present in the social amoeba, likely including the isomer described in humans (1,5-$InsP_8$), would be synthesised in lower concentrations by Ppip5k and other enzymes (**Figure 5.9**).

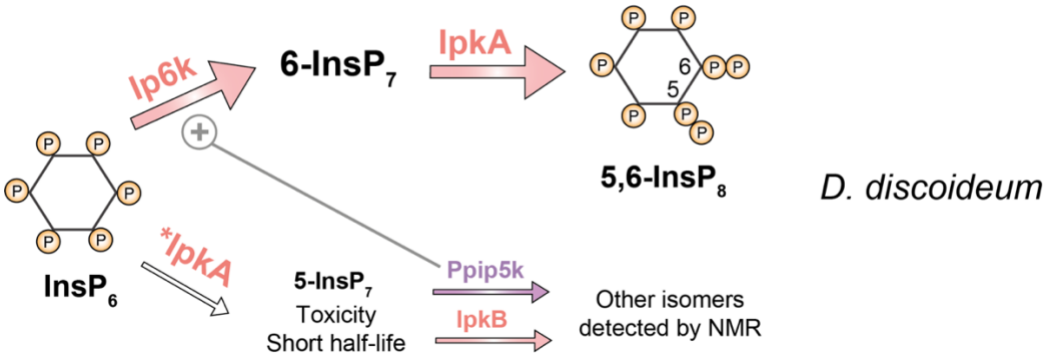

Figure 5.9. Current hypothesis for inositol phosphate synthesis in *D. discoideum*. A selective pressure (5-InsP$_7$ toxicity) would have resulted in the adaptive evolution of *D. discoideum* IP6K homologue as a 6-kinase instead of a 5-kinase. This would have been coupled to the catalytic specification of the expanded IPK members IpkA and IpkB. IpkA would have evolved as a 5-kinase capable of using 6-InsP$_7$ as a substrate to generate the likely predominant 5,6-InsP$_8$ isomer in *D. discoideum*. Any catalytic activity of ipkA phosphorylating InsP$_6$ at position 5 would have generated 5-InsP$_7$. IpkB would have evolved to use 5-InsP$_7$ as a substrate to result in its short half-life and lack of detection by NMR. Ppip5k would have used any 5-InsP$_7$ to likely generate 1,5-InsP$_8$, the isomer present in yeast and mammalian cells. A Ppip5k-dependent increase in Ip6k activity could act as a buffering mechanism to shift the synthesis of InsP$_7$ during development towards 6-InsP$_7$ and its use by IpkA to generate the primary *D. discoideum* isomer 5,6-InsP$_8$.

The presence of cellular 6-InsP$_7$, detected by NMR in the wild type amoeba, would have been coupled to the specialisation of an IPK enzyme capable of using this isomer as a substrate. This enzyme would be IpkA, given its in vitro specificity (Livermore, 2016) for 6-InsP$_7$ and its involvement in the majority of InsP$_8$ synthesis in the social amoeba (**Figure 5.8**).

Given the lack of clear *ipkA* homologues, excepting those in closely related amoebozoan species, one could assume that the specificity of this

IPK member developed posterior to the branching of Amoebozoa-Opistokhonta from a common eukaryotic ancestor.

Both 5-$InsP_7$ and 1-$InsP_7$ have been suggested to be present in human and yeast cells in varying proportions (Lin et al., 2009), whereas a single isomer of 4/6-$InsP_7$ is detected by NMR in the social amoeba. The hypothesis of 5-$InsP_7$ toxicity in the amoeba would account for the required selective pressure driving the catalytic specialization of *D. discoideum* Ip6k as a carbon-6 pyrophosphorylating enzyme (**Figure 5.10**).

The primary $InsP_8$ isomer in *D. discoideum* is 5,6-$InsP_8$, as previously detected by NMR (Laussmann et al., 1996). Other isomers detected by the highly sensitive ^{13}C-NMR technique are expected to be present in lower concentrations. Synthesis of certain amounts of 5-$InsP_7$ could be mediated by IpkA using $InsP_6$ as substrate. This isomer is not present in the $InsP_7$ NMR spectrum so its synthesis would require a rapid conversion to $InsP_8$ by different enzymes.

Pyrophosphorylation of 5-$InsP_7$ at position 1 by *D. discoideum* Ppip5k could resolve the presence of a pyrophosphate at position 1 on the C-13 NMR spectrum of $InsP_8$ (**Figure 3.2**). It is worth noting that the presence of a 2-PP in $InsP_8$ species purified from the amoeba, as detected by NMR (**Figure 3.2**), was unprecedented. We could speculate that such pyrophosphorylation could result from the action of IP5-2K (an enzyme evolutionarily derived from IPK (Gonzalez et al., 2010)) in order to reduce 5-$InsP_7$ concentrations in the amoeba.

Synthesis of 5,6-$InsP_8$ requires the presence of IpkA, since the *ipkA* knockout strain is depleted of $InsP_8$. This synthesis of $InsP_8$ could be regulated indirectly by *ppip5k* since the *ppip5k* knockout strain shows a 50% reduction in $InsP_8$ as well as $InsP_7$ concentration. The reduction in $InsP_7$ levels in *ppip5k* - amoeba is unlikely Ppip5k-generated, since the presence of 1-$InsP_7$ is not detected by NMR. An upregulation of Ip6k

activity by *ppip5k* would increase the levels of its product (6-InsP$_7$), increasing substrate availability for the synthesis of 5,6-InsP$_8$ by IpkA. Therefore, the existence of a *ppip5k* function in promoting and sustaining Ip6k activity can be hypothesised and would account for the detected *ppip5k* knockout phenotype.

The upregulation of InsP$_7$ synthesis by *ppip5k* could act as a buffering mechanism for achieving the correct isomeric balance throughout development. IpkA expression is upregulated upon starvation (Livermore, 2016), so one would expect a higher synthesis of undesirable 5-InsP$_7$ in the amoeba at this stage. The coupling of 5-InsP$_7$ synthesis to its phosphorylation by Ppip5k would ensure a decrease in 5-InsP$_7$ levels. A subsequent Ip6k upregulation would ensure and an increase in 6-InsP$_7$ levels to supply substrate for an increased IpkA activity. Hence, the induction of Ip6k activity by *ppip5k* would shift the pool of available InsP$_7$ towards 6-InsP$_7$, the isomer that IpkA can use to generate the predominant 5,6-InsP$_8$ pool in the amoeba.

Two possibilities could account for the regulation of Ip6k by *ppip5k*: a product-dependent or a product-independent one. In a product-dependent scenario, fortuitous synthesis of a detrimental levels 5-InsP$_7$ would be followed by Ppip5k phosphorylation, generating 1,5-InsP$_8$ in *D. discoideum*. This isomer is found in humans and yeast, and partially detected in the closely related amoeba *H. pallidum*. The presence of 1,5-InsP$_8$ could have an effect on Ip6k activity, leading to an increase in Ip6k-generated InsP$_7$ and, in turn, an increase in IpkA-generated InsP$_8$.

The following rationale supports the product-dependent mode of upregulation of ipkA by Ppip5k. Mammalian and yeast cells without *ppip5k* are depleted of InsP$_8$ and show an accumulation of its precursor InsP$_7$. The amoeba strain *ipkA* $^-$ is depleted of InsP$_8$ and displays no accumulation of the InsP$_7$ precursor. If indeed, amoeba Ip6k activity relies on *ppip5k* using IpkA-generated 5-InsP$_7$ as a substrate, *ipkA* $^-$ would lack

the substrate necessary for Ppip5k to upregulate Ip6k activity. The failed upregulation of Ip6k activity *ipkA* - *D. discoideum* strain would be detected as a lack of accumulation of the $InsP_7$ substrate required for $InsP_8$ synthesis.

IpkB is seen to phosphorylate 5-$InsP_7$ specifically in vitro (Livermore, 2016), an isomer that is not found in the wild type amoeba, as described by NMR (**Figure 3.2**). Conversion of any undesired levels of 5-$InsP_7$ to $InsP_8$ by IpkB could lead to the generation of a specific isomer have a yet unknown structure and activity. To further investigate IpkB function, a *ppip5k* knockout strain could be employed, given that IpkB would be expected to deal with the majority of 5-$InsP_7$ conversion to $InsP_8$ in a *ppip5k* - genetic background.

The *ip6k -/ppip5k* - strain is not completely depleted of $InsP_7$, implying an alternative enzymatic source. Such enzyme could be IpkA, generating tolerated levels of 5-$InsP_7$. A more likely candidate would be IpkB. Its upregulation could act as a form of compensation to achieve $InsP_7$ levels required for basic cell function.

This account of the results obtained would argue for the adaptive evolution of Ip6k in *D. discoideum* as a 6-kinase instead of a 5-kinase. This would account for the description of amoeba and human/yeast IP6Ks as heterofunctional homologues (**Figure 5.10**). Position 6 of the inositol ring is used by the IPK family member IPMK, perhaps even for pyrophosphorylation as demonstrated *in vitro* (Saiardi et al., 2001b). Evolution of Ip6k as a 6-kinase in the amoeba would be coupled to the retention of expanded IPK members and their evolution as and IpkA (5-kinase recognising 6-$InsP_7$ to generate 5,6-$InsP_7$) and IpkB (5-$InsP_7$ kinase). The presence of IPK members with the main function cellular of $InsP_8$ synthesis is unprecedented and had thus far been reserved for PPIP5K members, turning IpkA/IpkB and PPIP5K into analogues (**Figure 5.10**).

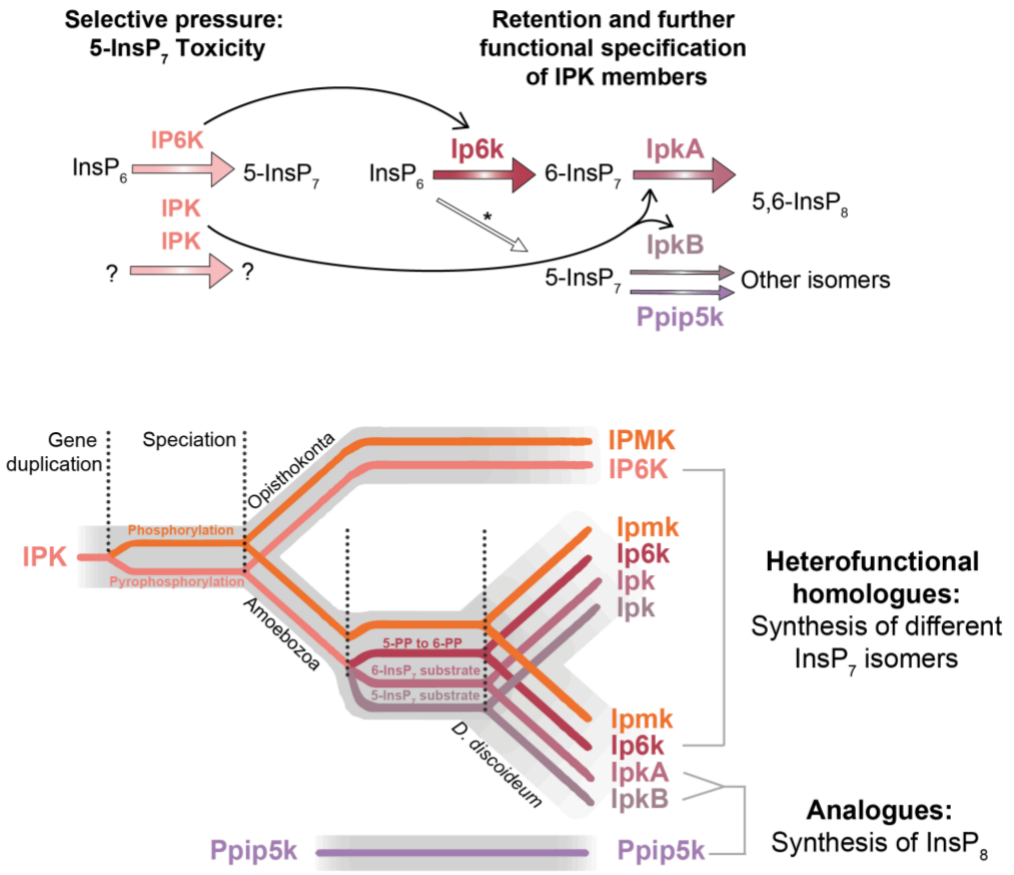

Figure 5.10. Schematic hypothesis for the evolution of inositol phosphate synthesis in *D. discoideum*. An expansion of the IPK family would have been seen in *D. discoideum* and higher eukaryotes. A further expansion of pyrophosphorylating IPK members would have occurred in the social amoeba. Selective pressures would have evolved Ip6k as a 6-InsP$_7$-synthesising enzyme, turning *D. discoideum* and *H. sapiens* IP6K members into heterofunctional homologues. An expanded IPK member (IpkA) would have specialised to use this as a substrate, replacing Ppip5k for the synthesis of a major InsP$_8$ pool in the amoeba. Another expanded IPK member, IpkB would have evolved to use 5-InsP$_7$ as a substrate to decrease the cellular concentration of this isomer. Both IpkA and IpkB would have become analogues of Ppip5k, due to their primary involvement in InsP$_8$ synthesis, a function previously undetected in the IPK family.

The discovery of IPK members with the primary function of InsP$_8$ synthesis therefore raised a question in terms of the emergence of a

PPIP5K activity. If the emergence of $InsP_8$ synthesis in IPK families was widespread, it could have preceded the emergence of PPIP5K enzymes. It could be further speculated that the emergence of the highly specific and tightly regulated bifunctional PPIP5K activity could have turned certain IPK members redundant in the synthesis of $InsP_8$, with exceptional cases in which the specificity of the isomers generated by IPK enzymes poses a functional advantage and allows retention of amplified IPK genes.

Hence, to identify broader catalytic activities of IPK members across eukaryotes and couple their emergence to the presence of other inositol phosphate kinase families, an evolutionary approach was required.

6. Evolution of the inositol phosphate kinase pathway

6.1. Introduction

Given that the physiological catalytic activity of IpkA was detected as the synthesis of $InsP_8$, a function not attributed to IPK family enzymes, an evolutionary approach was necessary to understand the evolution of the inositol phosphate code (Saiardi, 2017). Such an approach would dissect the established definitions of inositol phosphate kinase catalysis and aid in our understanding of the multiplicity of inositol phosphate isomers present in the social amoeba.

For this analysis, the entire inositol phosphate pathway had to be considered, given that functional redundancies would be coupled to the emergence of kinase activities across all families. The integration of our knowledge from all 4 families of inositol phosphate kinases was also required to accurately depict the development of new catalytic activities.

6.2. Results

6.2.1. Identification of new members

In order to further locate ipkA evolutionarily, due to its lack of clear mammalian or yeast homologues, a comparative evolutionary approach was undertaken. The initial approach, which recapitulated previous attempts in the lab, resided in the collection representative inositol phosphate kinases across available sequences. The different genomes were scored based on the number of members for each of the inositol phosphate kinase family.

An initial collection of sequences involved members of eukaryotic organisms, since the occurrence of inositol phosphate kinases in the tree of life had been traced to the origin of the eukaryotic cell (Irvine and Schell, 2001; Livermore et al., 2016b). Only recently, an ITPK1 member was detected in an archaeal organism (Desfougères et al., 2019), which was hence included in this study.

An investigation of viral and bacterial genomes revealed the presence of inositol phosphate kinase family members, previously dismissed by the literature (Irvine and Schell, 2001; Livermore et al., 2016b). Representatives from these were therefore included in this study.

Table 6.1 shows the representative species analysed in this study along with a respective scoring for the presence of IPK, IPK1, ITPK1 and PPIP5K family members in their genomes.

Table 6.1. Inositol phosphate kinase members across different species

Other	Domain	Eukaryotic Subkingdom	TaxID	Species	Abb.	IPK	IPPK	ITPK1	PPIP5K
Life	Eukaryota	Opisthokonta	6239	*Caenorhabditis elegans*	Ce	5	1	0	1
			5207	*Cryptococcus neoformans*	Cn	3	1	0	1
			7955	*Danio rerio*	Dr	10	1	2	3
			7227	*Drosophila melanogaster*	Dm	4	1	0	1
			9606	*Homo sapiens*	Hs	7	1	1	2
			6087	*Hydra vulgaris*	Hv	5	1	3	3
			10090	*Mus musculus*	Mm	7	1	1	2
			4932	*Saccharomyces cerevisiae*	Sc	2	1	0	1
			4896	*Schizosaccharomyces pombe*	Sp	2	1	0	1
		Amoebozoa	44689	*Dictyostelium discoideum*	Dd	4	1	1	1
			5759	*Entamoeba histolytica*	Ehi	5	0	2	0
			13642	*Heterostelium pallidum*	Pp	4	1	1	1
		Archaeplastida	3702	*Arabidopsis thaliana*	At	2	6	4	2
			3055	*Chlamydomonas reinhardtii*	Cr	1	2	3	2
			2769	*Chondrus crispus*	Cc	1	1	1	1
			4530	*Oryza Sativa*	Os	1	1	6	2
		SAR	353152	*Cryptosporidium parvum*	Cp	1	0	0	1
			1519565	*Fistulifera solaris*	Fs	2	1	2	2
			2315210	*Hondaea fermentalgiana*	Hf	2	1	0	1
			403677	*Phytophthora infestans*	Pi	1	1	2	2
			37360	*Plasmodiophora brassicae*	Pb	1	1	0	1
			5833	*Plasmodium falciparum*	Pf	3	0	0	0
			46433	*Reticulomyxa filosa*	Rf	2	1	3	1
			5911	*Tetrahymena thermophila*	Tt	2	0	1	1
		Excavata	5741	*Giardia intestinalis*	Gi	1	1	0	1
			5664	*Leishmania major*	Lm	2	1	1	1
			5722	*Trichomonas vaginalis*	Tv	8	1	3	0
			5691	*Trypanosoma brucei*	Tb	2	1	1	0
		Hacrobia	2903	*Emiliania huxleyi*	Eh	9	0	2	6
			55529	*Guillardia theta*	Gt	6	1	1	1
	Bacteria	N/A	237018	*Algoriphagus aquimarinus*	Aa	1	0	0	0
			1352	*Enterococcus faecium*	Ef	1	0	0	0
	Archaea	N/A	2214	*Methanosarcina acetivorans*	Ma	1	0	0	0
			1538547	*Lokiarchaeum sp. GC14_75*	Ls	0	0	4	0
N/A	Virus	N/A	2487775	*Terrestrivirus sp.*	Ts	1	0	0	0
			1977638	*Hokovirus HKV1*	Hh	0	0	1	0

Interestingly, members of certain taxa showed patterns in their absence of certain kinases. In order to determine with precision the origin of these kinase absences, an approach relying on whole proteomes was employed.

6.2.2. Absence of inositol phosphate kinases across eukaryotes

To assess the absence of certain inositol phosphate kinases in eukaryotes, reference eukaryotic proteomes were analysed. Such an approach would guarantee the completeness of genome sequencing, bypassing the possibility of accounting for multiple gene isoforms and reducing the incidence of false positives. A certain kinase absence at the proteome level would provide reliable information on the *bona fide* nature of such an absence.

The analysis of specific inositol phosphate kinase absences was performed at the level of species and traced back along the eukaryotic tree of life for identifications of taxa with a total loss of a particular inositol phosphate kinase. A colour-coded and condensed tree depicting IPK, IP5-2K and ITPK1 kinase absence across NCBI taxa is represented in **Figure 6.1**.

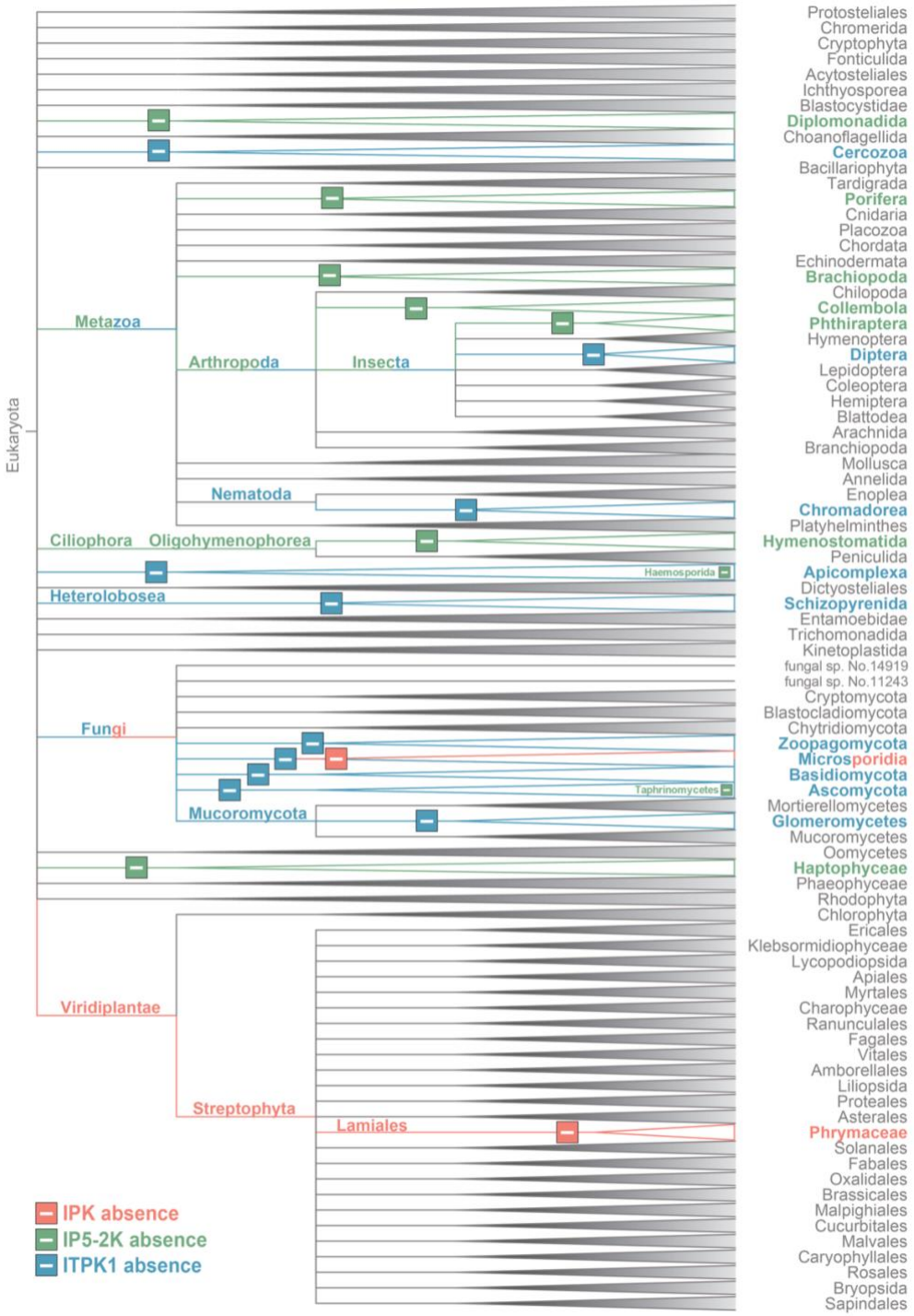

Figure 6.1. Inositol phosphate kinase absence across eukaryotes with reference proteomes. Loss of IPK is detected with a lower frequency than the loss of IP5K-2K or IPK. A previously described loss of ITPK1 in fungi was revealed to be less widespread than expected. PPIP5K was not analysed due to the lack of an InterPro entry for this family. Taxa are labelled as a kinase loss if a given enzyme is absent from all reference proteomes contained in the taxa.

As seen in this analysis, the cellular slime moulds or Dictyosteliales, which this study has focused on thus far, do not show an absence of IPK, IP5-2K or ITPK1 in all of the reference proteomes analysed. Such property allows them to be ideal model organisms for the study of inositol pyrophosphates in higher complexity organisms. This is in contrast with yeast, a model that was key in the development of the inositol phosphate field and which remarkably lacks enzymes of the ITPK1 family.

From this tree, it became evident that certain generalisations previously made did not apply to the realm of complexity of certain eukaryotic taxa. Fungi had been believed to lack ITPK1 (Saiardi et al., 2018). However, this analysis revealed that it is only a fraction of species in this taxon which have a loss of this enzyme.

A frequent loss of IP5-2K in Metazoa was not evident previous to this study and its relevance lies in the attributable function of this enzyme in the synthesis of $InsP_6$ by catalysis of the rate-limiting step of pyrophosphorylation at the carbon on position 2 of the inositol ring. One would expect that this enzyme would be required in all Metazoa for the further synthesis of $InsP_6$ and inositol pyrophosphate species. This seeming not to be the case points towards the potential catalytic flexibility of inositol phosphate enzymes or the identification of alternative kinases that lie outside the major families already described.

That a large fraction of plants does not have major kinase losses highlighted the functional relevance of these molecules in such organisms. Accumulating evidence supports this (Kuo et al., 2018; Laha et al., 2019), and our understanding of inositol phosphate synthesis in plants is beginning to flourish.

6.2.3. Location in the tree of life

In addition to kinase absence, frequent cases of gene amplification were detected from the quantitative study of species under analysis (**Table 6.1**). Such losses and amplifications and their taxonomic distributions are best represented in the form of a tree of life diagram (**Figure 6.2**). In this ‘timetree’, length of branches is to scale and corresponds to the evolutionary divergence of species. The different taxa were labelled according to their definition in the open tree of life taxonomy database.

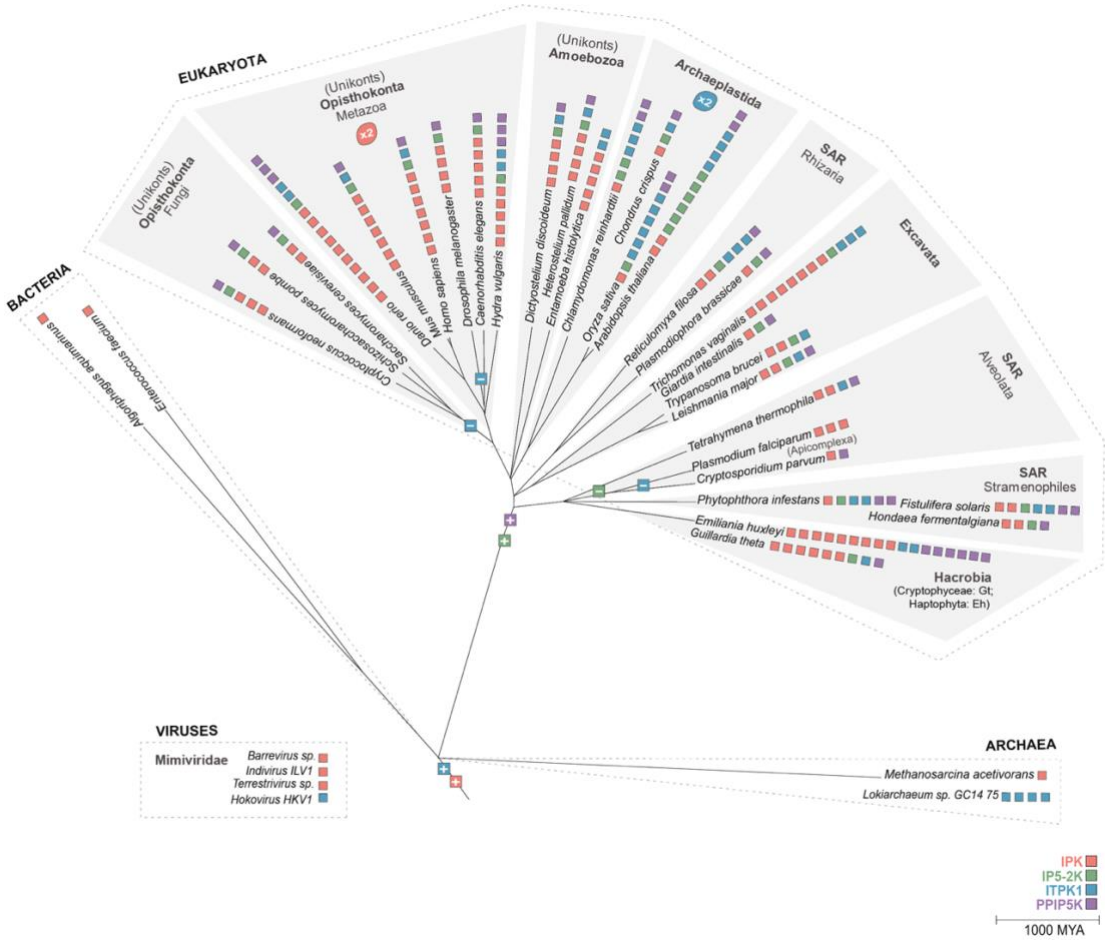

Figure 6.2. Inositol phosphate kinase members across the tree of life. An expansion of IPK in Opisthokonta is detected, whereas an ITPK1 expansion is detected in Archaeplastida. The emergence of PPIP5K and IP5-2K seems to be contemporary to the emergence of eukaryotes, whereas ITPK1 and IPK seem to be present before the branching of Eukaryota and in large viruses. Viruses are represented next to the tree of life due to their unclear taxonomic classification. Tree branching generated with timetree.org.

From these results, amplification of the IPK family is evident in Metazoa. The complexity of these organisms points towards a need for functional specialization that was accomplished by catalytic diversification into subfamilies.

The ITPK1 loss, which although not complete (**Figure 6.1**), is seen in many fungal species, could be attributable to a general kinase loss in this

taxon (Goldberg et al., 2006). A process reduction of genome size in this taxon closely related to Metazoa could underlie this phenomenon.

Archaeplastida have a considerable amplification in ITPK1 members. Such characteristic could be attributed to increased ploidy. Remarkably, likely increases in ploidy are not accompanied by amplification of IPK members, therefore implying a reduction of the IPK family by gene loss. One could hypothesise the parallel development of PP-InsP synthesising activity of Archaeplastida ITPK1 enzymes (Laha et al., 2019), in order to overcome a lack of functional diversity in PP-InsP synthesis.

A widespread lack of IP5-2K duplication and the tendency for this gene to be present as a single copy could be attributable to the environmental excess of phytate. Availability of extracellular phytate could imply that different species could rely on exogenous sources of $InsP_6$ without needing to amplify their enzymatic synthesis machinery.

In many Alveolata, which are primarily single-celled organisms, there is a loss of IP5-2K. This could arise from some of their preferred modes of nutrition: predation and intracellular parasitism. Such a mode of nutrition would also imply the availability of $InsP_6$ which could be coupled to the redundancy in its cellular synthesis, leading to functional gene loss throughout evolution. One particularly remarkable example of taxa in Alveolata which shows gene loss is Apicomplexa. Species in this taxon are obligate parasites and also show an ITPK1 loss, reflecting the tendency for loss of inositol phosphate kinases in cases where parasitism is the mode of nutrition and these molecules can be obtained from exogenous sources.

6.3. Discussion

The general absence of inositol phosphate kinases in eukaryotes can be understood under the light of functional redundancy and genomic simplification. In contrary, gene amplification could arise from a need for functional diversification or compartmentalisation of inositol phosphates. The model organism used in this study, *D. discoideum,* seemed to be an optimal candidate for the deciphering of inositol phosphate pathways in higher eukaryotes, given the predominant kinase loss in the preferred non-metazoan model organism, yeast (Goldberg et al., 2006).

A limitation of this analysis has resided in a lack of resolution across different IPK members, which show 3 distinct catalytic activities. As has been described, some of these activities have not been possible to trace to a characterised enzyme. One such example is that of *A. thaliana* whose IP6K enzyme remains unidentified. One possible solution to this conundrum could reside in the catalytic activities of uncharacterized members of closely related families. The IP5-2K family is evolutionarily close to the IPK family (Gonzalez et al., 2010), therefore certain uncharacterised members of this family in *A. thaliana* could be catalysing the addition of a pyrophosphate moiety to $InsP_6$ for the formation of higher phosphorylated species.

An additional time limitation of this study precluded the comparative phylogenetic analysis of *ipkA* and other inositol phosphate kinase sequences from *D. discoideum* with others present in the tree of life across the thoroughly researched higher eukaryotes (yeast and humans). An identification of IPK enzymes resembling *ipkA* in eukaryotic organisms that branched before Amoebozoa could argue for a widespread $InsP_8$-synthesising activity in the IPK family. This family could have expanded before eukaryotic branching into different taxa, from a multifunctional kinase activity that specialised into different catalytic activities.

Following the development of an $InsP_8$-synthesising activity in a subtype of IPKs, these could have been superseded by the bifunctional enzyme PPIP5K. A potential ‘IP7K’ resulting from IPK expansion could have become redundant and replaced by the presence of PPIP5K. The presence of *ipkA* in the *D. discoideum* genome would constitute in this case an instance of the retention of a gene that would have become redundant in other species. Such retention could have taken place in order to supply for the large requisite of inositol pyrophosphate concentrations in the amoeba. Additionally, the requirement for specific inositol pyrophosphate isomers synthesised by *ipkA* could have led to its retention in the *D. discoideum* genome.

The detected presence of inositol phosphate kinases in Archaea and Bacteria, most often IPK and ITPK1 can aid our understanding of the evolutionary antiquity of the inositol phosphate pathway. Most likely, these two enzymes acted in synchronicity to generate what we know today as the inositol phosphate pathway in Eukaryotic cells.

Remarkably, the presence of inositol phosphate kinases in viruses seems restricted to large viruses of the Mimiviridae family. These giant viruses infect unicellular eukaryotes and seem to have IPK and ITPK1. One promising hypothesis for their relative location in the tree of life stems from their possible reductive evolution. These viruses may have originated prior to the radiation of the eukaryotic phylum and may have contributed to its diversification and the development of inositol phosphate synthesis in higher Eukaryotes.

7. Conclusions

This work analysed inositol pyrophosphate structure in *D. discoideum*, revealing a higher isomeric diversity than previously identified. It also described the serendipitous discovery of an inhibitory effect of the buffer MES on synthesis of inorganic polyP in the social amoeba. Additional inositol pyrophosphate enzymes were brought to light by the detection of involvement of IpkA in the synthesis of the majority of the $InsP_8$ pool in the amoeba. An evolutionary analysis was initiated, whereby the presence of inositol phosphate kinases, previously thought to be restricted to Eukaryotes, was extended across the tree of life and viral species. Further work will be necessary to elucidate the functions of these molecules across the tree of life and deploy the translational potential of these findings.

8. Appendix

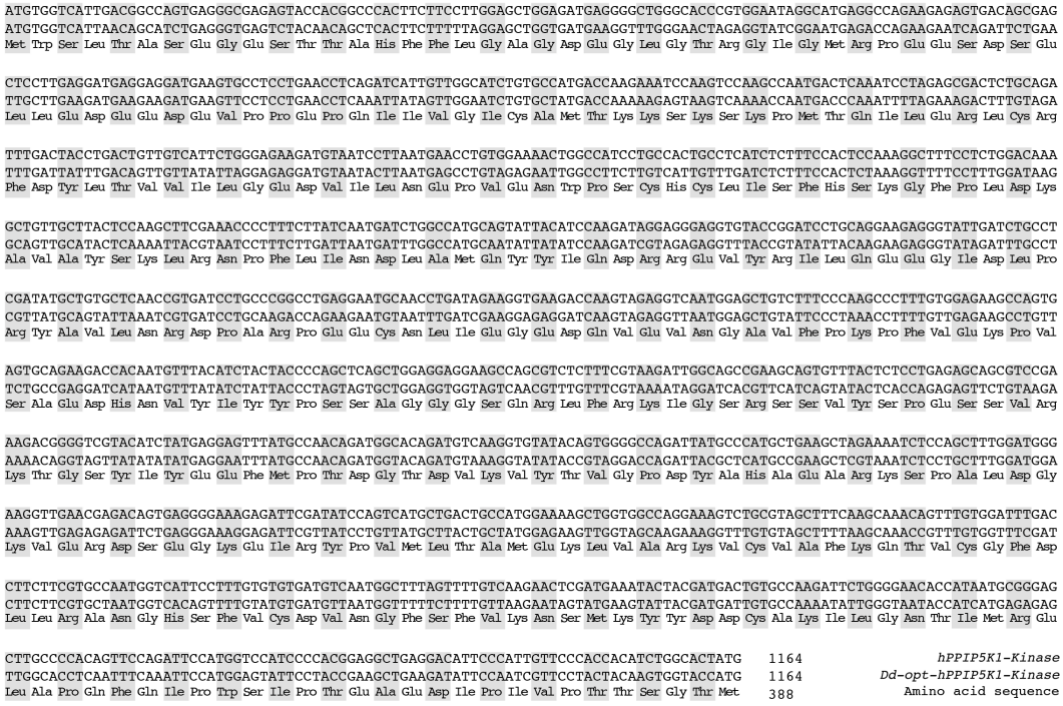

Figure 8.1. Codon optimisation of the kinase region of hPPIP5K1. Optimisation of codons was achieved with an IDT™ SciTools® tool and manual adjusting was performed to prevent the presence of unwanted restriction sites.

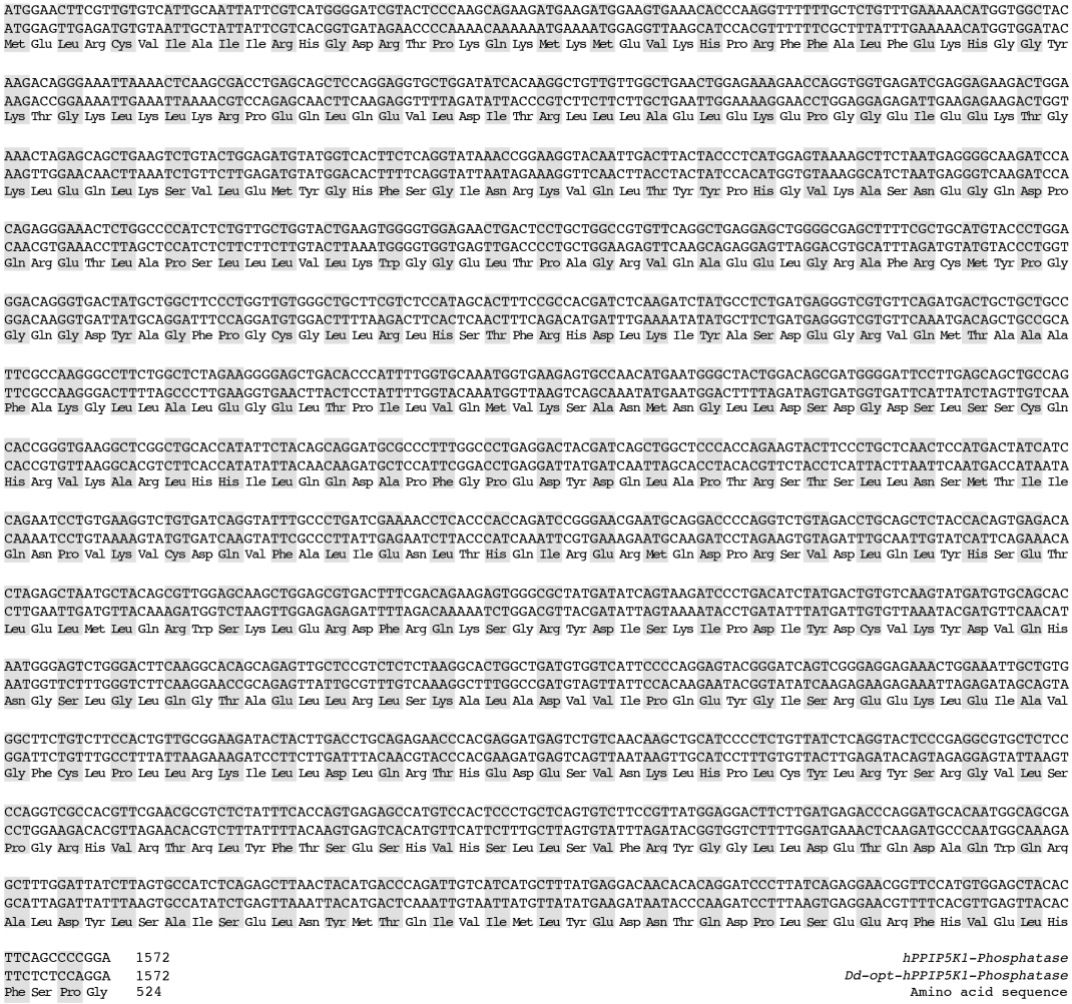

Figure 8.2. Codon optimisation of the phosphatase region of hPPIP5K1. Optimisation of codons was obtained with an IDT™ SciTools® tool and manually adjusted to prevent the presence of unwanted restriction sites.

9. References

Ahn, K., and Kornberg, A. (1990). Polyphosphate kinase from Escherichia coli. Purification and demonstration of a phosphoenzyme intermediate. J. Biol. Chem. *265*, 11734–11739.

Albert, C., Safrany, S.T., Bembenek, M.E., Reddy, K.M., Reddy, K., Falck, J., Bröcker, M., Shears, S.B., and Mayr, G.W. (1997). Biological variability in the structures of diphosphoinositol polyphosphates in Dictyostelium discoideum and mammalian cells. Biochem. J. *327*, 553–560.

Annesley, S.J., and Fisher, P.R. (2009). Dictyostelium discoideum-a model for many reasons. Mol. Cell. Biochem. *329*, 73–91.

Ansermet, C., Moor, M.B., Centeno, G., Auberson, M., Hu, D.Z., Baron, R., Nikolaeva, S., Haenzi, B., Katanaeva, N., Gautschi, I., et al. (2017). Renal fanconi syndrome and hypophosphatemic rickets in the absence of xenotropic and polytropic retroviral receptor in the nephron. J. Am. Soc. Nephrol. *28*, 1073–1078.

Arya, R., Bhattacharya, A., and Saini, K.S. (2008). Dictyostelium discoideum —a promising expression system for the production of eukaryotic proteins . FASEB J. *22*, 4055–4066.

Azevedo, C., and Saiardi, A. (2006). Extraction and analysis of soluble inositol polyphosphates from yeast. Nat. Protoc. *1*, 2416–2422.

Azevedo, C., and Saiardi, A. (2017). Eukaryotic Phosphate Homeostasis: The Inositol Pyrophosphate Perspective. Trends Biochem. Sci. *42*, 219–231.

Azevedo, C., Livermore, T., and Saiardi, A. (2015). Protein polyphosphorylation of lysine residues by inorganic polyphosphate. Mol. Cell *58*, 71–82.

Balla, T. (2013). Phosphoinositides: Tiny lipids with giant impact on cell

regulation. Physiol. Rev. *93*, 1019–1137.

Banfic, H., Bedalov, A., York, J.D., and Visnjic, D. (2013). Inositol pyrophosphates modulate S phase progression after pheromone-induced arrest in saccharomyces cerevisiae. J. Biol. Chem. *288*, 1717–1725.

Barker, C.J., Wright, J., Hughes, P.J., Kirk, C.J., and Michell, R.H. (2004). Complex changes in cellular inositol phosphate complement accompany transit through the cell cycle. Biochem J *380*, 465–473.

Bennett, M., Onnebo, S.M.N., Azevedo, C., and Saiardi, A. (2006). Inositol pyrophosphates: Metabolism and signaling. Cell. Mol. Life Sci. *63*, 552–564.

Berridge, M.J. (1993). Inositol Trisphosphate and Calcium Signalling. Nature *361*, 315–325.

Berridge, M.J. (2009). Inositol trisphosphate and calcium signalling mechanisms. Biochim. Biophys. Acta - Mol. Cell Res.

Bonner, J.T., and Savage, L.J. (1947). Evidence for the formation of cell aggregates by chemotaxis in the development of the slime mold Dictyostelium discoideum. J. Exp. Zool. *106*, 1–26.

Burton, A., Azevedo, C., Andreassi, C., Riccio, A., and Saiardi, A. (2013). Inositol pyrophosphates regulate JMJD2C-dependent histone demethylation. Proc. Natl. Acad. Sci. *110*, 18970–18975.

Chakraborty, A., Koldobskiy, M.A., Bello, N.T., Maxwell, M., Potter, J.J., Juluri, K.R., Maag, D., Kim, S., Huang, A.S., Megan, J., et al. (2010). Inositol pyrophosphates inhibit Akt signaling, regulate insulin sensitivity and weight gain. Cell *143*, 897–910.

Choi, K., Mollapour, E., and Shears, S.B. (2005). Signal transduction during environmental stress: InsP8operates within highly restricted contexts. Cell. Signal. *17*, 1533–1541.

Desfougères, Y., and Saiardi, A. (2020). Dictyostelium discoideum as a Model to Study Inositol Polyphosphates and Inorganic Polyphosphate. In Inositol Phosphates Methods and Protocols, G.J. Miller, ed. (Humana Press), pp. 59–71.

Desfougères, Y., Wilson, M.S.C., Laha, D., Miller, G.J., and Saiardi, A. (2019). ITPK1 mediates the lipid-independent synthesis of inositol phosphates controlled by metabolism. Proc. Natl. Acad. Sci. U. S. A. *116*, 24551–24561.

Desfougères, Y., Saiardi, A., and Azevedo, C. (2020). Inorganic polyphosphate in mammals: where's Wally? Biochem. Soc. Trans. *0*, 95–101.

Draškovič, P., Saiardi, A., Bhandari, R., Burton, A., Ilc, G., Kovačevič, M., Snyder, S.H., and Podobnik, M. (2008). Inositol Hexakisphosphate Kinase Products Contain Diphosphate and Triphosphate Groups. Chem. Biol. *15*, 274–286.

Dubois, E., Scherens, B., Vierendeels, F., Ho, M.M.W., Messenguy, F., and Shears, S.B. (2002). In Saccharomyces cerevisiae, the inositol polyphosphate kinase activity of Kcs1p is required for resistance to salt stress, cell wall integrity, and vacuolar morphogenesis. J. Biol. Chem. *277*, 23755–23763.

Eichinger, L., Pachebat, J.A., Glöckner, G., Rajandream, M.-A., Sucgang, R., Berriman, M., Song, J., Olsen, R., Szafranski, K., Xu, Q., et al. (2005). The genome of the social amoeba Dictyostelium discoideum. Nature *435*, 43–57.

Escalante, R., and Cardenal-Muñoz, E. (2019). The Dictyostelium discoideum model system. Int. J. Dev. Biol. *63*, 317–320.

Europe-Finner, G.N., and Newell, P.C. (1985). Inositol 1,4,5-triphosphate induces cyclic GMP formation in Dictyostelium discoideum. Biochem. Biophys. Res. Commun. *130*, 1115–1122.

Europe-Finner, G.N., Gammon, B., and Newell, P.C. (1991). Accumulation of [3H]-inositol into inositol polyphosphates during development of Dictyostelium. Biochem. Biophys. Res. Commun. *181*, 191–196.

Feoktistova, A., Mccollum, D., Ohi, R., and Gould, K.L. (1999). a Gene That Interacts with Mutations in the Arp2 / 3 Complex and Actin.

Friedrich, M., Meier, D., Schuster, I., and Nellen, W. (2015). A simple retroelement based knock-down system in Dictyostelium: Further Insights into RNA Interference Mechanisms. PLoS One *10*, 1–17.

Fu, C., Xu, J., Li, R.J., Crawford, X.A., Khan, A.B., Ma, T.M., Cha, J.Y., Snowman, A.M., Pletnikov, M. V., and Snyder, S.H. (2015). Inositol hexakisphosphate kinase-3 regulates the morphology and synapse formation of cerebellar purkinje cells via spectrin/adducin. J. Neurosci. *35*, 11056–11067.

Gokhale, N.A., Zaremba, A., Janoshazi, A.K., Weaver, J.D., and Shears, S.B. (2013). PPIP5K1 modulates ligand competition between diphosphoinositol polyphosphates and PtdIns(3,4,5)P3 for polyphosphoinositide-binding domains. Biochem. J. *453*, 413–426.

Goldberg, J.M., Manning, G., Liu, A., Fey, P., Pilcher, K.E., Xu, Y., and Smith, J.L. (2006). The Dictyostelium Kinome—Analysis of the Protein Kinases from a Simple Model Organism. PLoS Genet. *2*, e38.

Gonzalez, B., Banos-Sanz, J.I., Villate, M., Brearley, C.A., and Sanz-Aparicio, J. (2010). Inositol 1,3,4,5,6-pentakisphosphate 2-kinase is a distant IPK member with a singular inositide binding site for axial 2-OH recognition. Proc. Natl. Acad. Sci. *107*, 9608–9613.

Gu, C., Wilson, M.S.C., Jessen, H.J., Saiardi, A., Shears, S.B., Wilson, M., Livermore, T., Saiardi, A., Shears, S., Shears, S., et al. (2016). Inositol Pyrophosphate Profiling of Two HCT116 Cell Lines Uncovers Variation in InsP8 Levels. PLoS One *11*, e0165286.

Gu, C., Nguyen, H.N., Ganini, D., Chen, Z., Jessen, H.J., Gu, Z., Wang, H., and Shears, S.B. (2017). KO of 5-InsP7 kinase activity transforms the HCT116 colon cancer cell line into a hypermetabolic, growth-inhibited phenotype. Proc. Natl. Acad. Sci. U. S. A. *114*, 11968–11973.

Harmel, R.K., Puschmann, R., Nguyen Trung, M., Saiardi, A., Schmieder, P., and Fiedler, D. (2019). Harnessing 13C-labeled myo-inositol to interrogate inositol phosphate messengers by NMR. Chem. Sci. *10*, 5267–5274.

Hoeller, O., and Kay, R.R. (2007). Chemotaxis in the Absence of PIP3 Gradients. Curr. Biol. *17*, 813–817.

Hsieh, P.C., Shenoy, B.C., Jentoft, J.E., and Phillips, N.F.B. (1993). Purification of Polyphosphate and ATP Glucose Phosphotransferase from Mycobacterium tuberculosis H37Ra: Evidence That Poly(P) and ATP Glucokinase Activities Are Catalyzed by the Same Enzyme. Protein Expr. Purif. *4*, 76–84.

Iijima, M., Huang, Y.E., and Devreotes, P. (2002). Temporal and spatial regulation of chemotaxis. Dev. Cell *3*, 469–478.

Illies, C., Gromada, J., Fiume, R., Leibiger, B., Yu, J., Juhl, K., Yang, S.-N., Barma, D.K., Falck, J.R., Saiardi, A., et al. (2007). Requirement of Inositol Pyrophosphates for Full Exocytotic Capacity in Pancreatic β Cells. Science (80-.). *318*, 1299–1302.

Insall, R., Kuspa, A., Lilly, P.J., Shaulsky, G., Levin, L.R., Loomis, W.F., and Devreotes, P. (1994). CRAC, a cytosolic protein containing a pleckstrin homology domain, is required for receptor and G protein-mediated activation of adenylyl cyclase in Dictyostelium. J. Cell Biol. *126*, 1537–1545.

Irvine, R.F. (2016). A short history of inositol lipids. J. Lipid Res. *57*, 1987–1994.

Irvine, R.F., and Schell, M.J. (2001). Back in the water: the return of the inositol phosphates. Nat. Mol. Cell Biol.

Jadav, R.S., Chanduri, M.V.L., Sengupta, S., and Bhandari, R. (2013). Inositol pyrophosphate synthesis by inositol hexakisphosphate kinase 1 is required for homologous recombination repair. J. Biol. Chem. *288*, 3312–3321.

Katz, K.S., and Ratner, D.I. (1988). Homologous recombination and the repair of double-strand breaks during cotransformation of Dictyostelium discoideum. Mol. Cell. Biol. *8*, 2779–2786.

King, J., Keim, M., Teo, R., Weening, K.E., Kapur, M., McQuillan, K., Ryves, J., Rogers, B., Dalton, E., Williams, R.S.B., et al. (2010). Genetic control of lithium sensitivity and regulation of inositol biosynthetic genes. PLoS One *5*.

Kornberg, A., Rao, N.N., and Ault-riché, D. (1999). I Norganic P Olyphosphate : 89–125.

Krupovic, M., Dolja, V. V., and Koonin, E. V. (2019). Origin of viruses: primordial replicators recruiting capsids from hosts. Nat. Rev. Microbiol. *17*, 449–458.

Kuo, H.-F., Hsu, Y.-Y., Lin, W.-C., Chen, K.-Y., Munnik, T., Brearley, C.A., and Chiou, T.-J. (2018). Arabidopsis inositol phosphate kinases IPK1 and ITPK1 constitute a metabolic pathway in maintaining phosphate homeostasis. Plant J. *95*, 613–630.

Laha, D., Parvin, N., Hofer, A., Giehl, R.F.H., Fernandez-Rebollo, N., Von Wirén, N., Saiardi, A., Jessen, H.J., and Schaaf, G. (2019). Arabidopsis ITPK1 and ITPK2 Have an Evolutionarily Conserved Phytic Acid Kinase Activity. ACS Chem. Biol. *14*, 2127–2133.

Laussmann, T., Eujen, R., Weisshuhn, C.M., and Thiel, U. (1996). Structures of diphospho-myo-inositol pentakisphosphate and

bisdiphospho- myo-inositol tetrakisphosphate from Dictyostelium resolved by NMR analysis. Biochem. J. *315*, 715–720.

Laussmann, T., Reddy, K.M., Reddy, K.K., Falck, J.R., and Vogel, G. (1997). Diphospho-myo-inositol phosphates from Dictyostelium identified as D-6-diphospho-myo-inositol pentakisphosphate and D-5,6-bisdiphospho-myo-inositol tetrakisphosphate. Biochem. J. *322*, 31–33.

Laussmann, T., Pikzack, C., Thiel, U., Mayr, G.W., and Vogel, G. (2000). Diphospho-myo-inositol phosphates during the life cycle of Dictyostelium and Polysphondylium. Eur. J. Biochem. *267*, 2447–2451.

Lenburg, M.E., and O'Shea, E.K. (1996). Signaling phosphate starvation. Trends Biochem. Sci. *21*, 383–387.

Lev, S., Li, C., Desmarini, D., Saiardi, A., Fewings, N.L., Schibeci, S.D., Sharma, R., Sorrell, T.C., and Djordjevic, J.T. (2015). Fungal inositol pyrophosphate IP7 is crucial for metabolic adaptation to the host environment and pathogenicity. MBio *6*, 1–15.

Levi, S., Polyakov, M., and Egelhoff, T.T. (2000). Green fluorescent protein and epitope tag fusion vectors for Dictyostelium discoideum. Plasmid.

Lin, H., Fridy, P.C., Ribeiro, A.A., Choi, J.H., Barma, D.K., Vogel, G., Falck, J.R., Shears, S.B., York, J.D., and Mayr, G.W. (2009). Structural analysis and detection of biological inositol pyrophosphates reveal that the family of VIP/Diphosphoinositol pentakisphosphate kinases Are1/3-kinases. J. Biol. Chem. *284*, 1863–1872.

Livermore, T.M. (2016). Developing Dictyostelium discoideum as a model to study the synthesis and metabolism of inositol pyrophosphates and inorganic polyphosphate. PhD Thesis, University College London.

Livermore, T.M., Chubb, J.R., and Saiardi, A. (2016a). Developmental accumulation of inorganic polyphosphate affects germination and

energetic metabolism in Dictyostelium discoideum. Proc. Natl. Acad. Sci. *113*, 201519440.

Livermore, T.M., Azevedo, C., Kolozsvari, B., Wilson, M.S.C., and Saiardi, A. (2016b). Phosphate, inositol and polyphosphates. Biochem. Soc. Trans. *44*, 253–259.

Lonetti, A., Szijgyarto, Z., Bosch, D., Loss, O., Azevedo, C., and Saiardi, A. (2011). Identification of an evolutionarily conserved family of inorganic polyphosphate endopolyphosphatases. J. Biol. Chem. *286*, 31966–31974.

Losito, O., Szijgyarto, Z., Resnick, A.C., and Saiardi, A. (2009). Inositol pyrophosphates and their unique metabolic complexity: Analysis by gel electrophoresis. PLoS One *4*, 2–10.

Loss, O., Azevedo, C., Szijgyarto, Z., Bosch, D., and Saiardi, A. (2011). Preparation of Quality Inositol Pyrophosphates. JoVE e3027.

Luo, H.R., Huang, Y.E., Chen, J.C., Saiardi, A., Iijima, M., Ye, K., Huang, Y., Nagata, E., Devreotes, P., and Snyder, S.H. (2003). Inositol Pyrophosphates Mediate Chemotaxis in< i> Dictyostelium</i> via Pleckstrin Homology Domain-PtdIns (3, 4, 5) P3 Interactions. Cell *114*, 559–572.

Maeda, Y., and Chida, J. (2013). Control of Cell Differentiation by Mitochondria, Typically Evidenced in Dictyostelium Development. Biomolecules *3*, 943–966.

Mayr, G.W. (1988). A novel metal-dye detection system permits picomolar-range h.p.l.c. analysis of inositol polyphosphates from non-radioactively labelled cell or tissue specimens. Biochem. J *254*, 585–591.

Mayr, G.W., Radenberg, T., Thiel, U., Vogel, G., and Stephens, L.R. (1992). Phosphoinositol diphosphates: non-enzymic formation in vitro and occurrence in vivo in the cellular slime mold Dictyostelium. Carbohydr.

Res. *234*, 247–262.

McCutcheon, M. (1946). CHEMOTAXIS IN LEUKOCYTES. Physiol. Rev. *26*, 319–336.

Moreno, S.N.J., and Docampo, R. (2013). Polyphosphate and Its Diverse Functions in Host Cells and Pathogens. PLoS Pathog. *9*, 5–7.

Morrison, B.H., Haney, R., Lamarre, E., Drazba, J., Prestwich, G.D., and Lindner, D.J. (2009). Gene deletion of inositol hexakisphosphate kinase 2 predisposes to aerodigestive tract carcinoma. Oncogene *28*, 2383–2392.

Morrissey, J.H., Choi, S.H., and Smith, S.A. (2012). Polyphosphate: An ancient molecule that links platelets, coagulation, and inflammation. Blood *119*, 5972–5979.

Mulugu, S., Bai, W., Fridy, P.C., Bastidas, R.J., Otto, J.C., Dollins, D.E., Haystead, T.A., Ribeiro, A.A., and York, J.D. (2007). A Conserved Family of Enzymes That Phosphorylate Inositol Hexakisphosphate. Science (80-.). 106–110.

Muramoto, T., Iriki, H., Watanabe, J., and Kawata, T. (2019). Recent Advances in CRISPR/Cas9-Mediated Genome Editing in Dictyostelium. Cells *8*, 46.

Myre, M.A. (2012). Clues to γ-secretase, huntingtin and Hirano body normal function using the model organism Dictyostelium discoideum. J. Biomed. Sci. *19*, 1–11.

Nichols, J.M.E., Veltman, D., and Kay, R.R. (2015). Chemotaxis of a model organism: Progress with Dictyostelium. Curr. Opin. Cell Biol. *36*, 7–12.

Ohashi, K., Kawai, S., and Murata, K. (2012). Identification and characterization of a human mitochondrial NAD kinase. Nat. Commun. *3*.

Onnebo, S.M.N., and Saiardi, A. (2009). Inositol pyrophosphates modulate hydrogen peroxide signalling. Biochem. J. *423*, 109–118.

Di Paolo, G., and De Camilli, P. (2006). Phosphoinositides in cell regulation and membrane dynamics. Nature *443*, 651–657.

Pearson, W.R. (2013). An Introduction to Sequence Similarity ("Homology") Searching. Curr. Protoc. Bioinforma. *42*, 3.1.1-3.1.8.

Pesesse, X., Choi, K., Zhang, T., and Shears, S.B. (2004). Signaling by higher inositol polyphosphates: Synthesis of bisdiphosphoinositol tetrakisphosphate ("InsP8") is selectively activated by hyperosmotic stress. J. Biol. Chem. *279*, 43378–43381.

Pisani, F., Livermore, T., Rose, G., Chubb, J.R., Gaspari, M., and Saiardi, A. (2014). Analysis of Dictyostelium discoideum inositol pyrophosphate metabolism by gel electrophoresis. PLoS One *9*, 1–9.

Rao, N.N., Gómez-García, M.R., and Kornberg, A. (2009). Inorganic Polyphosphate: Essential for Growth and Survival. Annu. Rev. Biochem. *78*, 605–647.

Rullich, C.C., and Kiefer, J. (2018). Enantioselective Raman spectroscopy (esR) for distinguishing between the enantiomers of 2-butanol. Analyst *143*, 3040–3048.

Saiardi, A. (2017). Has Inositol Played Any Role in the Origin of Life? Life *7*, 24.

Saiardi, A., Erdjument-Bromage, H., Snowman, A.M., Tempst, P., and Snyder, S.H. (1999). Synthesis of diphosphoinositol pentakisphosphate by a newly identified family of higher inositol polyphosphate kinases. Curr. Biol. *9*, 1323–1326.

Saiardi, A., Caffrey, J.J., Snyder, S.H., and Shears, S.B. (2000). The inositol hexakisphosphate kinase family. Catalytic flexibility and function in yeast vacuole biogenesis. J. Biol. Chem. *275*, 24686–24692.

Saiardi, A., Nagata, E., Luo, H.R., Snowman, A.M., and Snyder, S.H. (2001a). Identification and Characterization of a Novel Inositol Hexakisphosphate Kinase. J. Biol. Chem. *276*, 39179–39185.

Saiardi, A., Nagata, E., Luo, H.R., Sawa, A., Luo, X., Snowman, A.M., and Snyder, S.H. (2001b). Mammalian inositol polyphosphate multikinase synthesizes inositol 1,4,5-trisphosphate and an inositol pyrophosphate. Proc. Natl. Acad. Sci. *98*, 2306–2311.

Saiardi, A., Sciambi, C., McCaffery, J.M., Wendland, B., and Snyder, S.H. (2002). Inositol pyrophosphates regulate endocytic trafficking. Proc. Natl. Acad. Sci. U. S. A. *99*, 14206–14211.

Saiardi, A., Azevedo, C., Desfougères, Y., Portela-Torres, P., and Wilson, M.S.C. (2018). Microbial inositol polyphosphate metabolic pathway as drug development target. Adv. Biol. Regul. *67*, 74–83.

Schell, M.J. (2010). Inositol trisphosphate 3-kinases: Focus on immune and neuronal signaling. Cell. Mol. Life Sci. *67*, 1755–1778.

Sekine, R., Kawata, T., and Muramoto, T. (2018). CRISPR/Cas9 mediated targeting of multiple genes in Dictyostelium. Sci. Rep. *8*, 8471.

Shears, S.B. (2015). Inositol pyrophosphates: Why so many phosphates? Adv. Biol. Regul. *57*, 203–216.

Shen, X., Xiao, H., Ranallo, R., Wu, W.H., and Wu, C. (2003). Modulation of ATP-dependent chromatin-remodeling complexes by inositol polyphosphates. Science (80-.). *299*, 112–114.

Smith, R., Wright, K.L., and Ashton, L. (2016). Raman spectroscopy: an evolving technique for live cell studies. Analyst *141*, 3590–3600.

Steger, D.J., Haswell, E.S., Miller, A.L., Wente, S.R., and OòShea, E.K. (2003). Regulation of Chromatin Remodeling by Inositol Polyphosphates. *299*, 114–116.

Stephens, L.R., and Irvine, R.F. (1990). Stepwise phosphorylation of myo-inositol leading to myo-inositol hexakisphosphate in Dictyostelium. Nature *346*, 580–583.

Stephens, L.R., Hawkins, P.T., Barker, C.J., and Downes, C.P. (1988). Synthesis of myo-inositol 1,3,4,5,6,-pentakisphosphate from inositol phosphates generated by receptor activation. Biochem. J. *253*, 721–733.

Stephens, L.R., Hawkins, P.T., Stanley, A.F., Moore, T., Poyner, D.R., Morris, P.J., Hanley, M.R., Kay, R.R., and Irvine, R.F. (1991). myo-Inositol pentakisphosphates Structure, biological occurrence and phosphorylation to myo-inositol hexakisphosphate. *275*, 485–499.

Streb, H., Irvine, R.F., Berridge, M.J., and Schulz, I. (1983). Release of Ca2+ from a nonmitochondrial intracellular store in pancreatic acinar cells by inositol-1,4,5-trisphosphate. Nature *306*, 67–69.

Thota, S.G., and Bhandari, R. (2015). The emerging roles of inositol pyrophosphates in eukaryotic cell physiology. J. Biosci. *40*, 593–605.

Tsui, M.M., and York, J.D. (2010). Roles of inositol phosphates and inositol pyrophosphates in development, cell signaling and nuclear processes. *50*, 324–337.

Vanhaesebroeck, B., Stephens, L., and Hawkins, P. (2012). PI3K signalling: The path to discovery and understanding. Nat. Rev. Mol. Cell Biol. *13*, 195–203.

Veltman, D.M., Akar, G., Bosgraaf, L., and Van Haastert, P.J.M. (2009). A new set of small, extrachromosomal expression vectors for Dictyostelium discoideum. Plasmid.

Wang, H., Falck, J.R., Hall, T.M.T., and Shears, S.B. (2012). Structural basis for an inositol pyrophosphate kinase surmounting phosphate crowding. Nat. Chem. Biol. *8*, 111–116.

Wang, H., DeRose, E.F., London, R.E., and Shears, S.B. (2014). IP6K

structure and the molecular determinants of catalytic specificity in an inositol phosphate kinase family. Nat. Commun. *5*, 4178.

Wang, H., Nair, V.S., Holland, A.A., Capolicchio, S., Jessen, H.J., Johnson, M.K., and Shears, S.B. (2015). Asp1 from Schizosaccharomyces pombe Binds a [2Fe-2S]2+ Cluster Which Inhibits Inositol Pyrophosphate 1-Phosphatase Activity. Biochemistry *54*, 6462–6474.

Wild, R., Gerasimaite, R., Jung, J.Y., Truffault, V., Pavlovic, I., Schmidt, A., Saiardi, A., Jacob Jessen, H., Poirier, Y., Hothorn, M., et al. (2016). Control of eukaryotic phosphate homeostasis by inositol polyphosphate sensor domains. Science (80-.). *352*, 986–990.

Wilson, M.S., Jessen, H.J., and Saiardi, A. (2019). The inositol hexakisphosphate kinases IP6K1 and -2 regulate human cellular phosphate homeostasis, including XPR1-mediated phosphate export. J. Biol. Chem. *294*, 11597–11608.

Wilson, M.S.C., Livermore, T.M., and Saiardi, A. (2013). Inositol pyrophosphates: between signalling and metabolism. Biochem. J. *452*, 369–379.

Wilson, M.S.C., Bulley, S.J., Pisani, F., Irvine, R.F., and Saiardi, A. (2015). A novel method for the purification of inositol phosphates from biological samples reveals that no phytate is present in human plasma or urine. Open Biol. *5*, 150014.

Zhang, C., Majerus, P.W., and Wilson, M.P. (2011). Regulation of inositol 1,3,4-trisphosphate 5/6-kinase (ITPK1) by reversible lysine acetylation. *109*, 2290–2295.

Acknowledgements

I would like to thank everyone in the Saiardi laboratory for their support throughout my studies. I would like to especially thank my supervisor Adolfo, for his mentoring and support throughout the course of my postgraduate experience and allowing me to pursue a career path that would suit me. I would like to thank Julie Pitcher for her mentoring and administrative help throughout my studies. I would also like to thank my committee for their discussions and support during my project. I would like to thank collaborators at the FMP in Berlin, the Orengo laboratory and Riana Gaifulina and Geraint Thomas at UCL. Finally, I would like to thank everyone at the LMCB for creating a great work atmosphere.